

UNCLASSIFIED

AD NUMBER

ADB019123

LIMITATION CHANGES

TO:

Approved for public release; distribution is unlimited.

FROM:

Distribution authorized to U.S. Gov't. agencies only; Test and Evaluation; DEC 1974. Other requests shall be referred to Air Force Armament Laboratories, Eglin AFB, FL 32542.

AUTHORITY

AFATL per DTIC form 55

THIS PAGE IS UNCLASSIFIED

THIS REPORT HAS BEEN DELIMITED
AND CLEARED FOR PUBLIC RELEASE
UNDER DOD DIRECTIVE 5200.20 AND
NO RESTRICTIONS ARE IMPOSED UPON
ITS USE AND DISCLOSURE.

DISTRIBUTION STATEMENT A

APPROVED FOR PUBLIC RELEASE;
DISTRIBUTION UNLIMITED.



AFATL-TR-74-202 ✓

2

8

AIMABLE WARHEAD SAFING AND ARMING (S&A) DEVICE

AD B019123

1 FMC CORPORATION,
2 DEFENSE TECHNOLOGY LABORATORIES, *Santa Clara*
3 MICRONICS DEPARTMENT, *- new*
1400 NORTH BURTON PLACE *410 235*
2 ANAHEIM, CALIFORNIA 92806

DDC
RECEIVED
JUN 20 1977
A

DECEMBER 1974

FINAL REPORT: JUNE 1973-DECEMBER 1974

Distribution limited to U. S. Government agencies only; this report documents test and evaluation; distribution limitation applied December 1974. Other requests for this document must be referred to the Air Force Armament Laboratory (DLJF), Eglin Air Force Base, Florida 32542.

AIR FORCE ARMAMENT LABORATORY

AIR FORCE SYSTEMS COMMAND • UNITED STATES AIR FORCE

EGLIN AIR FORCE BASE, FLORIDA



AD No.
DDC FILE COPY

UNCLASSIFIED

SECURITY CLASSIFICATION OF THIS PAGE (When Data Entered)

19 REPORT DOCUMENTATION PAGE		READ INSTRUCTIONS BEFORE COMPLETING FORM	
18	1. REPORT NUMBER AFATL TR-74-202	2. GOVT ACCESSION NO.	3. RECIPIENT'S CATALOG NUMBER
6	4. TITLE (and Subtitle) AIMABLE WARHEAD SAFING AND ARMING (S&A) DEVICE.	9	5. TYPE OF REPORT & PERIOD COVERED Final Report, June 1973 to December 1974
10	7. AUTHOR(s) Louis Vaida	15	6. PERFORMING ORG. REPORT NUMBER F08635-73-C-0144
	9. PERFORMING ORGANIZATION NAME AND ADDRESS FMC Corporation Defense Technology Laboratory 1400 North Burton Place Anaheim, California 92806	16	10. PROGRAM ELEMENT, PROJECT, TASK AREA & WORK UNIT NUMBERS Project No. 670A Task No. VII Work Unit No. 8247
	11. CONTROLLING OFFICE NAME AND ADDRESS Air Force Armament Laboratories Armament Development and Test Center Eglin Air Force Base, Florida 32542	11	12. REPORT DATE December 1974
	14. MONITORING AGENCY NAME & ADDRESS (if different from Controlling Office) 81p.		13. NUMBER OF PAGES 77
			15. SECURITY CLASS. (of this report) UNCLASSIFIED
			15a. DECLASSIFICATION DOWNGRADING SCHEDULE
16. DISTRIBUTION STATEMENT (of this Report) Distribution limited to U. S. Government agencies only; this report documents test and evaluation; distribution limitation applied December 1974. Other requests for this document must be referred to the Air Force Armament Laboratory (DLJF) Eglin Air Force Base, Florida 32542.			
17. DISTRIBUTION STATEMENT (of the abstract entered in Block 20, if different from Report)			
18. SUPPLEMENTARY NOTES Available in DDC.			
19. KEY WORDS (Continue on reverse side if necessary and identify by block number) Aimable Warhead Cylindrical Warhead Quadrifid Explosive Detonators Safing and Arming Device Target Detection Device (TDD)			
20. ABSTRACT (Continue on reverse side if necessary and identify by block number) The aimable warhead safing and arming device is an improved mechanism with the capability of selective multiple explosive output functions. Four independent explosive functions are electrically initiated which are physically separated 90 degrees about the cylindrical warhead's roll axis. The unique construction consists of a modified spheroid rotor designed to contain four quadrifid explosive detonators which can be fired individually, in pairs, in a complement of three, or salvo. The spherical rotor also provides means for rotor latching,			

UNCLASSIFIED

SECURITY CLASSIFICATION OF THIS PAGE(When Data Entered)

20. ABSTRACT (CONCLUDED)

→ cam functions, escapement (timing) drive, and electrical switching functions. This spherical rotor concept results in a physically balanced device which is insensitive to dynamic shock and vibration. ←

UNCLASSIFIED

SECURITY CLASSIFICATION OF THIS PAGE(When Data Entered)

PREFACE

The Engineering Design and Development Program for the Aimable Warhead Safing and Arming Device (AWSAD) was conducted by FMC Corporation, Micronics Department, Defense Technology Laboratories, 1400 North Burton Place, Anaheim, California 92806, under Contract F08635-73-C-0144 with the Air Force Armament Laboratory, Armament Development and Test Center, Eglin Air Force Base, Florida 32542. Mr. Richard B. Mabry, Jr. (DLJF) managed this development program for the Air Force Armament Laboratory. The program was conducted during the period from June 1973 to December 1974.

This technical report has been reviewed and is approved for publication.

FOR THE COMMANDER


WILLIAM F. BROCKMAN, Colonel, USAF
Chief, Munitions Division

SEARCHED	INDEXED
SERIALIZED	FILED
APR 1974	
FBI - MEMPHIS	
BY: [Signature]	
[] [] []	

TABLE OF CONTENTS

Section	Title	Page
I	INTRODUCTION	1
II	TECHNICAL DESCRIPTION	2
III	TEST PROCEDURES AND RESULTS	9
IV	CONCLUSIONS	16

LIST OF FIGURES

Figure	Title	Page
1	Aimable Cylindric Warhead (ACW)	17
2	Comparison of Dual and Single Detonator Initiation. . .	18
3	Aimable Warhead With AWSAD.	19
4	Cross Section of AWSAD.	20
5	AWSAD Functional Flow Chart (Motor Thrust for Complete Arming Cycle Mode).	21
6	Mechanical and Electrical Functional Diagram.	23
7	Aimable Warhead Safing and Arming Device Layout	25
8	AWSAD Functional Flow Chart - Short Burn Motor (Motor Thrust for Commit Time Period Mode)	29
9	Escapement and Driving Elements	31
10	Rotor Assembly With Timing Spring	32
11	Rotor Frame Assembly	33
12	Setback Weight Assembly	34
13	Solenoid Frame Assembly	35
14	Setback Weight Latch Linkage.	36
15	Commit and Pre-Arm Latch Linkage.	37
16	Forward Frame Assembly.	38
17	Safing and Arming Device, Components Array.	39
18	Rear View of Components Array	40
19	Front View of Components Array.	41
20	Bottom View of Safing and Arming Mechanism.	42
21	Side View of Safing and Arming Mechanism.	43
22	Top View of Safing and Arming Mechanism	44
23	Side View of Safing and Arming Device	45
24	Top View of Safing and Arming Device.	46
25	Bottom View of Safing and Arming Device	47
26	Acceleration Values Versus RPM for Centrifuge Tests . .	48
27	Fixture Orientation - Axial	49
28	Fixture Oriented for Loading.	50
29	Centrifuge Fixture in Axial Position.	51
30	Spring System Characteristics	52
31	AWSAD Acceleration Test No. 1	53
32	AWSAD Centrifuge Test No. 1	54
33	AWSAD Acceleration Test No. 2	55
34	AWSAD Centrifuge Test No. 2	56
35	Force Vectors at 45-Degree Lateral Centrifuge Test. . .	57
36	Acceleration Test Equipment Setup	58
37	Typical Oscilloscope Trace (0.02 Second/CM Sweep Rate).	59
38	Typical Oscilloscope Trace (0.10 Second/CM Sweep Rate).	60
39	Explosive Train Test Setup	61
40	Aimable Explosive Train, Test No. 1	62
41	Aimable Explosive Train, Test No. 2	63

LIST OF FIGURES (CONCLUDED)

Figure	Title	Page
42	Aimable Explosive Train, Test No. 3	64
43	Aimable Explosive Train, Test No. 4	65
44	Aimable Explosive Train, Test No. 5	66
45	Aimable Explosive Train, Test No. 6	67
46	Aimable Explosive Train, Test No. 7	68
47	Aimable Explosive Train, Test No. 8	69
48	Detail of Hydra Substrate Test Sample	70

LIST OF TABLES

Table	Title	Page
1	AWSAD Centrifuge Test No. 1 Results	71
2	AWSAD Centrifuge Test No. 2 Results	72
3	Measured Loads of Spring Functions	73

SECTION I

INTRODUCTION

The aimable cylindrical warhead (ACW) was developed under Air Force contract F08635-71-C-0019 and is documented in AFATL-TR-74-56 dated March 1974. The concept employs a fragmenting cylindrical case surrounding a cylindrical explosive charge as shown in Figure 1. To obtain the directional effects of Figure 2, available with this warhead, a safing and arming (S&A) device with four independent explosive outputs is required with the outputs radially side firing from the center of the device. The S&A explosive outputs must initiate the explosive hydra network without initiating the warhead's main charge. The hydra initiation network and associated boosters are detailed in AFATL-TR-74-56.

The objective of this phase of the aimable warhead safing and arming device (AWSAD) development was to determine the design and fabrication feasibility of an S&A device that would be compatible with the physical and functional requirements of the ACW. Because no missile system had been identified for ACW application, it was necessary to anticipate missile acceleration profiles and configure the AWSAD to properly function under the anticipated conditions. These conditions included arm during boost, arm at boost termination, arm after boost termination, and arm upon receipt of an externally generated electrical command, provided proper motor burn had occurred.

The AWSAD design selected consists of a spheroid rotor containing four independent detonators which end fire into four independent output leads to initiate selected quadrants of the ACW. The rotor is driven into line by a linear setback weight with both the setback weight and rotor being retarded by runaway escapements. The setback weight mechanism is a derivative of that utilized on the prototype AGM-65A safety, arming and fuzing unit. This setback mechanism establishes a driving force level to the rotor that is proportional to boost acceleration levels and incorporates a feature to allow the weight to be locked back at a variable position, thus maintaining the force level on the rotor even after boost fall-off. The detonator to be used as specified by the sponsor was the miniature precision detonator developed under contract F08635-73-C-0156 and documented in AFATL-TR-74-101 dated June 1974. This detonator is a redesigned USAF Microdetonator, P/N 66A11302, and will function within 10 microseconds with less than 1 microsecond jitter to provide the precision required for ACW arming. Independent solenoids lock the setback weight and rotor in the safe and armed position.

This document describes the AWSAD design and functional testing.

SECTION II

TECHNICAL DESCRIPTION

AWSAD TECHNICAL DESCRIPTION

General

The aimable warhead safing and arming device (AWSAD) is required in order to maintain the warhead in a safe condition until a proper sequence of dynamic and electrical inputs are sensed, at which time the AWSAD arms the warhead and responds to the electrical command inputs from an external fuze signal-processor unit.

In this program, the AIM-9L air-to-air missile was utilized to develop the motor thrust versus time profiles and to determine the warhead specifications and physical size requirements for the AWSAD engineering prototype. The objective for extending the use of this AWSAD to other missiles with similar size and weight requirements, including missiles with a high thrust and short-burn mission profile, was also realized.

The following technical description for the AWSAD includes an explanation of the mechanical and electrical functions of the mechanism. Figures illustrating the detail parts with their descriptive function and relative position and location are included for further clarification.

ACW/AWSAD Interface

The interface between the ACW and AWSAD is shown in Figure 3. The AWSAD is inserted into the S&A liner against the aft plug of the warhead aft enclosure. The end bell of the AWSAD is aligned by the guide pin in the forward closure. This alignment provides the registry between the output leads of the AWSAD and the corresponding input receptors of the hydra substrates illustrated in Figure 4. Singular or multiple substrates can be initiated by the AWSAD to produce the optimum propagation of the warhead fragmentation. The crossover charges at either end of the warhead provide explosive continuity independent of the direction of propagation.

AWSAD Functional Characteristics

The time-based sequence of events internal to the AWSAD is presented in Figure 5 for a mission profile which has motor thrust for the complete safe-to-arm cycle. This sequence is representative of one of the most complex possible but can be simplified dependent upon system parameters.

The intent-to-launch signal initiates the sequence and provides motor ignition. The AWSAD latching solenoid is energized, which frees the

setback weight and arming rotor (Figure 6). The resultant positive thrust due to proper motor ignition causes the setback weight to move aft relative to the latched position due to its own inertia.

The rate of movement of the setback weight is regulated by the damping escapement. At the same time, the return spring for sensing g-level loads is compressed, the rotor drive spring is loaded for rotational torque (energized), and the interlock rod moves aft. The interlock rod was designed to provide setback weight position intelligence to the electronic package area, if a specific application required such intelligence.

The setback weight extension actuates the commit lever which lifts the pre-arm lever and releases the arming rotor in conjunction with the latching solenoid action. By appropriate selection of stroke, cam rise and the setback weight damping escapement, this function corresponds to the specified commit timing. The arming rotor can then revolve at a rate determined by the torque applied by the timing spring and the regulation by the rotor escapement.

If missile power allocations are restrictive, the arming rotor is configured to operate an electrical switch which de-energizes the latching solenoid and causes the latch to ride on the periphery of the arming rotor. Through the mechanical linkage the setback latch lever is held out of engagement with the sawtooth rack of the setback weight. If power allocations permit, the solenoid would remain energized until arming; however, the arming rotor would prevent setback latching in the case of power failure.

The arming rotor continues to revolve at a rate proportional to the g-level load, and is arrested at the pre-arm position by the pre-arm lever against the pre-arm stop on the rotor. The time period from the start of rotation to the pre-arm position is equivalent to the specified arm time and corresponds to the missile's safe separation distance.

The arming rotor remains at the pre-arm stop position until an external electrical command again actuates the pre-arm solenoid coil. This command can be the output of an electronic timer or a direct output from the missile's guidance which could initiate or delay the arming function for a prescribed time period. The withdrawal of the pre-arm latch releases the arming rotor a second time and permits it to rotate with a snap action to the full arm position. The snap action of the arming rotor is due to its disengagement from the gear teeth of the rotor escapement. When the arming rotor is in the full arm position, it is locked into position by the latching solenoid lever, entering the stop position on the rotor and, through a mechanical linkage, the setback weight is locked by the latch setback lever.

Until the moment of the snap rotation of arming rotor, the setback weight and arming rotor are not latched and any decay in motor thrust below a specified g-level load will cause the setback weight to drive the arming rotor back to the original safe position through the setback weight extension's contact point with the rotor.

When the arming rotor is in the full-arm position, all electrical arming circuits to the four detonators are completed (closed). An electrical firing command from the missile's target detecting device to the associated quadrifid firing circuits will initiate the required detonator(s) to produce the optimum (aimed) warhead propagation.

The AWSAD can be recycled from the full-arm position to the safe position by simultaneously energizing both solenoid coils. (The g-level load must be less than that required to cause movement of the setback weight from the safe position.) With both solenoid coils energized, the arming rotor is free to return to the safe position due to the return spring force exerted against the rotor by the setback weight extension.

AWSAD Electrical Characteristics

The electrical input parameters were not defined for the electrical/mechanical interface for this program. Figure 6 illustrates a suggested schematic which could be used as a baseline for any future design considerations. It must be stressed that a definitive interface must be specified to integrate the electrical design with the mechanical parameters required.

In Figure 6, intent-to-launch command (+28 vdc) is applied to pin F of connector P1. Current flows through the normally closed switch S1 and energizes coil assembly K1. This operates the solenoid latch mechanism which unlocks the arming rotor and the setback weight. This circuit is completed to 28 vdc common at pin G. Diode CR1 blocks the current flow so that coil assembly K2 cannot be energized.

Input (+) power from pin F can pass through normally closed switch S2 to an indicator to show that the mechanism is in the safe position. When K1 is energized, S2 will open and provide a monitoring function at pin H that the arming function has been initiated.

Positive acceleration will cause the setback weight to move aft, loading the return spring and timing spring, and if the acceleration level is greater than the minimum commit level, the bias spring will also be compressed. Simultaneously the interlock rod causes switching poles S3 and S4 to transfer. Switch S3, illustrated as normally closed, opens the circuit to the target detector interlock at pins B and C. This could also be a circuit closing function if the target detecting device circuitry required it.

Switch S4 is an interlock to the electronic timer. This timer will not operate unless the setback weight has moved aft and closed switch S4.

The setback weight extension cams the commit lever and causes the pre-arm lever to unlatch the rotor. The compressed timing spring causes the rotor to rotate and transfers switches S1 and S5. The transfer of switch S1 causes the coil assembly K1 to de-energize and permit the rotor latch lever to ride on the periphery of arming rotor preventing the setback lever from engaging the setback weight. Electrical power from pin F can now pass through switches S1 and S4 and energize the electronic timer. The transfer of switch S5 closes the circuit from the timer to coil assembly K2. An input signal into the electronic timer to vary the arming point at pin D can pass through S5 and energize K2. If K2 is energized, the pre-arm stop position becomes inoperative and, at the end of the safe separation time period, the rotor will immediately snap to the full-arm position. Normally, the rotor would stop at the pre-arm position and the electronic timer would complete its function and energize the coil assembly to complete the arming rotor transfer.

A timer override function at pin E can be provided so that power applied at pin E would pass through switch S5 and energize coil assembly K2. This circuit could also be used if an electronic timer is not utilized.

The snap-to-arm rotation of the arming rotor closes switches S6, S7, S8, S9, and S10. Switches S6 through S9 are detonator circuit switches and switch S10 completes each circuit to common or ground return. With these switches closed, any combination of detonators can be fired.

Pin A of the connector provides an input for recycling the AWSAD. Applied voltage through CR1 and CR2 will operate the K1 and K2 coil assemblies simultaneously. With the solenoid coils energized, the setback weight will return the arming rotor to the safe position.

AWSAD Mechanical Characteristics

Figure 7 is a detail drawing of the AWSAD. The detail parts list which corresponds to the find numbers in Figure 7 is shown in the legend to Figure 7.

The unique feature of the AWSAD is the arming rotor (2) as illustrated in the Figure 7 plan view, Sections A-A, B-B, and E-E. It consists of a spherical aluminum quadrifid with provisions for four micro-detonators. Each detonator has a single bridgewire with a dual insulated output electrical lead configuration. The leads exit from the ends of the shaft (26) and are attached and soldered to the rotor switch. Two rotor switches, one at each end of the rotor shaft, are required to provide the switching circuitry illustrated in Figure 5. The rotor switches are held in place on the shaft (26) by retaining ring (±07). The rotor

switches and circuit boards were not fabricated since the electrical considerations were beyond the scope of this program.

The arming rotor also provides the structural support for the gear sector assembly (33) and the gear sector spring (37) which engages the rotor escapement assembly (17). The spring acts as gear clutch when the gear sector first re-engages the input pinion of the escapement during the recycle to the safe position. In addition, the spacers (59) and (62) and pin (60) are supported in the rotor periphery. This pin provides the attachment point for the spring guide link (75), spring guide (76), and timing springs (85). The spacers act as cam rollers against which the setback weight extension (20) bears.

The center section of the rotor is cut away, similar to a spool, in order to provide accessibility for all operating shafts (69), tubes (68), and levers (66) and (38), and the mounting for the plate cams (21) and (22). The pre-arm lever (66) engages the pre-arm plate cam (21) and the rotor latch lever (38) mates and operates in the latch plate (22).

The rotor frame (3) is the central module of the mechanism. The side plates (9) and (90) are mounted to the frame. The plates have flanged radial bearings (106) which support the rotor shaft (26). The rotor frame also holds the four housing leads (64) which contain the explosive propagation element between the detonator and the hydra receptor charge of the warhead. The flanged shoulder bushing (84) is pressed into the frame and acts as a bearing for the rotor latch tube (68).

The aft frame (4) mounts to the rotor frame (3) and also supports the escapement mounting block (18). The setback damping escapement (42) engages a rack (19) that is attached to the setback weight (1). The escapement regulates the rate of setback weight motion. The rotor escapement (17) engages the gear sector (33) and provides the regulation for the arming rotor rotation. The aft frame (4) and rotor frame (3) supports the setback weight guide rods (28) which support the setback weight (1). The setback latch lever (63) is attached to the shaft (69) and is supported by the mounting block (18).

The setback weight (1) provides a structural component for many elements. The guide rod bushings (77) are pressed in the weight to provide a relative frictionless slide bearing support. The setback weight extension (20) is pressed and staked in place, and supports the rotor timing spring system (76), (85), and (75). In addition, the bias spring (85), the plunger (67), and retaining screw (88) operate within the setback weight structure. The interlock rod (70) which passes through the rotor latch tube (68) is attached to the setback weight and moves forward into the electronic module package. The commit lever (65) is attached to the rotor latch tube (68) and is actuated by a cam rise machined on the setback extension (20).

Section D-D illustrates the method in which a single unitized frame (8) provides the magnetic path and plunger (39) support for both coil assemblies (81). A forward pivot plate (6) and an aft pivot plate (7) are mounted to the frame (8) and provide bearing supports (71) and (72) for the setback weight latch shaft (69) and the rotor latch tube (68). The appropriate clevises (73) and (74) are mounted on the shaft and tube and coupled to their respective solenoid plungers (39). The plates and frame also form a modular structural member connecting the rotor frame (3) and the forward frame (5).

The forward frame (5) has a mounting cavity for an electronic module which may contain the electronic timer or an interface termination with a component board assembly. An evacuation tube (80) is solder-sealed to the rear flange. The appropriate connector can be crimped and solder-sealed into place. The rear flange contains a notch on its periphery for engagement with the warhead forward closure alignment pin. The aft end of the forward frame has a sealing groove into which the AWSAD housing (82) could be roll-crimped and sealed. Sections F-F and G-G depict how the safe indicator windows (89) are solder-sealed to the AWSAD housing. Section F-F depicts the window viewing the rotor latch lever (66) engagement into the cam plate (21) and a safe-arm indicator on the periphery of the rotor.

Section G-G illustrates the viewing window over the setback weight (1) and latch (63) engagement.

The aft end of the housing (82) is roll-crimped and sealed over the aft frame cap (79). The cap has an extension on it which engages the warhead aft plug (Figure 3).

Optional Configurations/Capabilities

Several optional configurations are easily accomplished with the AWSAD design including the following:

(1) For an arm-during-boost-only application (i.e., AIM-9L), the serrations on the setback weight and lever and on the setback weight may be eliminated.

(2) For an application not requiring the capability of external arming, one solenoid (81), the shaft latch clevis (73), and the rod interlock (70) may be eliminated.

(3) Operation as a timer. If the missile system parameters allow time to be utilized as the arming criteria (provided proper boost occurs), the input pinion rack setback weight (19), the escapement assembly setback weight (42), the serrations on the setback weight and

lever setback weight (63), the plunger setback weight (67), and associated spring may be eliminated.

Figure 8 illustrates the functional capability of the AWSAD when utilized in a missile with a high thrust, short burn propellant motor. The primary difference in this mission profile is that the positive acceleration for arming only lasts for a period equivalent to the commit time rather than for the complete arming function. In this mode, the setback weight can be latched in the aft position, proportional to the thrust level imposed, immediately after the commit time. A decay in thrust or motor burnout will not affect the arming function. All other functional operating characteristics are identical. The pre-arm cam plate (21) and the rotor switch would require modification to operate in this mode.

Figures 9 through 25 illustrate the detail parts with their relative position and location.

SECTION III

TEST PROCEDURES AND RESULTS

The testing efforts on this program included both acceleration tests to simulate a missile's dynamic environment for fuze arming and explosive train tests to demonstrate the capability of the AWSAD to detonate the ACW through the hydra substrate interface.

ACCELERATION (CENTRIFUGE) TESTING

Prior to conducting the centrifuge acceleration testing, calculations were made to determine the required rotational speeds of the centrifuge for their corresponding values of acceleration. The rotational speed, revolutions per minute (rpm), determines the acceleration sensed by the AWSAD specimen in the centrifuge test fixture. The radius from the center of rotation for the centrifuge to the center of mass of the AWSAD setback weight was measured as 20.25 inches. The applicable formula is $g = 2.842 RN^2/10^5$ where R is the radius and N is rpm. Figure 26 lists the values of rpm and resultant acceleration calculated for use during this test series.

Figures 27, 28, and 29 show the test fixture and the loaded test fixture in the centrifuge for these tests.

Tables 1 and 2 provide the data obtained on Centrifuge Tests No. 1 and No. 2 series. It should be stressed that the AWSAD did not pre-arm until a minimum acceleration level of 16g was attained. This value of g-load corresponds to a point just beyond the commit stroke level illustrated in Figure 30.

Since the AWSAD prototype had no electrical circuitry for sensing operating functions, an audio sensing setup was devised to determine the setback weight movement, escapement activity, etc. A time signal trace was initiated on an oscilloscope by a sound pickup (transducer) fixed to the frame of the test specimen.

At levels of 8, 10.5, and 12g, the setback weight had moved aft but the g force was not great enough to drive the commit lever up the cam rise to release the arming rotor. At 16g, the commit lever was actuated and the rotor lock lever released the arming rotor, permitting its rotation to the pre-arm position.

Table 3 gives the numerical spring system characteristics shown in graphical form in Figure 30.

Figures 31 and 32 are acceleration versus time curves plotted for the centrifuge test data. Figure 31 indicates that a three-element,

0.050-inch-thick aluminum pallet lever on the damping escapement results in a commit time in the range of 0.07 to 0.09 second. The pre-arm time agrees with the escapement distance integration curve, $S = 1/2at^2$,

where S = safe separation distance in feet

a = g level x 32.2 ft/sec/sec

t = time in seconds

Refer to Table 1. Example:

1st Case: g-level is 16.1g

Time is 0.86 second

$$S = \frac{16.1 \times 32.2 \times (0.86)^2}{2} = 191.7 \text{ feet}$$

or approximately 190 feet

2nd Case: g-level is 25.4g

Time is 0.68 second

$$S = \frac{25.4 \times 32.2 \times (0.68)^2}{2} = 189.1 \text{ feet}$$

or approximately 190 feet

Figure 32 shows the data from the first series of tests plotted on logarithmic graphs to illustrate the time span and differential from commit time to pre-arm time, using the three-element damping escapement and the four-element rotor time escapement.

The second series of tests were conducted in which the escapements were exchanged in the safing and arming mechanism. A four-element, 0.050-inch-thick aluminum pallet lever was used in the damping escapement, and the pallet lever in the four-element rotor time escapement was a 0.100-inch-thick brass configuration. The objective was to determine the effect on the timing parameters with no alteration to the spring-mass system of the setback weight and arming rotor.

Table 2 presents test data obtained on the second series of centrifuge runs. The commit time and pre-arm time were obtained from one oscilloscope trace. Figures 33 and 34 are acceleration-time curves plotted to represent the centrifuge-time trace data. Figure 33 indicates that a four-element, 0.050-inch-thick aluminum pallet lever in the damping escapement results in a commit time that represents a constant separation distance with respect to the setback weight acting as an integrating mass sensor. The curve will not be true to the theoretical curve since a small amount of energy is dissipated to release the rotor latch and operate the

commit lever by the cam rise of the setback weight extension. The commit time ranged from 0.5 second at 30.4g to 0.8 second at 16.6g. Applying the safe distance integration equation, $S = 1/2at^2$, these times result in a minimum separation distance of 123 feet and a maximum of 171 feet. The pre-arm curve using a four-element escapement with a 0.100-inch-thick brass pallet lever also illustrates a safe distance integrating trend indicative of a recoil pallet lever escapement. From the respective curves, it appears that both the arming rotor timing springs reached their maximum deflection at 25.4g since the time obtained at 30.4g was equal to that at 25.4g. Application of the distance integration equation, $S = 1/2at^2$, to a number of points below 25g results in a satisfactory correlation:

$$S_{25.37g} = 1/2 \times 25.37 \times 32.2 (1.60)^2 = 1,044 \text{ feet}$$

$$S_{20.12g} = 1/2 \times 20.12 \times 32.2 (1.76)^2 = 1,003 \text{ feet}$$

$$S_{16.63g} = 1/2 \times 16.63 \times 32.2 (1.84)^2 = 906 \text{ feet}$$

The acceleration time data from Table 2 was plotted on logarithmic chart paper in Figure 34. The time span and differential from commit time to pre-arm time is readily discernible.

Comparing Figure 32 to Figure 34 indicates the time variation and flexibility inherent in the design of the AWSAD mechanism. The commit time may be varied from approximately 0.08 second to 0.80 second, a factor of ten, by changing pallet levers and/or escapement gear ratios (three-element versus four-element). Pre-arm time was altered from 0.80 second to 1.8 seconds, a factor of 2.25, by changing pallet lever weights only. As shown, a longer pre-arm time can be obtained by increasing the pallet lever mass, and a much longer pre-arming time can be obtained by decreasing the rotor drive torque or changing the spring rate.

An additional experiment was conducted during each test series. A 45-degree lateral centrifuge run was conducted. The specific lateral acceleration versus time value is noted on each of Figures 31, 32, 33, and 34. The lateral run consisted of pre-positioning the fixture at 45 degrees to the normal axis with respect to the center of rotation of the centrifuge. At a rotational speed of 230 rpm or centrifugal force of 30.4g, the equivalent axial and lateral components of force are both equal to 21.5g at 45 degrees. Figure 35 presents the rationale for the test setup.

Figures 31 and 33 show that the lateral run times for the commit function fall within or near the equivalent abscissa point of each curve. An ordinate of 21.5g is used in each case; the three-element is 0.080 to 0.085 second and the four-element is 1.60 seconds. The small degree of variation indicates that the lateral load on the setback weight system was minimal.

The lateral results for the pre-arm times indicated a greater deviation from the curve for the axial runs. The four-element, 0.062-inch-thick lever escapement obtained a time of 0.81 second compared to the curve reading of 0.72 second.

The four-element 0.100-inch-thick brass lever escapement obtained a time of 2.1 seconds compared to the curve reading of 1.69 seconds.

The greater deviation of the pre-arm lateral runs can be attributed to the fact that the arming rotor of the prototype unit was not dynamically balanced. The lateral force produces a side load and couple on the bearing supports because of this imbalance.

The test equipment used during the acceleration time tests is listed in Figure 36. Photographs were taken of the oscilloscope trace obtained from the transducer pickup of the escapement operation. Figures 37 and 38 illustrate the typical trace obtained. Figure 37 reflects the use of a 0.02 second per centimeter sweep rate for the oscilloscope. The commit time is read from the beginning of the trace at point A to the start of the decay of the first amplitude level at point B. The solenoid energization of the setback weight latch starts the trace. The broad amplitude section of the trace is the hard driving audio sound of the damping escapement as the setback weight moves aft. The commit lever then is cammed up by the cam rise on the setback weight extension and the damping escapement amplitude drops off as the setback weight comes to rest. Actuation of the commit lever lifts the rotor latch and permits the arming rotor to rotate. The timing springs provide the torque and the gear sector drives the rotor time escapement. Figure 38 illustrates the pre-arm time from point A at the start of the trace to point C at the end of the trace. The commit time is also indicated at point B. The sweep rate of the oscilloscope is 0.10 second per centimeter in order to encompass the full pre-arm time interval.

These tests illustrate the flexibility of the basic design to provide the capability of adapting the AWSAD to any missile mission profile requirement.

EXPLOSIVE TRAIN TESTS

These tests were relevant to the explosive components included in the AWSAD design and the propagation of the explosive output through the warhead interface.

These tests provide a baseline configuration for design proof of a future number of explosive train tests to establish confidence in the safety and performance reliability of the AWSAD.

The explosive components consisted of:

(1) Microdetonator - This item was specified by the procuring agency. A complete AWSAD requires four microdetonators. One microdetonator was used in each of the tests.

(2) Case Lead - The case lead, when aligned with the microdetonator, provides an explosive output from the AWSAD to the warhead. The case leads are retained in a fixed position in the housing.

(3) Hydra Assemblies - Hydra assemblies are incorporated into the warhead with four inputs that align with the AWSAD outputs for quadrant selected initiation of the warhead.

In addition to the explosive components, hardware items were used to simulate the air gaps, barriers and dimensional interfaces.

The test equipment utilized for these tests is illustrated in Figure 39.

TEST CONFIGURATION-TEST NO. 1

A dent block test was conducted to provide visible evidence of the microdetonator and case lead explosive effects. The test configuration is shown in Figure 40 with a dent block.

Test Results

High order output for the microdetonator and lead was evident. Dent block evidence indicated a marginal condition with respect to the ability of the output to initiate the warhead hydra. No comparison dent block values were available for more detail analysis.

TEST CONFIGURATION-TEST NO. 2

The test configuration is shown in Figure 41 with a hydra assembly.

Test Results

Output from the microdetonator and lead was inadequate to initiate the hydra assembly. Explosive material in the V-shaped receptor area of the hydra was blasted out by the lead output with metal particles from the housing and liner simulators.

TEST CONFIGURATION-TEST NO. 3

The test configuration is shown in Figure 42. The microdetonator was mounted directly in contact with the AWSAD housing simulator, eliminating the case lead.

Test Results

High order detonation of the hydra input was evident. Propagation to the right leg of the hydra was uniform. Propagation of the left leg diminished as the detonation progressed to the left, indicating a possible inconsistency in hydra explosive density.

TEST CONFIGURATION-TEST NO. 4

Test No. 4 was a repeat of Test No. 2 to establish a second indication of the insufficient lead output in the event that a marginal condition existed. Figure 43 shows the test configuration.

Test Results

Results of this test were identical to Test No. 2.

TEST CONFIGURATION-TEST NO. 5

Test No. 5 was conducted using a hydra assembly as shown in Figure 44, except that the 0.100-inch-diameter end of the output lead was reversed to interface with the AWSAD housing simulator.

Test Results

Hardware used in Test No. 5 and the results of the detonation of the microdetonator and explosive train are shown in Figure 44. High order detonation of all explosive components was evident with uniform propagation of both legs of the hydra. Input to the hydra in this test is considered more violent and broader in penetration than desired and could cause warhead detonation at the interface.

TEST CONFIGURATION-TEST NO. 6

Components were assembled as shown in Figure 45 with a 0.062-inch-diameter case lead bore diameter with a 0.100-inch-diameter receptor end.

Test Results

As shown in Figure 45, high order uniform propagation of the explosive components was evident. The case lead bushing split in half causing a distortion of the output and a greater disruption at the hydra interface than desired.

TEST CONFIGURATION-TEST NO. 7

Test No. 7 was the same configuration as Test No. 6 except for the lead where a lead bore diameter of 0.052 inch was used. Figure 46 shows the test configuration.

Test Results

As shown in Figure 46, propagation of all explosives occurred. The lead bushing remained intact and produced a well-defined output into the hydra with a minimum of distortion. High order detonation of the hydra was evident. The end of the left leg was evidently of low density or contained a void causing the propagation to terminate prior to the end of the leg.

This configuration is considered to be close to an optimum design for the AWSAD.

TEST CONFIGURATION-TEST NO. 8

A test configuration as shown in Figure 47 was assembled to demonstrate the effects of the explosive configuration established in Test No. 7 when contained within the warhead explosive. To simulate this condition, the hydra was encased in an aluminum mold housing and filled with plaster of paris. Two RTV rubber attenuators were cemented, one on each side, to the hydra to absorb detonation energy adjacent to the hydra input (Figure 48).

Test Results

High order detonation of all explosives was evident as shown in Figure 47. Dents were evident in the mold housing where the ends of the hydra legs contacted the housing. A bulge in the housing was evident for the full diameter of the housing due to compression of the plaster of paris.

One side of the housing was milled to provide a window to examine the effect of the hydra. As would be expected, the plaster of paris was disintegrated causing a tunnel effect on the foil side of the hydra.

The attenuators were very effective in containing the simulated output of AWSAD.

SECTION IV

CONCLUSIONS

Based on the AWSAD design developed during this effort and the results of the preliminary testing performed, the following conclusions are made:

1. A safety and arming device which is compatible with the physical and functional characteristics of the aimable cylindrical warhead is feasible.
2. The safety and arming device can be adapted to arm either during boost, at boost fall termination, after boost, or upon electrical command.
3. The safety and arming device can be simplified if the device is optimized for a particular missile acceleration profile.
4. The S&A to warhead explosive train interface is the greatest risk area in any future development.

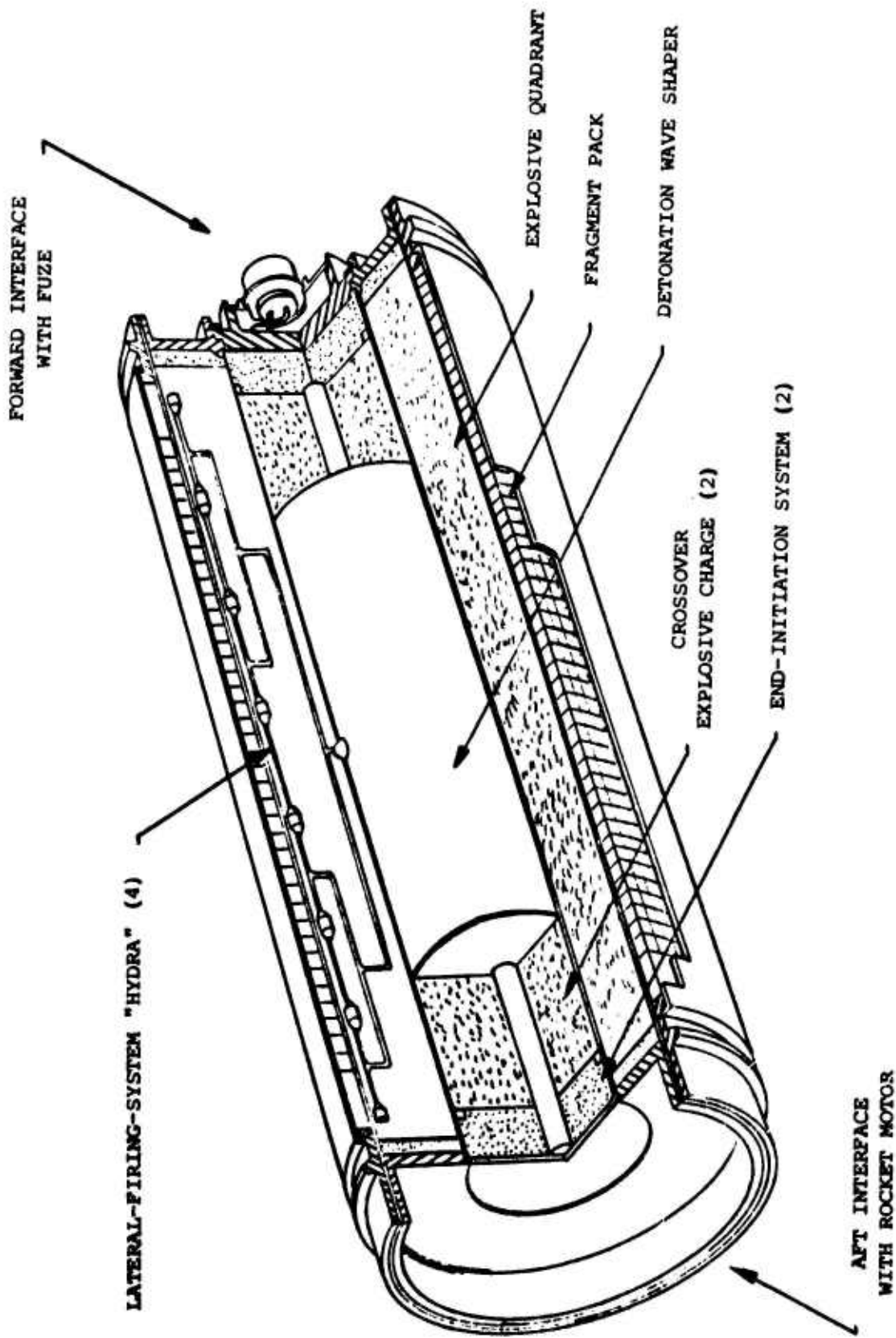
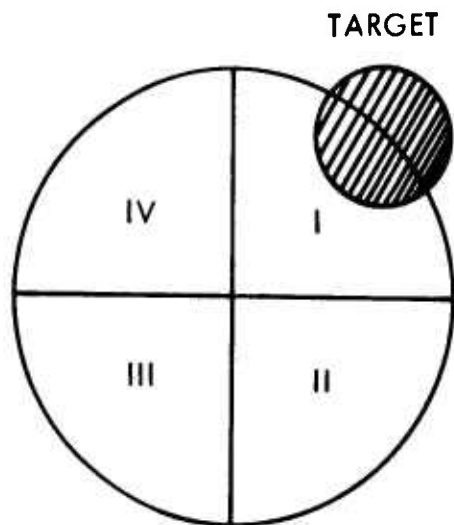
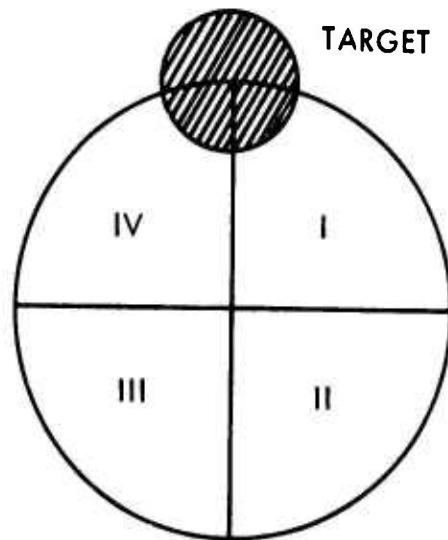


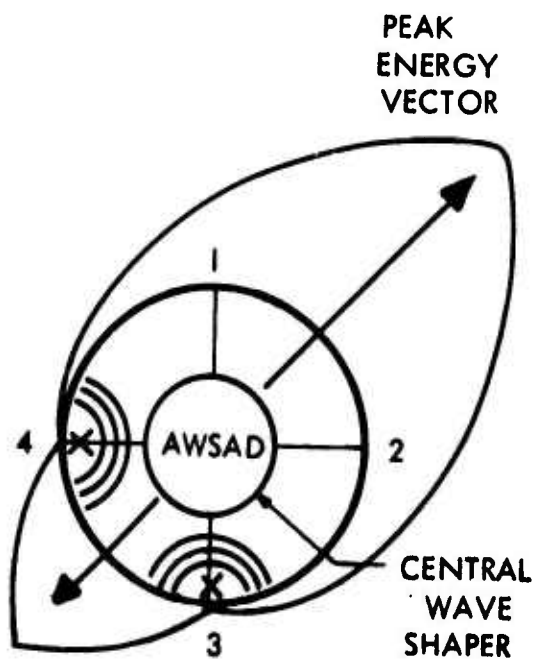
Figure 1. Aimable Cylindrical Warhead (ACW)



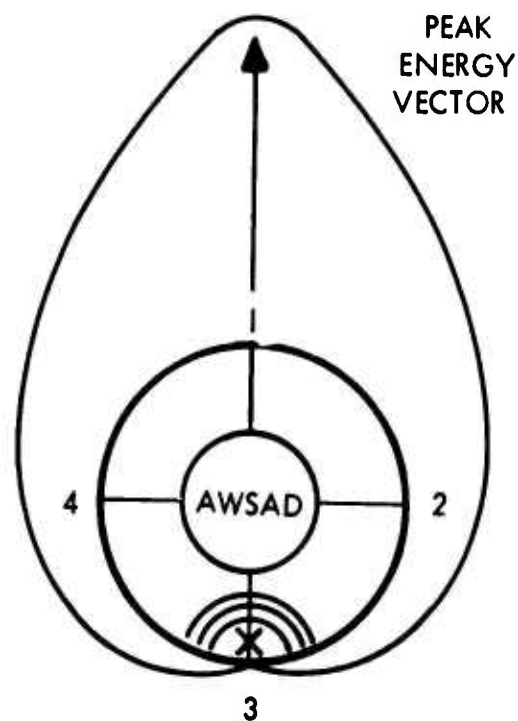
FOUR 90-DEG TARGET-DETECTOR SCANNING SECTORS. TARGET IN SECTOR I.



TARGET DETECTED SIMULTANEOUSLY IN SECTORS I AND IV.



DUAL-LINE ASYMMETRICAL INITIATION AT DETONATORS 3 AND 4.



SINGLE-LINE ASYMMETRICAL INITIATION AT DETONATOR 3.

Figure 2. Comparison of Dual and Single Detonator Initiation

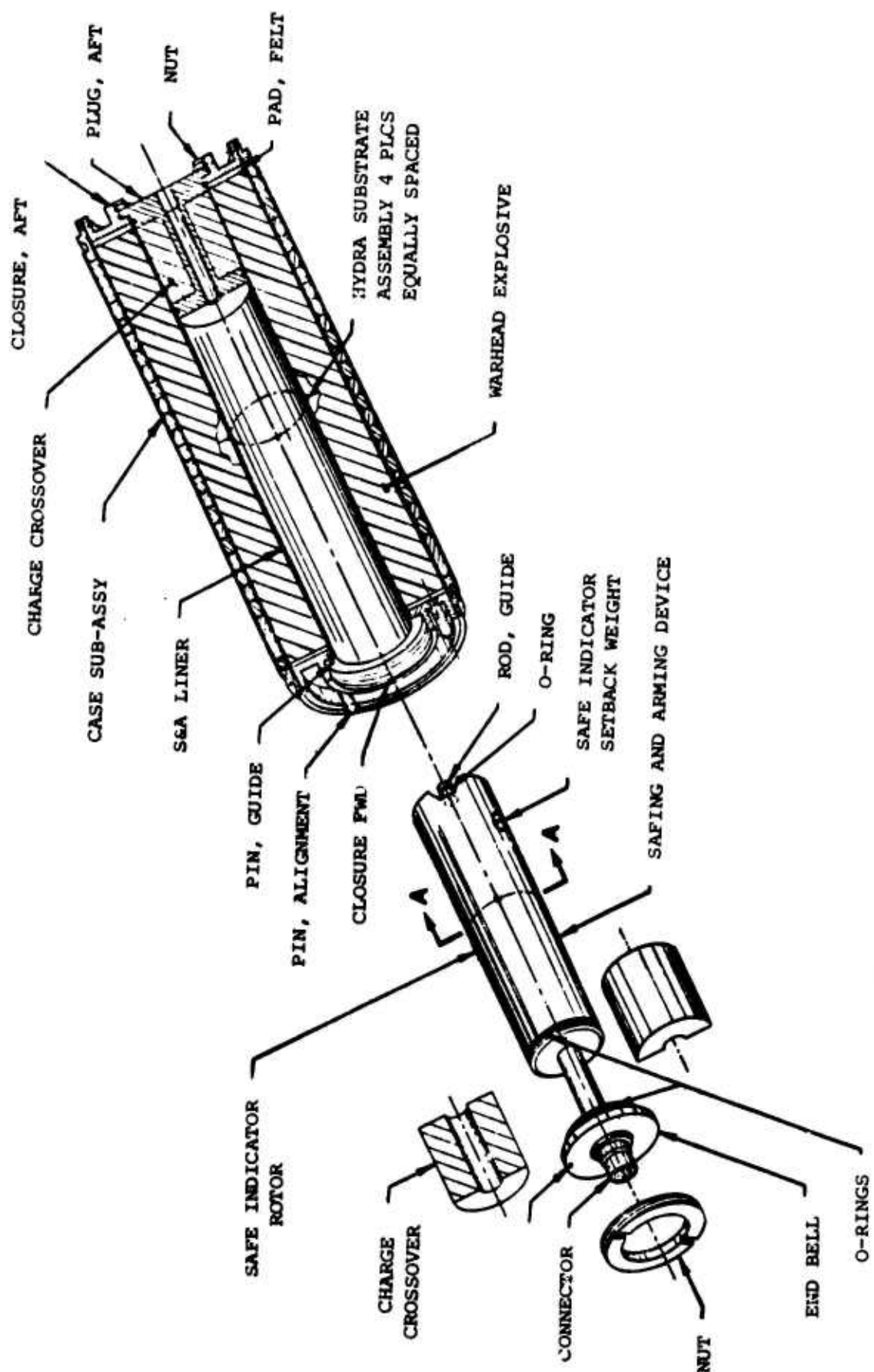


Figure 3. Aimable Warhead with AWSAD

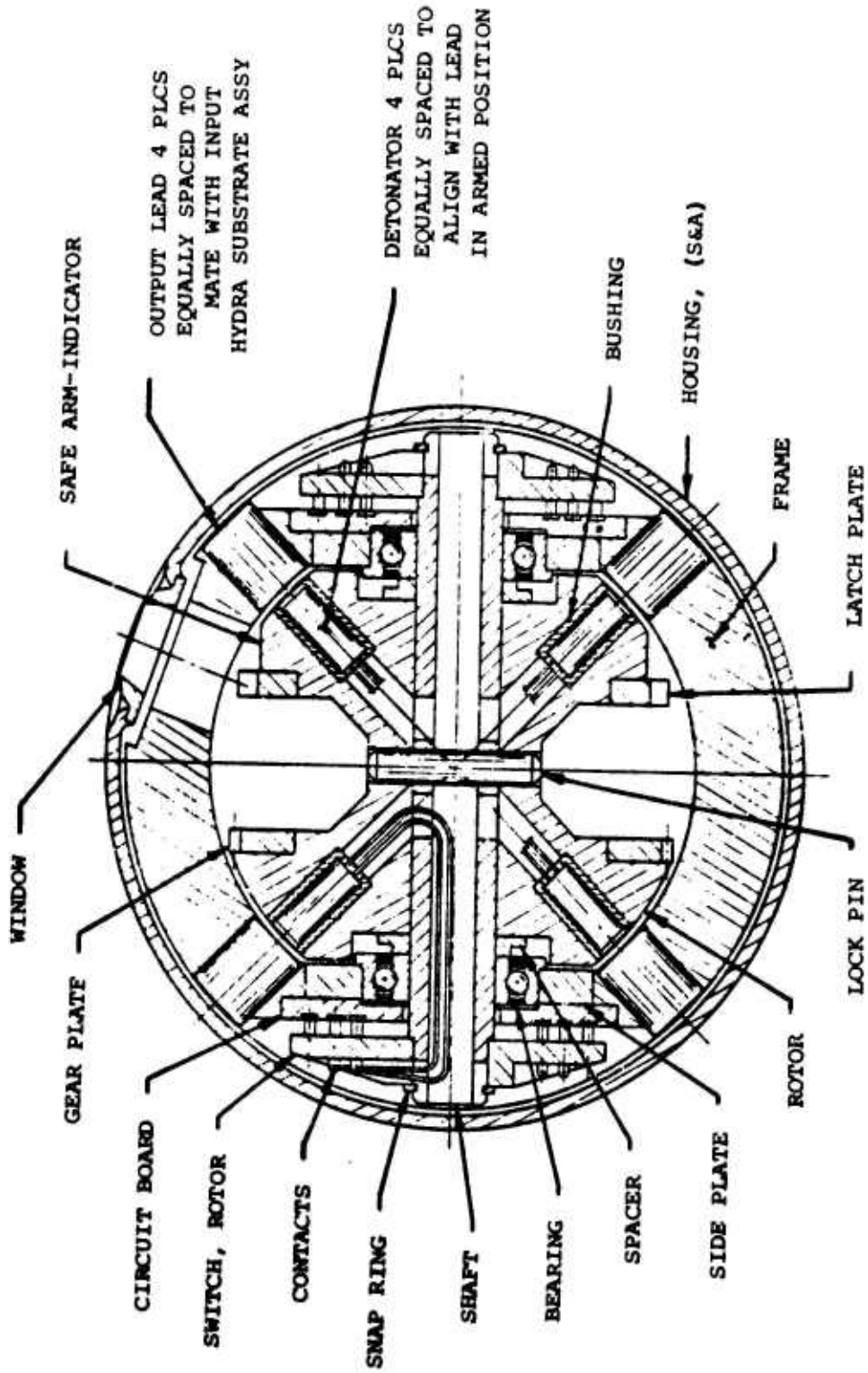
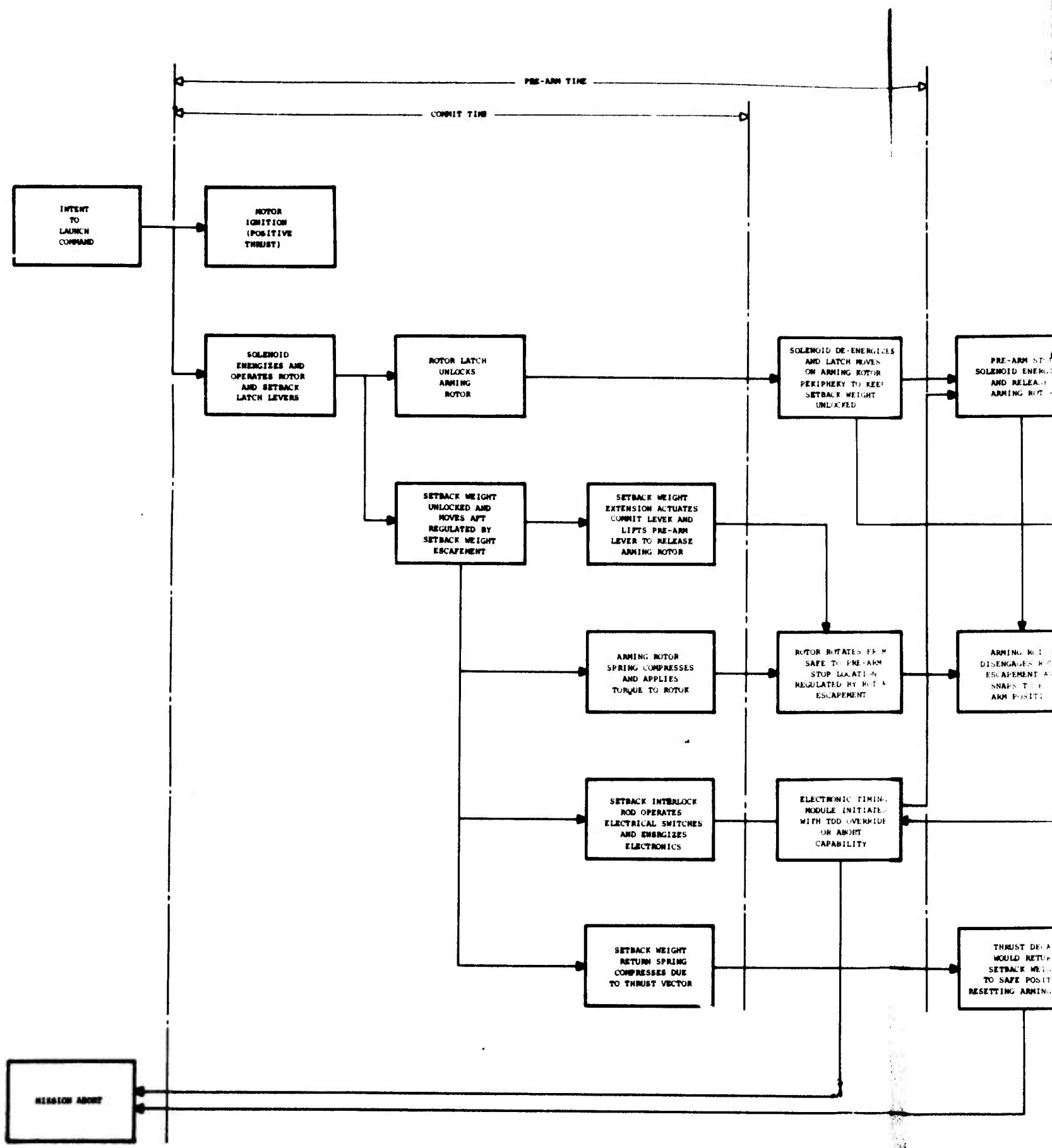
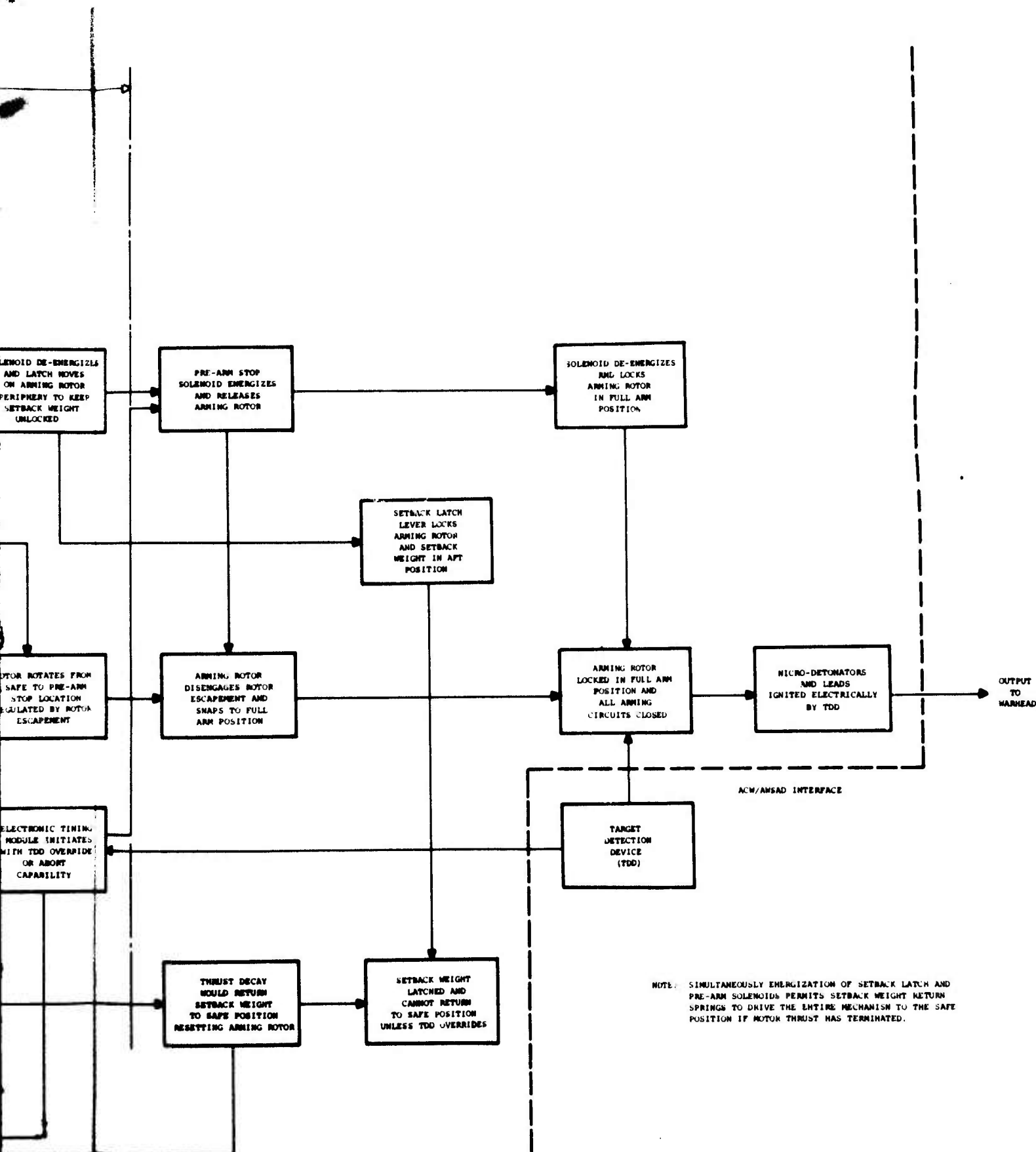


Figure 4. Cross Section of AWSAD

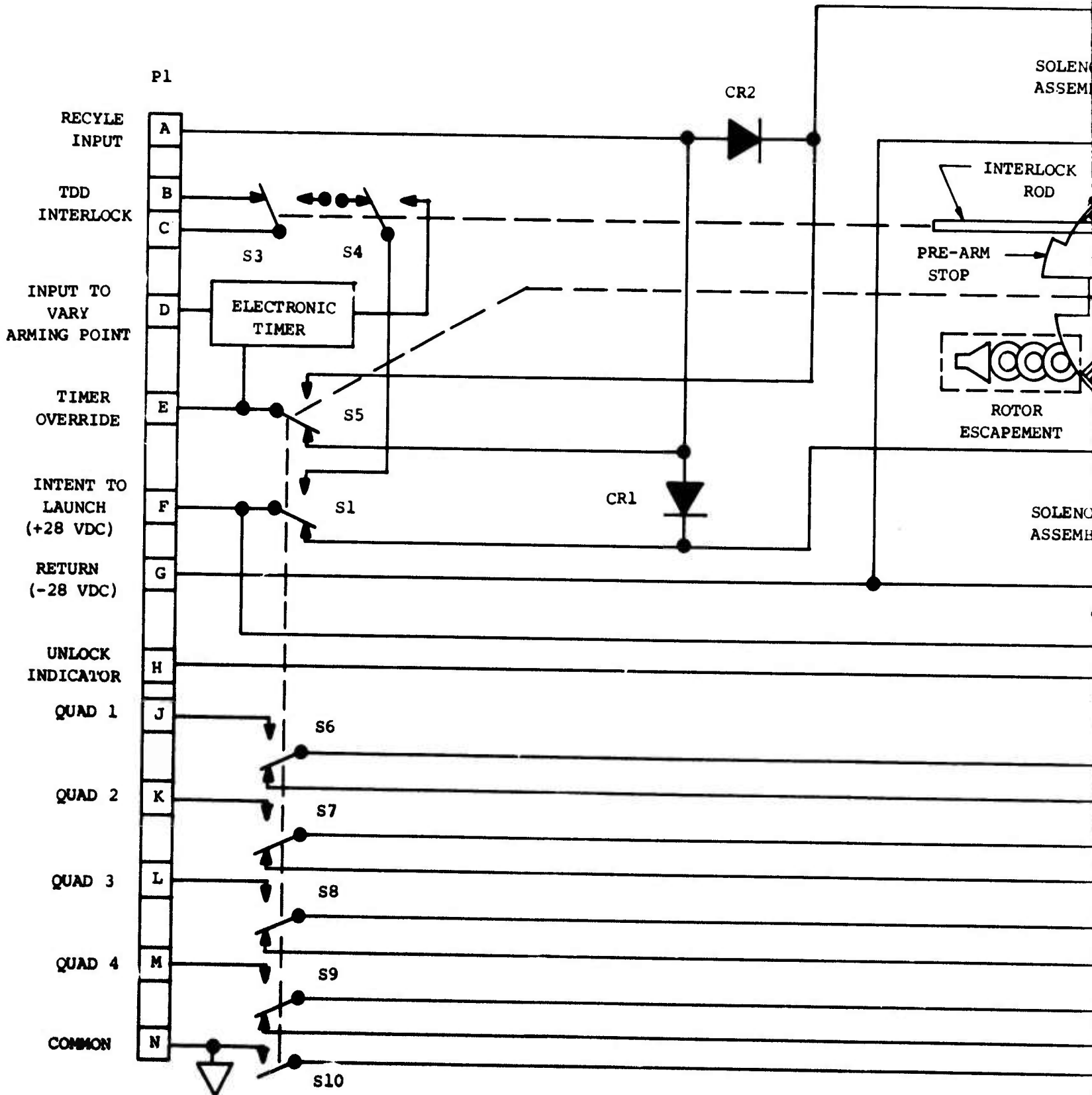




NOTE: SIMULTANEOUSLY ENERGIZATION OF SETBACK LATCH AND PRE-ARM SOLENOIDS PERMITS SETBACK WEIGHT RETURN SPRINGS TO DRIVE THE ENTIRE MECHANISM TO THE SAFE POSITION IF ROTOR THRUST HAS TERMINATED.

Figure 5. AWSAD Functional Flow Chart (Motor Thrust for Complete Arming Cycle Mode)

2



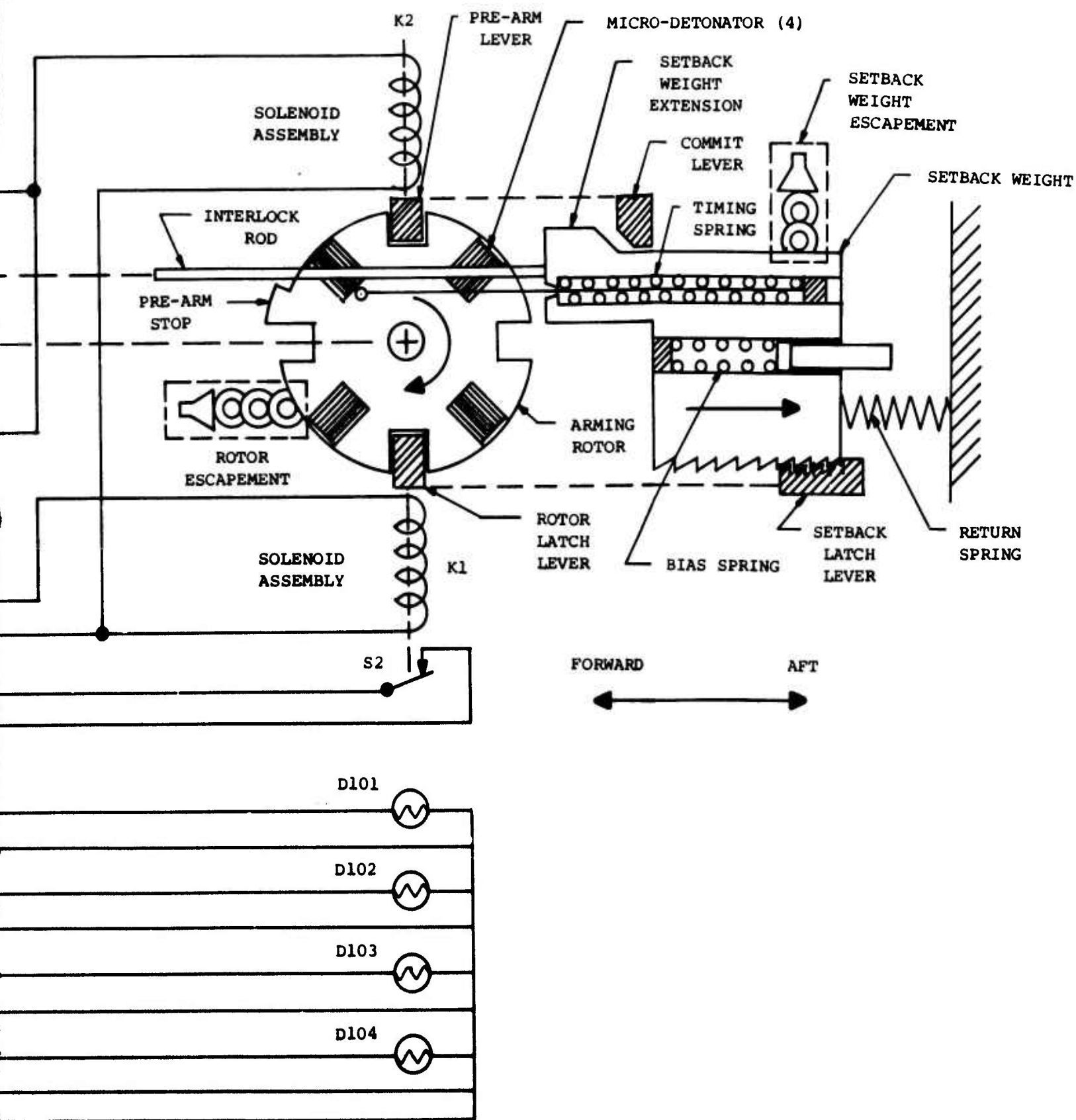
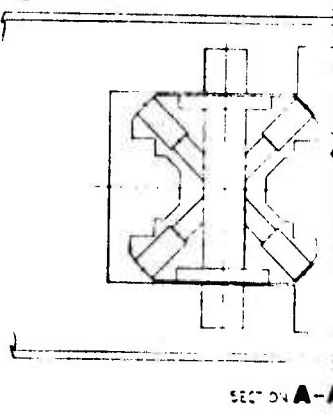
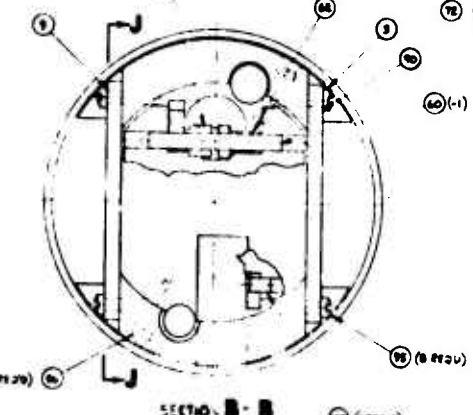
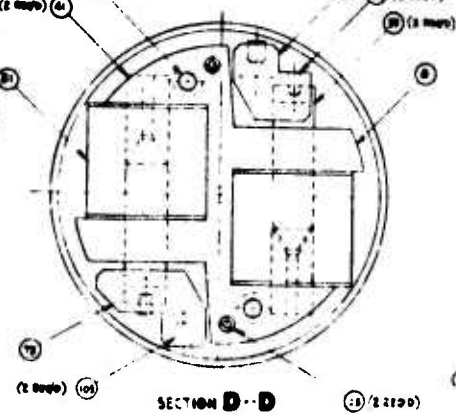
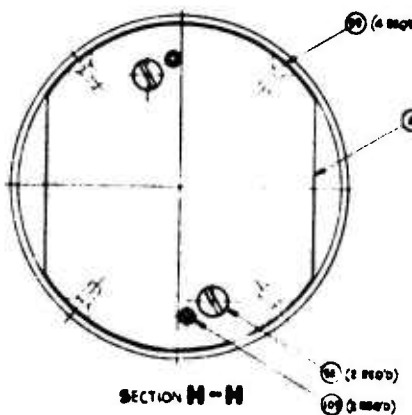
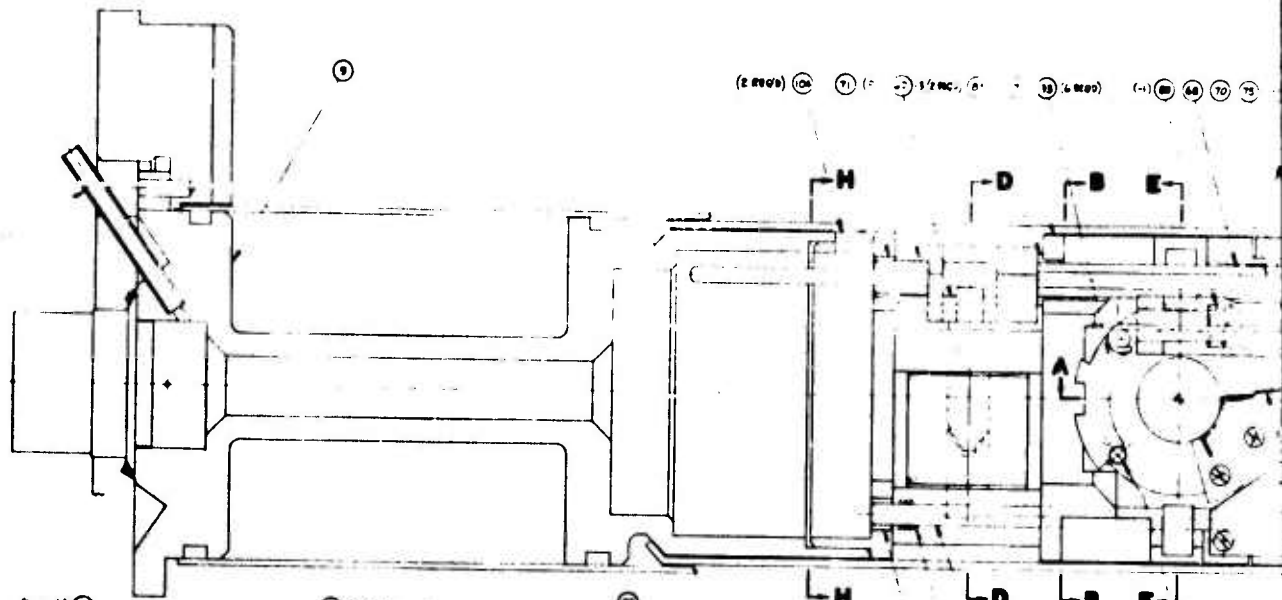


Figure 6. Mechanical and Electrical Functional Diagram

2



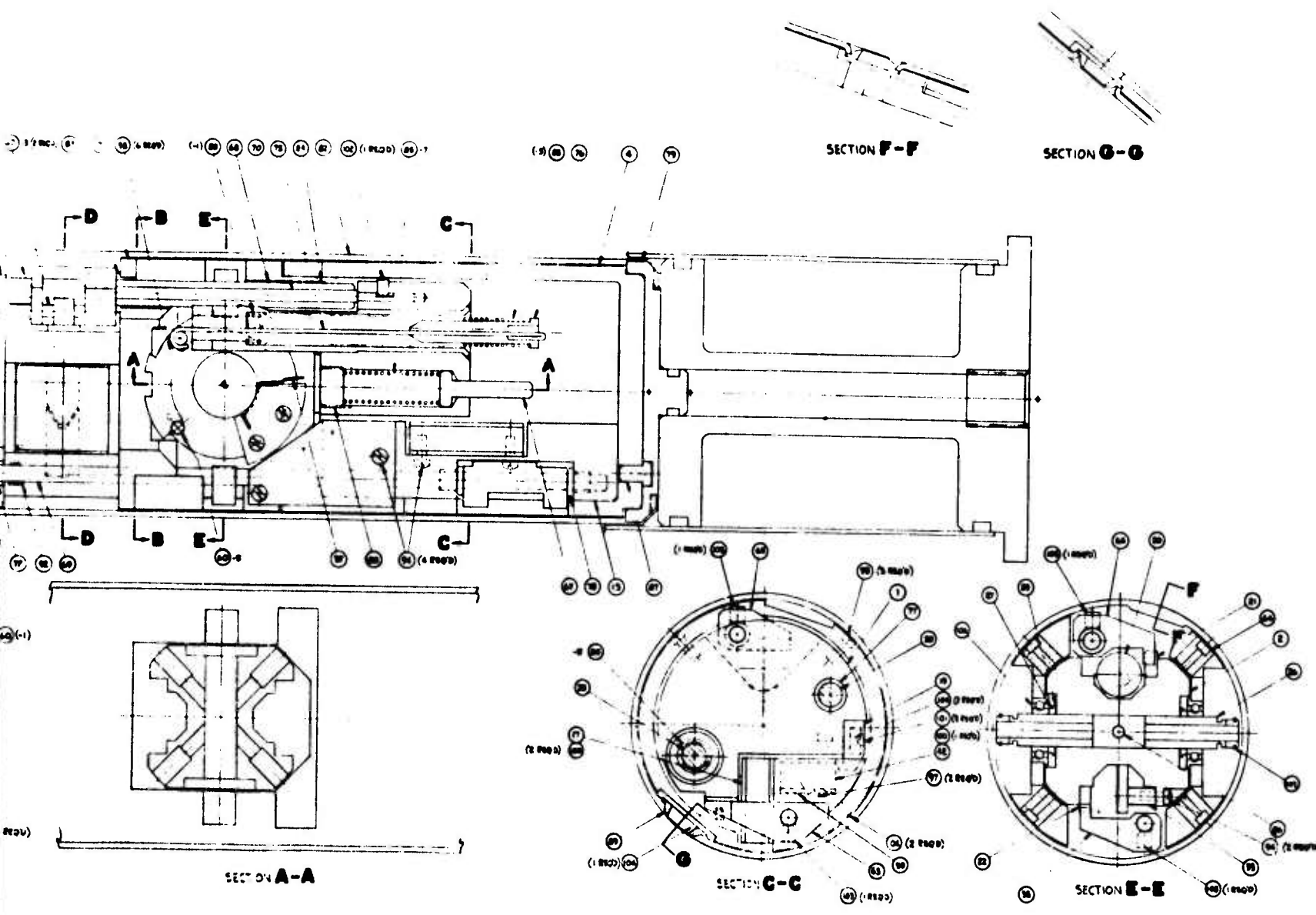


Figure 7. Aimable Warhead Safing and Arming Device - Layout

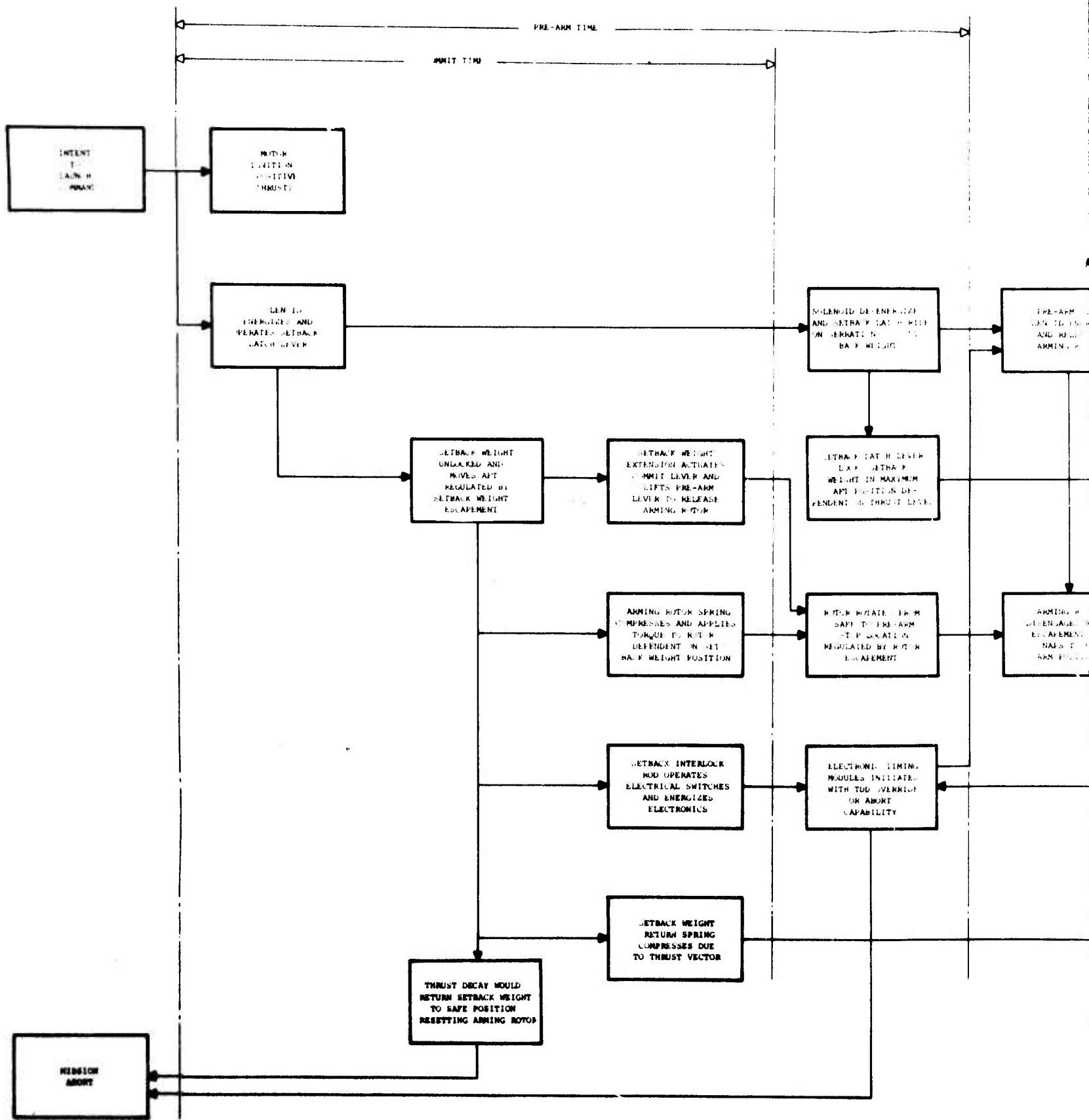
2

LEGEND (Figure 7)

1	Weight, Setback	30	Standoff, Gear Sector
2	Rotor, Arming	31	Plate Assembly, Rotor Escapement - Bottom
3	Frame, Rotor	32	Plate Assembly, Rotor Escapement - Top
4	Frame, Aft	33	Gear Sector Assembly
5	Frame, Forward	34	Gear, Escape - Rotor
6	Plate, Pivot-Forward	35	Pinion, Escape - Rotor
7	Plate, Pivot-Aft	36	Gear Escapement Assembly - Rotor
8	Frame, Solenoid	37	Spring, Gear Sector
9	Plate, Side-Rotor Frame	38	Lever, Rotor Latch
10	Plate, Rotor Escapement-Top	39	Plunger, Solenoid
11	Plate, Rotor Escapement-Bottom	40	Bobbin, Solenoid
12	Gear, Spur - Intermediate	41	Pole, Solenoid
13	Gear, Pinion - Intermediate	42	Escapement Assembly - Setback Weight
14	Gear & Pinion - Intermediate	43	Lever Assembly
15	Lever Assembly	44	Gear & Pinion Assembly - Input
16	Lamina, Pallet Lever	45	Gear & Pinion Assembly - Setback Weight
17	Escapement Assembly, Rotor	46	Pillar, Escapement - End
18	Block - Escapement Mounting, Aft Frame	47	Pillar, Escapement - Center
19	Rack - Input Pinion, Setback Weight	48	Plate, Escapement - Top
20	Extension, Setback Weight	49	Plate, Escapement - Bottom
21	Plate Cam, Pre-Arm	50	Shaft, Lever
22	Plate, Latch	51	Lever
23	Gear Sector	52	Spacer, Lever
24	Pillar No. 2, Escapement	53	Pallet, Lever
25	Pillar No. 1, Escapement	54	Gear, Pinion - Input
26	Shaft, Rotor Arming	55	Gear, Spur - Input
27	Spacer, Rotor Arming	56	Gear, Escapement
28	Guide Rod, Setback Weight		
29	Shim, Rotor Arming		

LEGEND (Figure 7) (Concluded)

57	Gear, Pinion - Setback	87	Pin, Alignment, Housing
58	Shim, Escapement	88	Screw, Plunger, Setback
59	Spacer, Rotor Pin-Plate	89	Frame, Window
60	Pin	90	Plate - Side, Rotor Stop
61	Insulator, Coil	91	Spring, Clevis, Rotor
62	Spacer, Rotor Pin	92	Spring, Clevis, Latch
63	Lever, Setback Latch	93	#1-72 UNF x 1/8 Fil Hd Scr
64	Housing, Lead	94	#1-72 UNF x 3/16 Fil Hd Scr
65	Lever, Commit	95	#2-56 UNC x 3/16 Pan Hd Slot Scr
66	Lever, Rotor, Pre-Arm	96	#2-56 UNC x 5/16 Pan Hd Slot Scr
67	Plunger, Setback Weight	97	#4-40 UNC x 3/16 Pan Hd Slot Scr
68	Tube, Rotor Latch	98	#4-40 UNC x 1/4 Pan Hd Slot Scr
69	Shaft, Setback Weight Latch	99	#2-56 UNC x 3/16 F1 Hd Slot Scr
70	Rod, Interlock	100	#0-80 UNF x 1/8 F1 Hd Slot Scr
71	Bushing, Large Pivot Plate	101	#4-40 UNC x 1/4 Soc Hd Cap Scr
72	Bushing, Small Pivot Plate	102	#2-56 UNC x 1/8 Soc Set Cup Pt
73	Clevis Shaft, Latch	103	#4-40 UNC x 1/8 Soc Cup Pt
74	Clevis Shaft, Rotor	104	1/16 Dia x 1/4 Lg Pin, Spring, Tub Sl
75	Link, Guide Spring	105	3/32 Dia x 1/4 lg Pin, Spring Tub Sl
76	Guide, Spring	106	Radial Retainer Flanged Open Bearing
77	Bushing, Setback Weight	107	External Series Retaining Ring
78	Bushing, Escapement Mounting Block		
79	Cap, Pin - Aft Frame		
80	Tube, Evacuator		
81	Coil Assembly		
82	Housing		
83	Clevis Spacer Flanged Bushing		
84	Bushing, Shoulder, Frame Rotor		
85	Spring Compression		
86	Pin, Rotor Shaft		



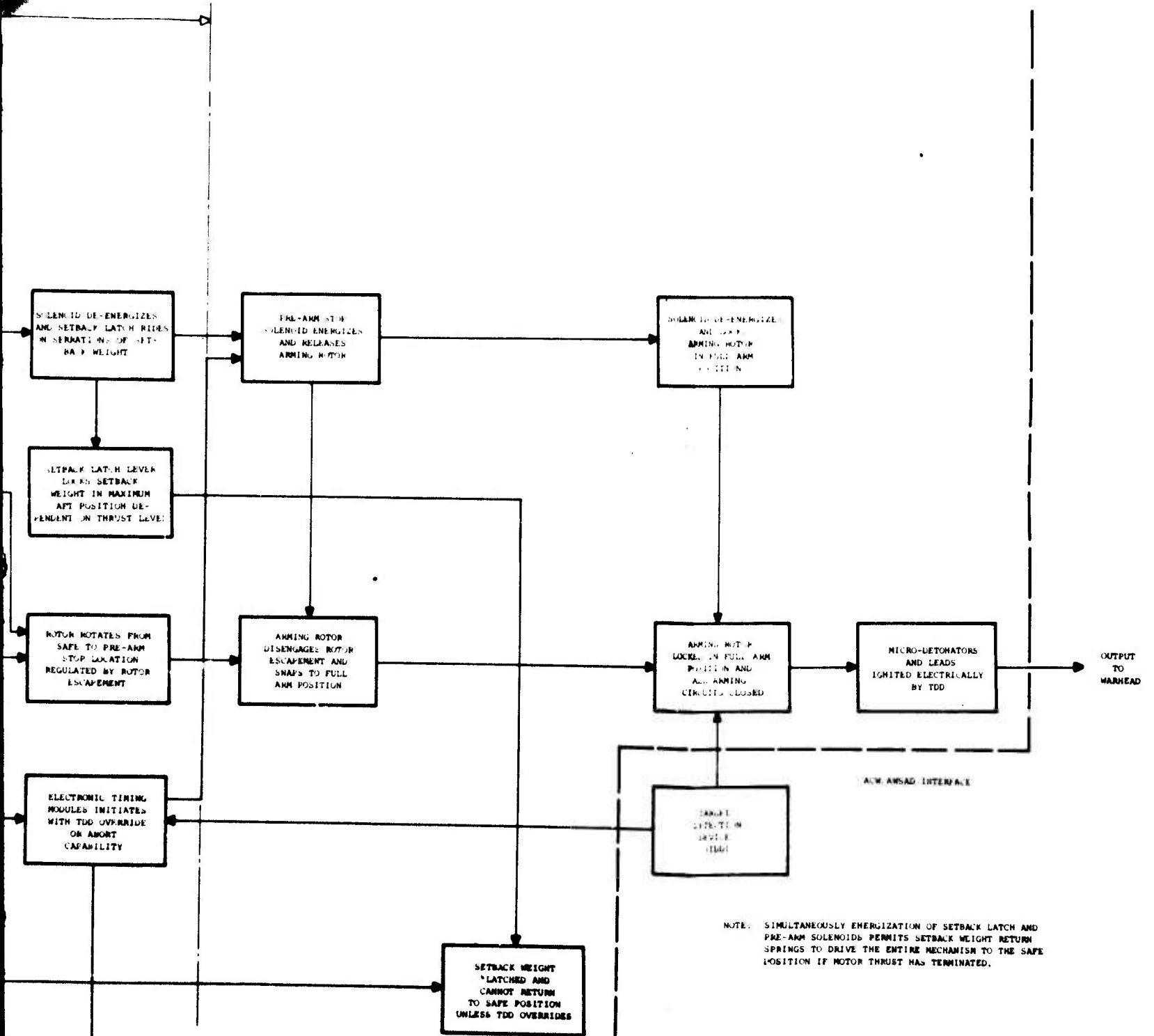


Figure 8. AWSAD Functional Flow Chart - Short Burn Motor (Motor Thrust for Commit Time Period Mode)

2

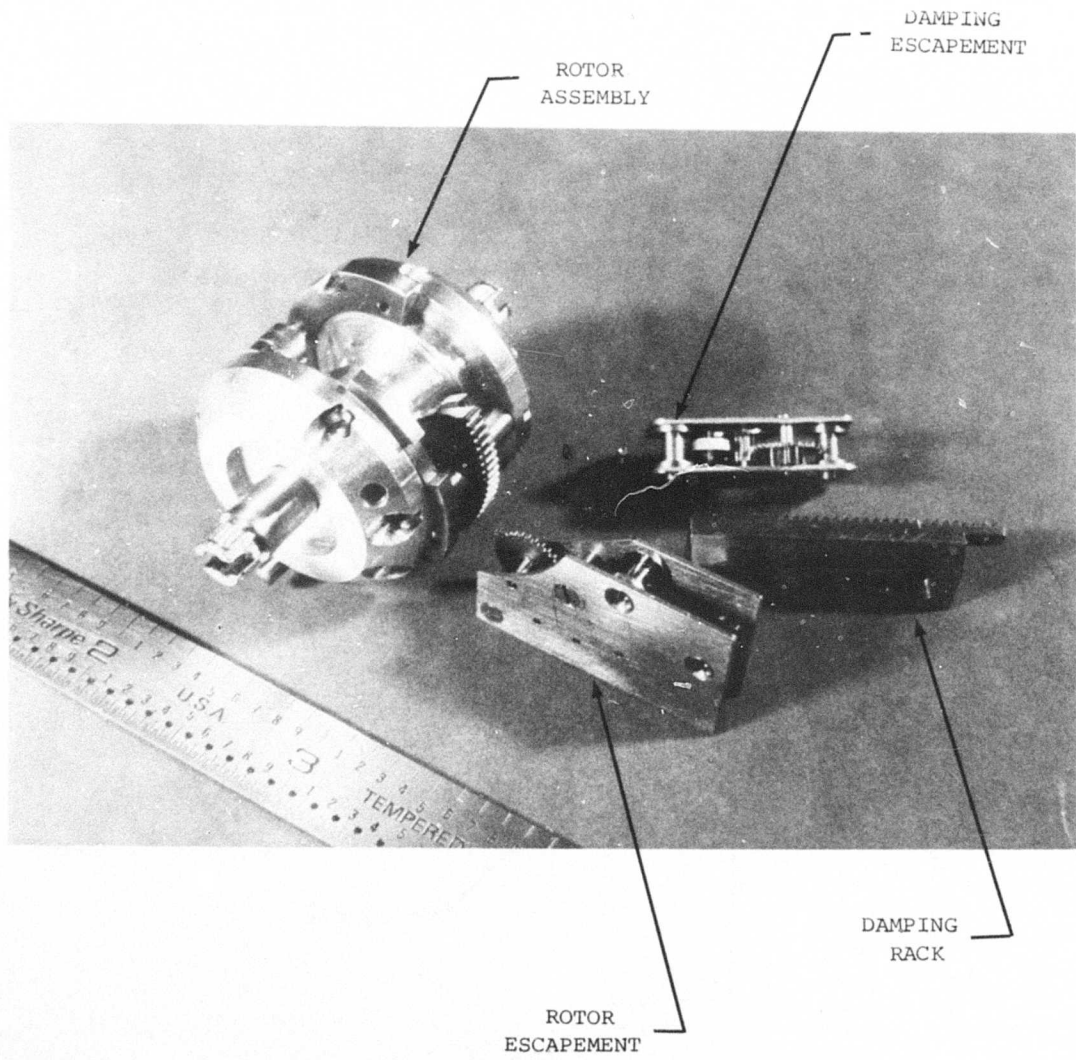


Figure 9. Escapement and Driving Elements

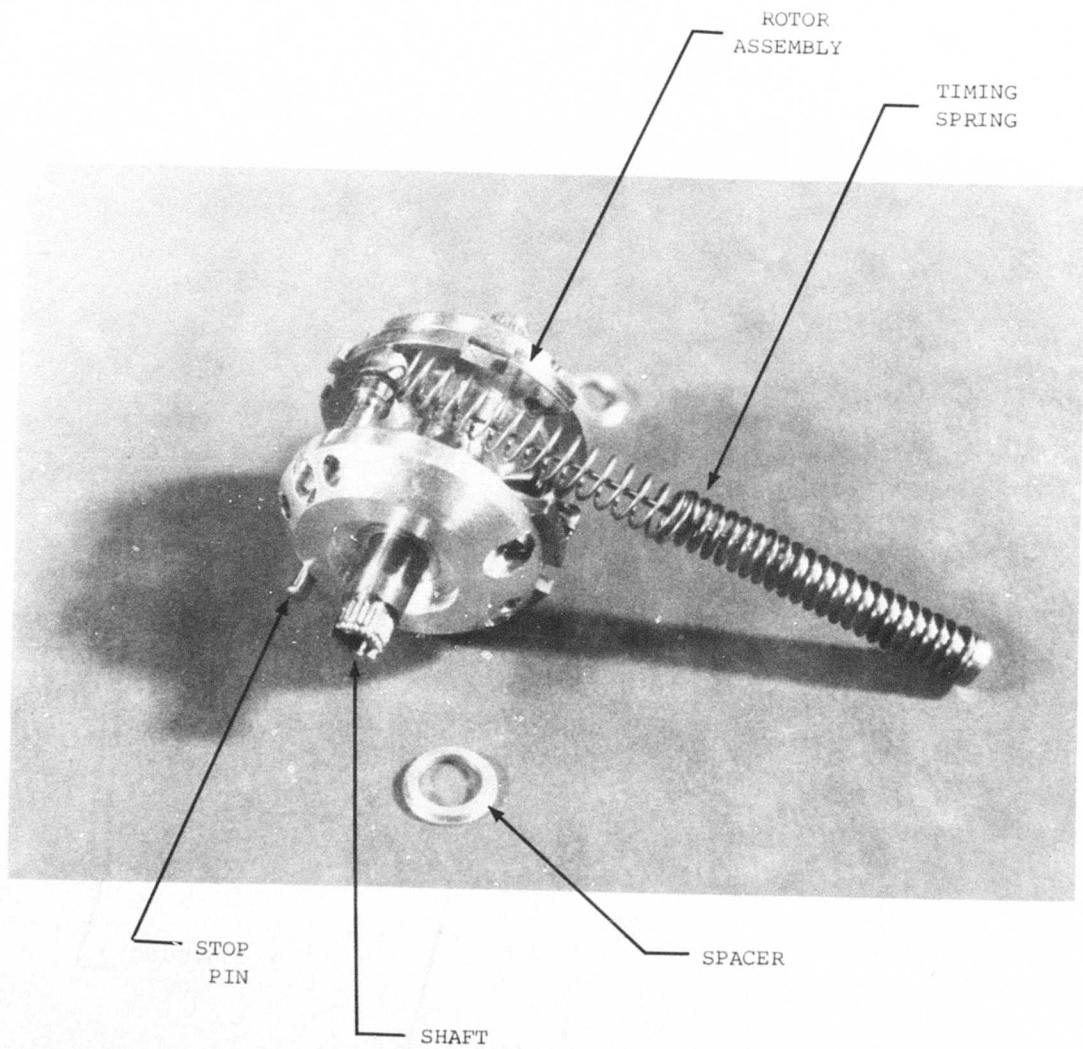


Figure 10. Rotor Assembly With Timing Spring

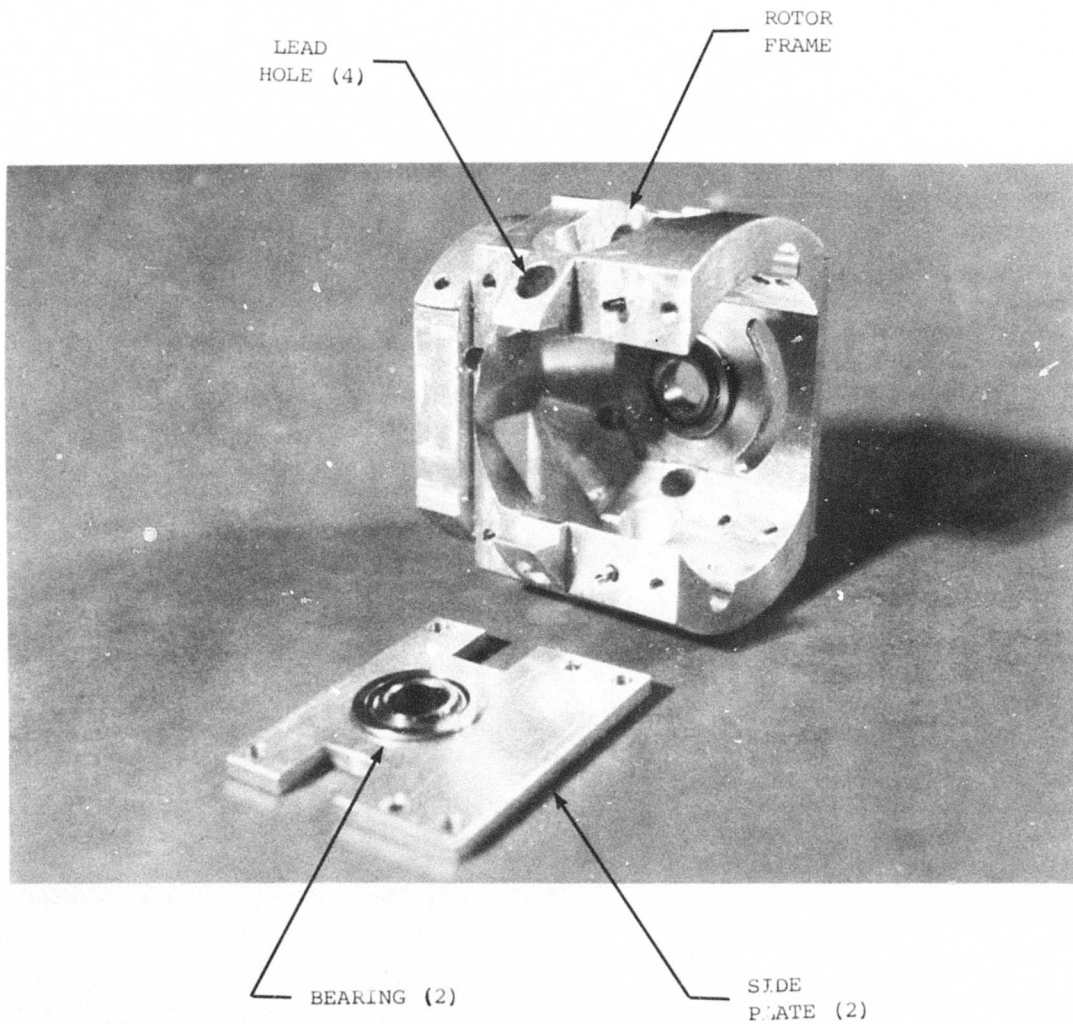


Figure 11. Rotor Frame Assembly

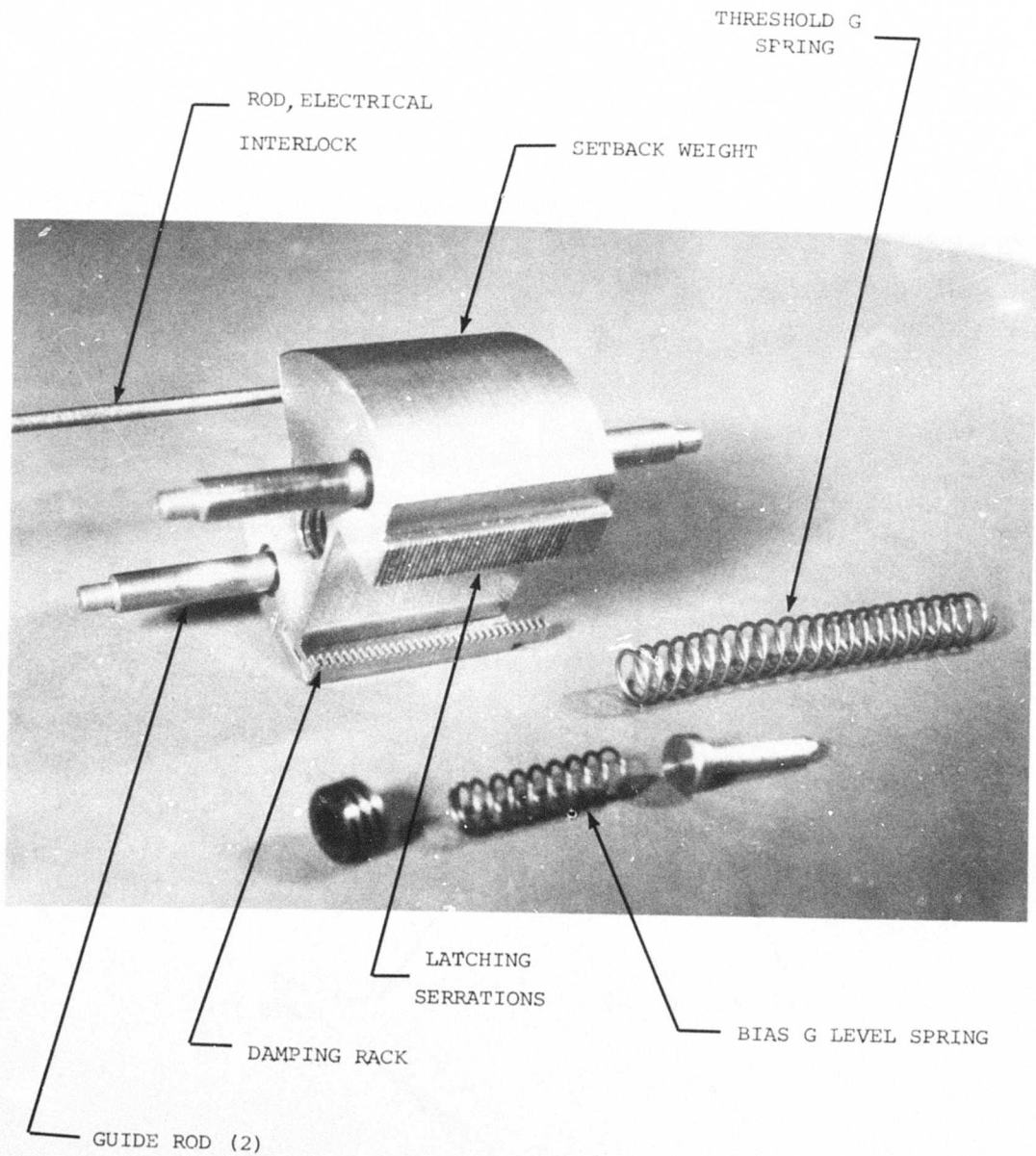


Figure 12. Setback Weight Assembly

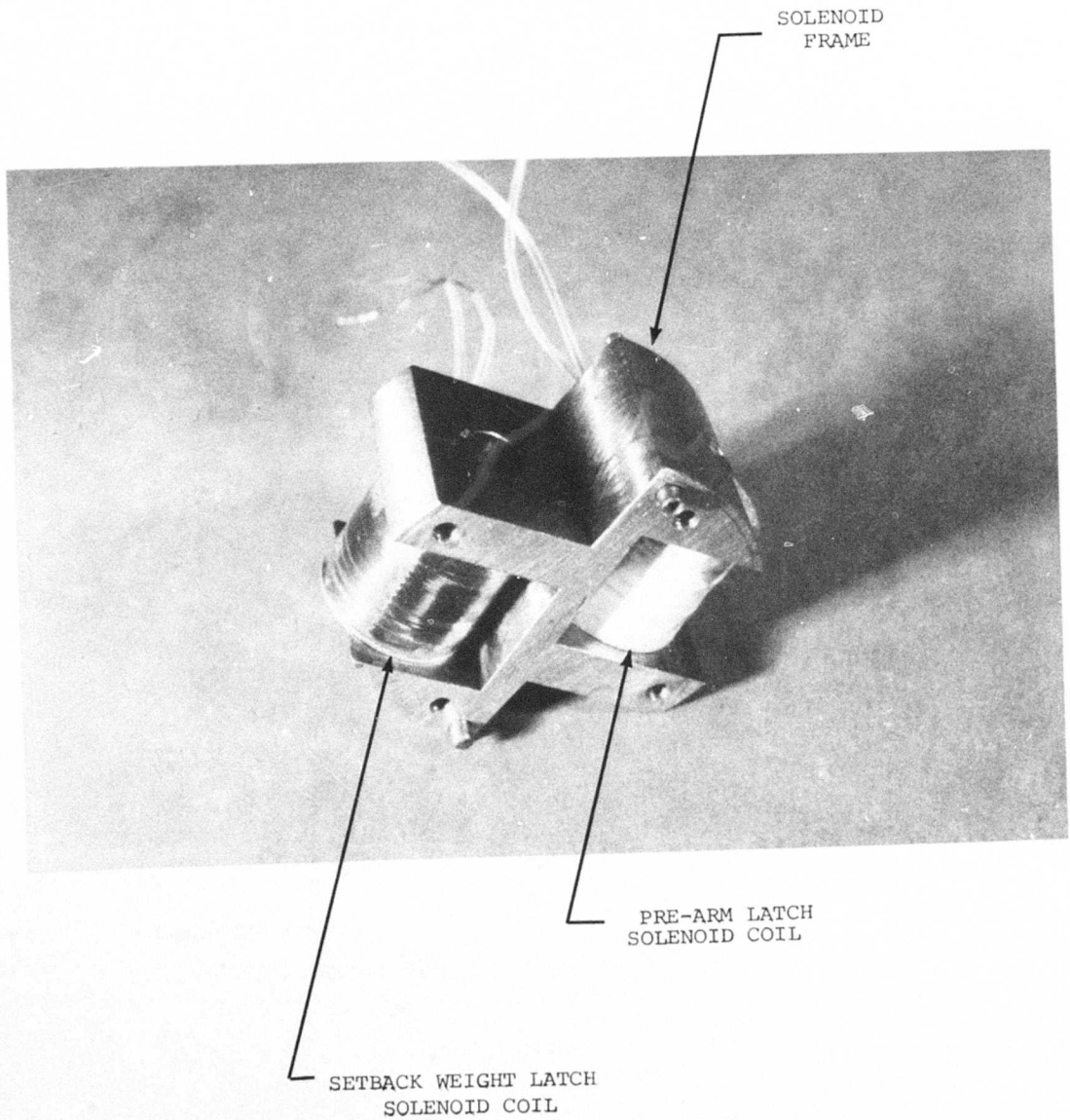


Figure 13. Solenoid Frame Assembly

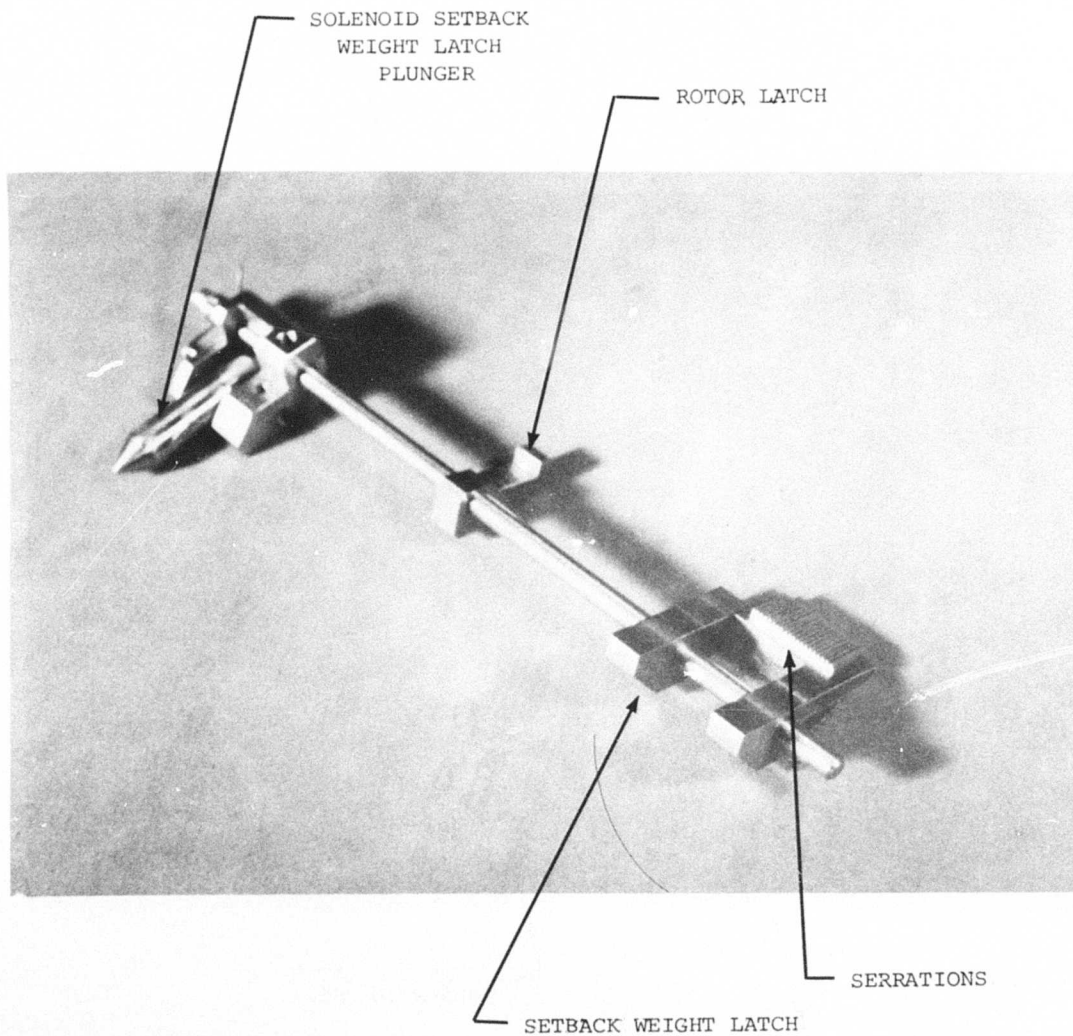


Figure 14. Setback Weight Latch Linkage

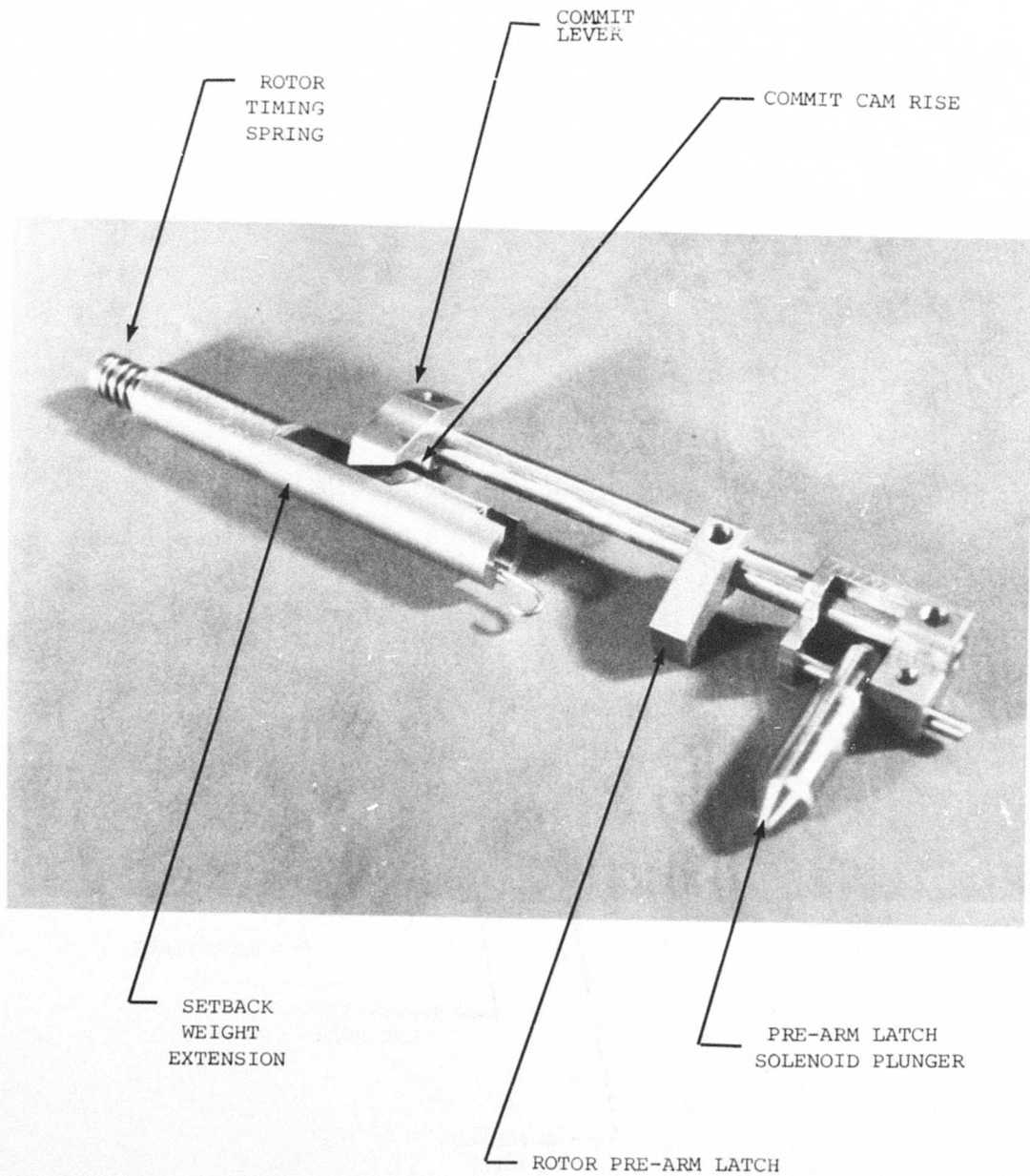


Figure 15. Commit and Pre-Arm Latch Linkage

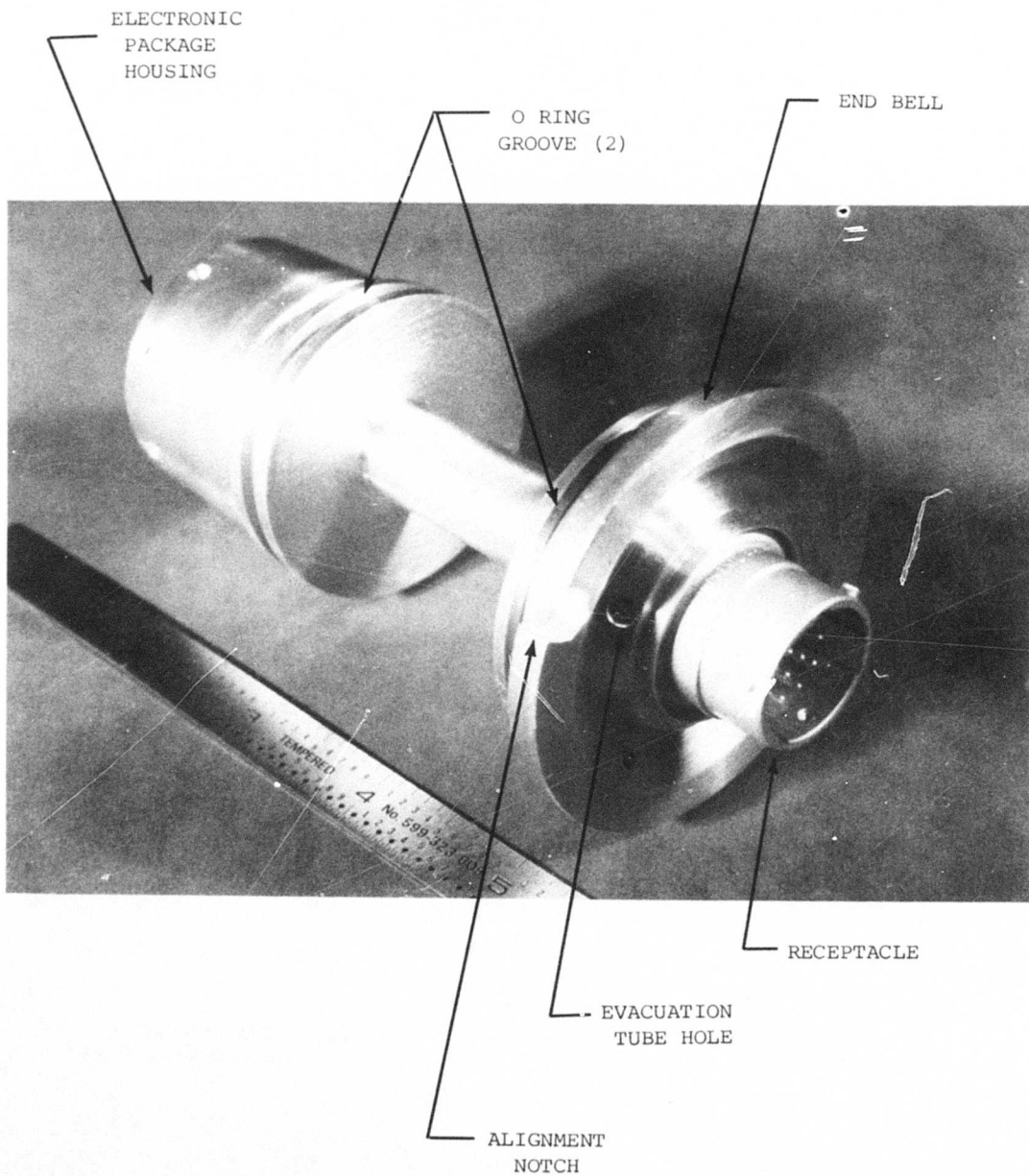


Figure 16. Forward Frame Assembly

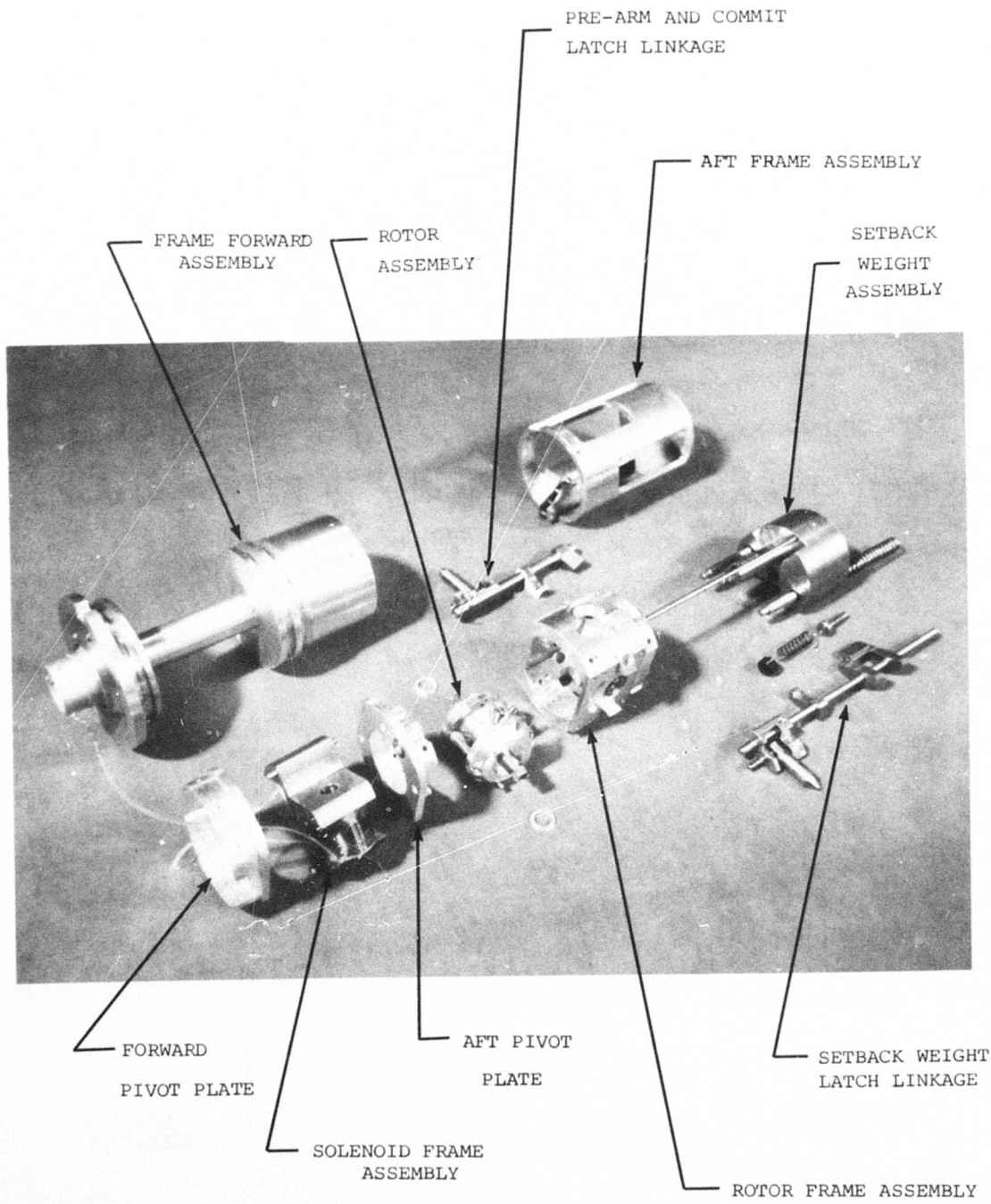
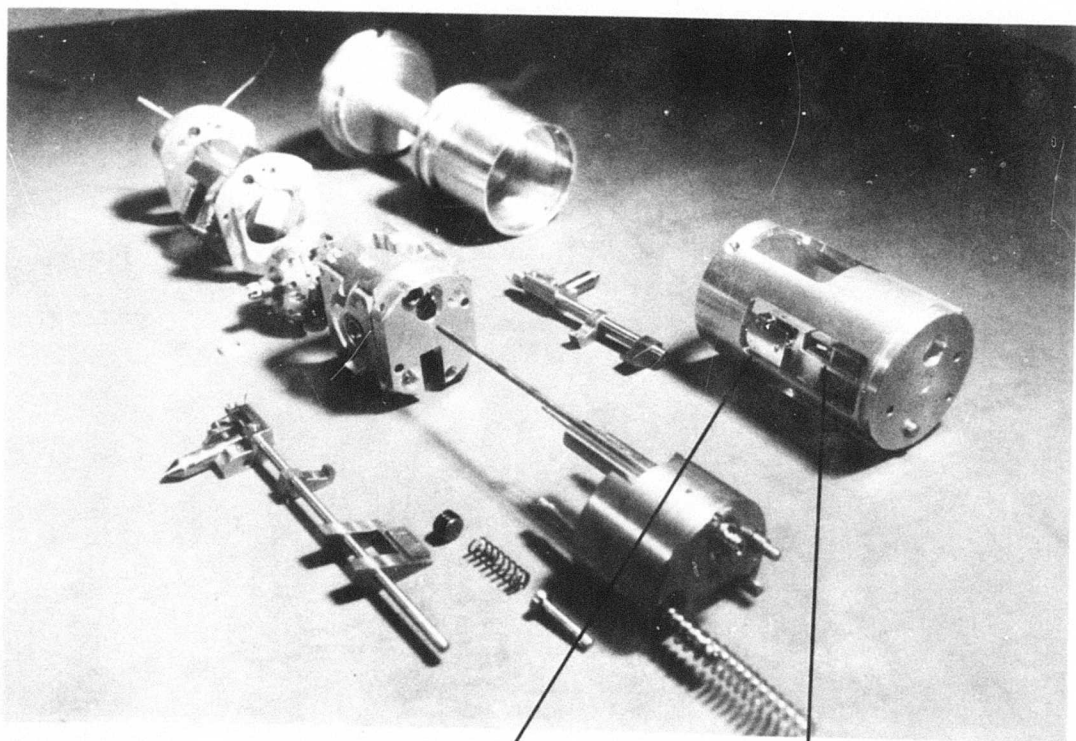


Figure 17. Safing and Arming Device, Components Array



ROTOR
ESCAPEMENT

DAMPING
ESCAPEMENT

Figure 18. Rear View of Components Array

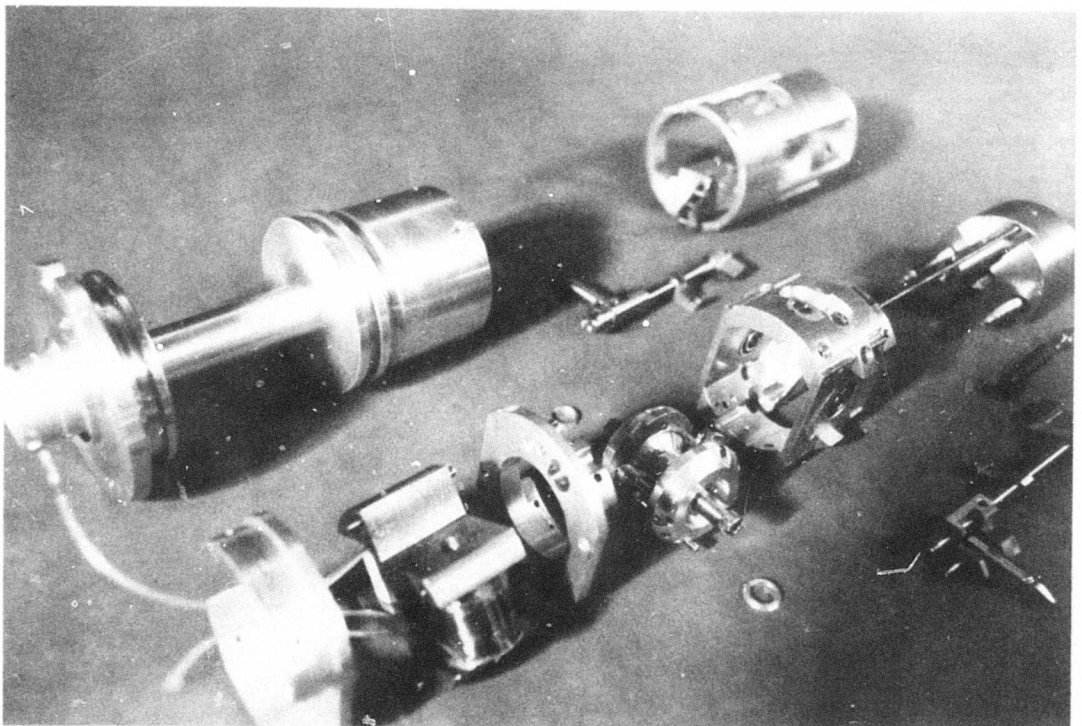


Figure 19. Front View of Components Array

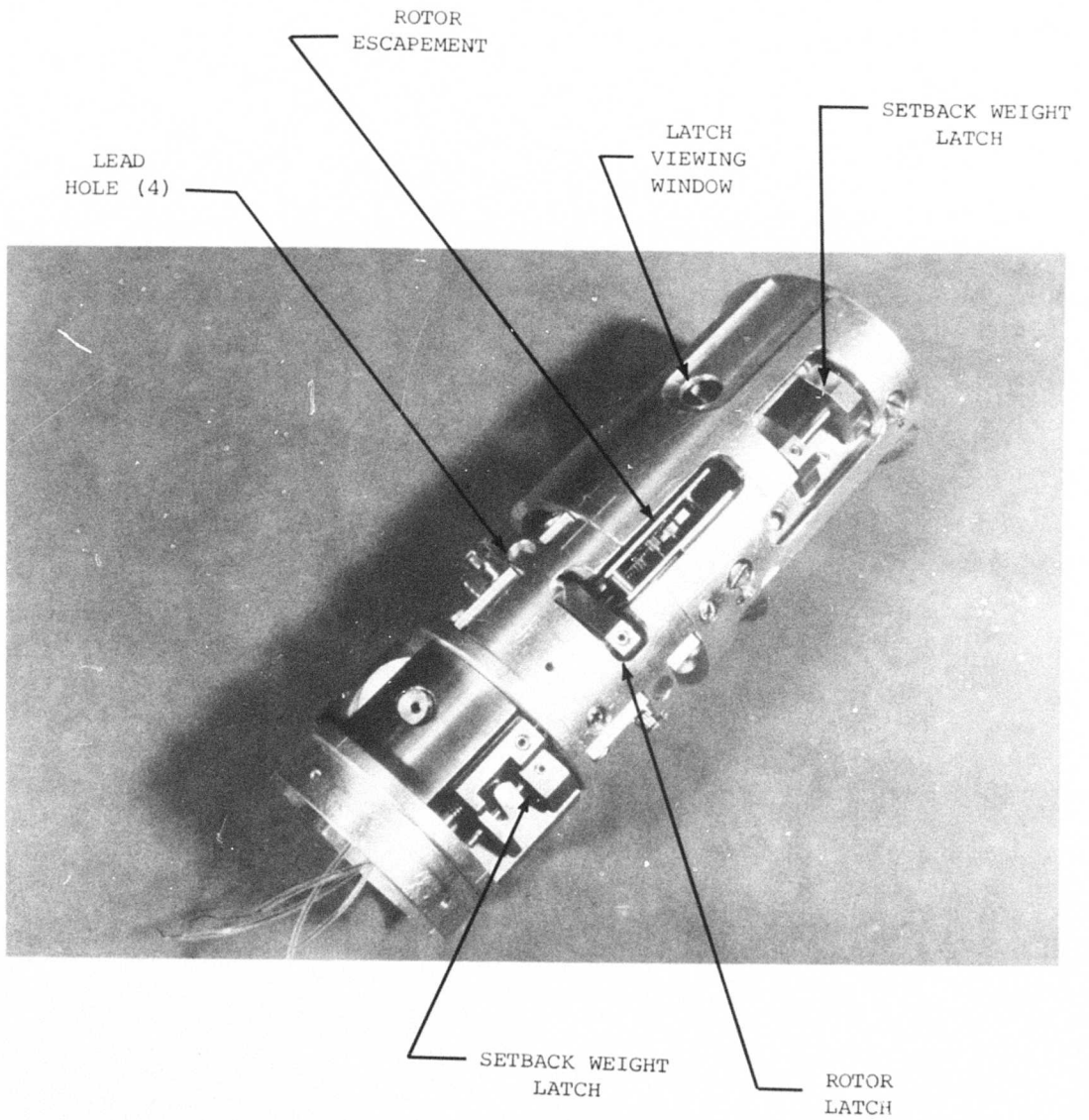


Figure 20. Bottom View of Safing and Arming Mechanism

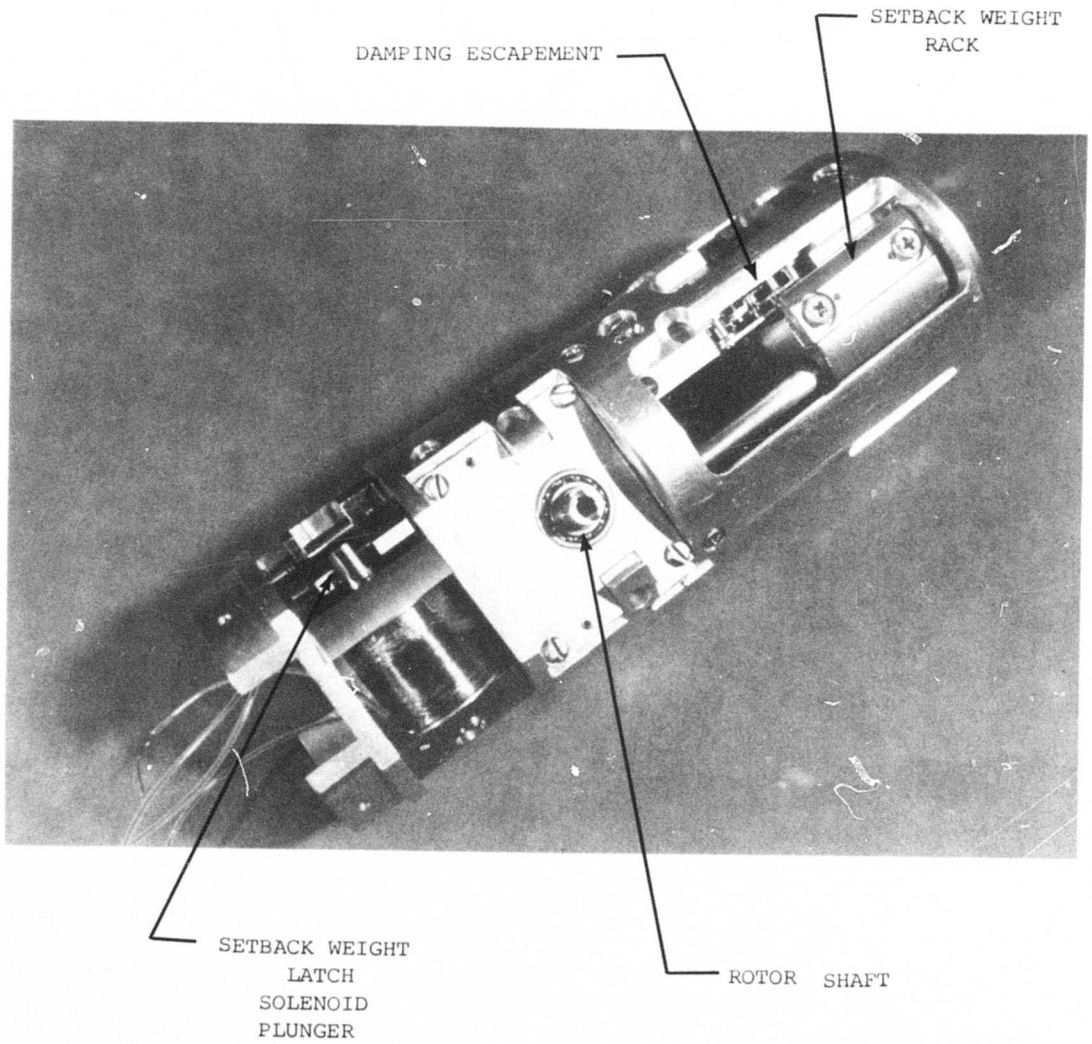


Figure 21. Side View of Safing and Arming Mechanism

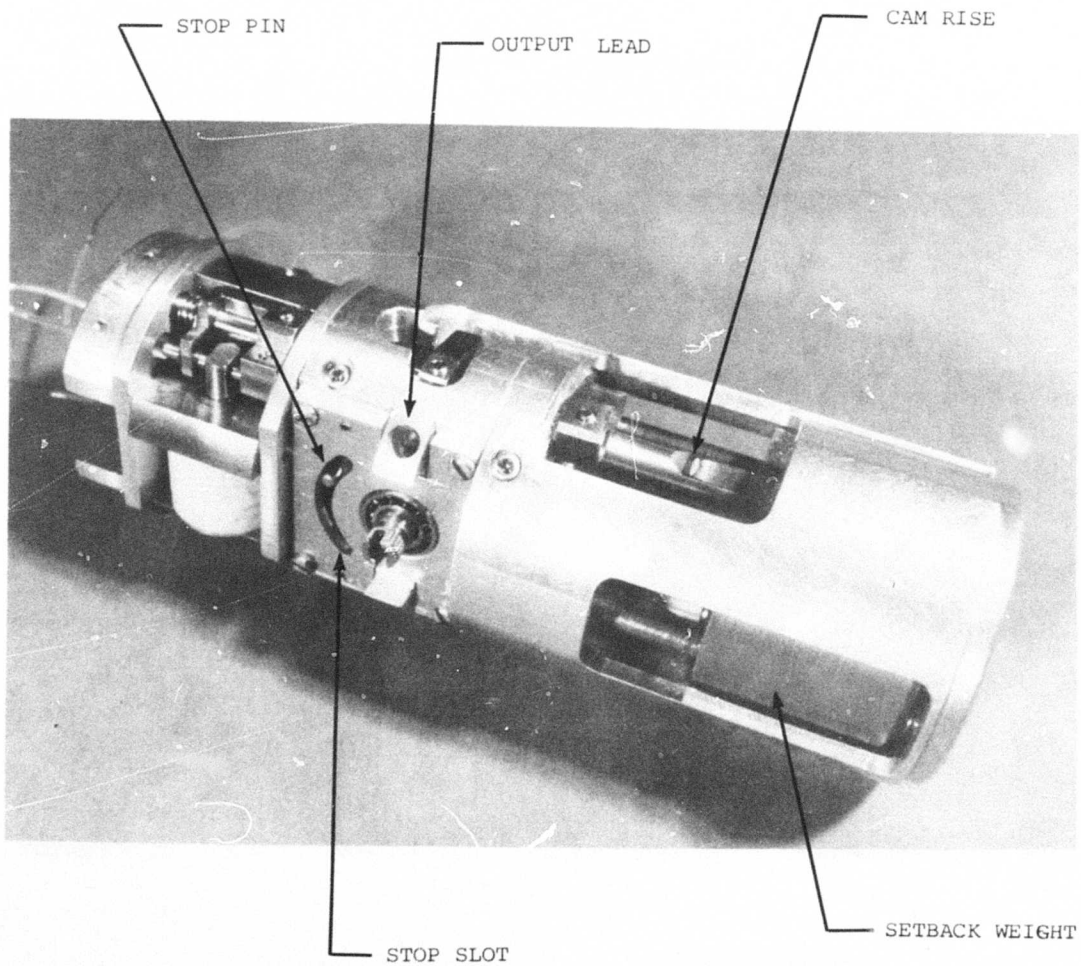


Figure 22. Top View of Safing and Arming Mechanism

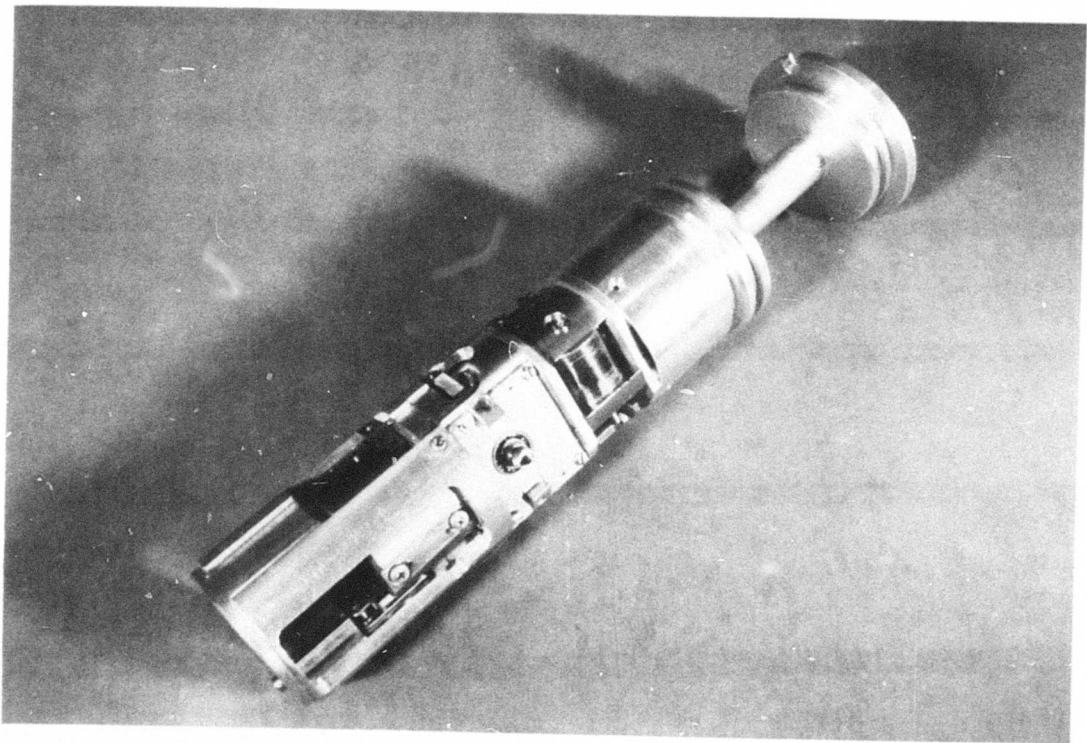


Figure 23. Side View of Safing and Arming Device

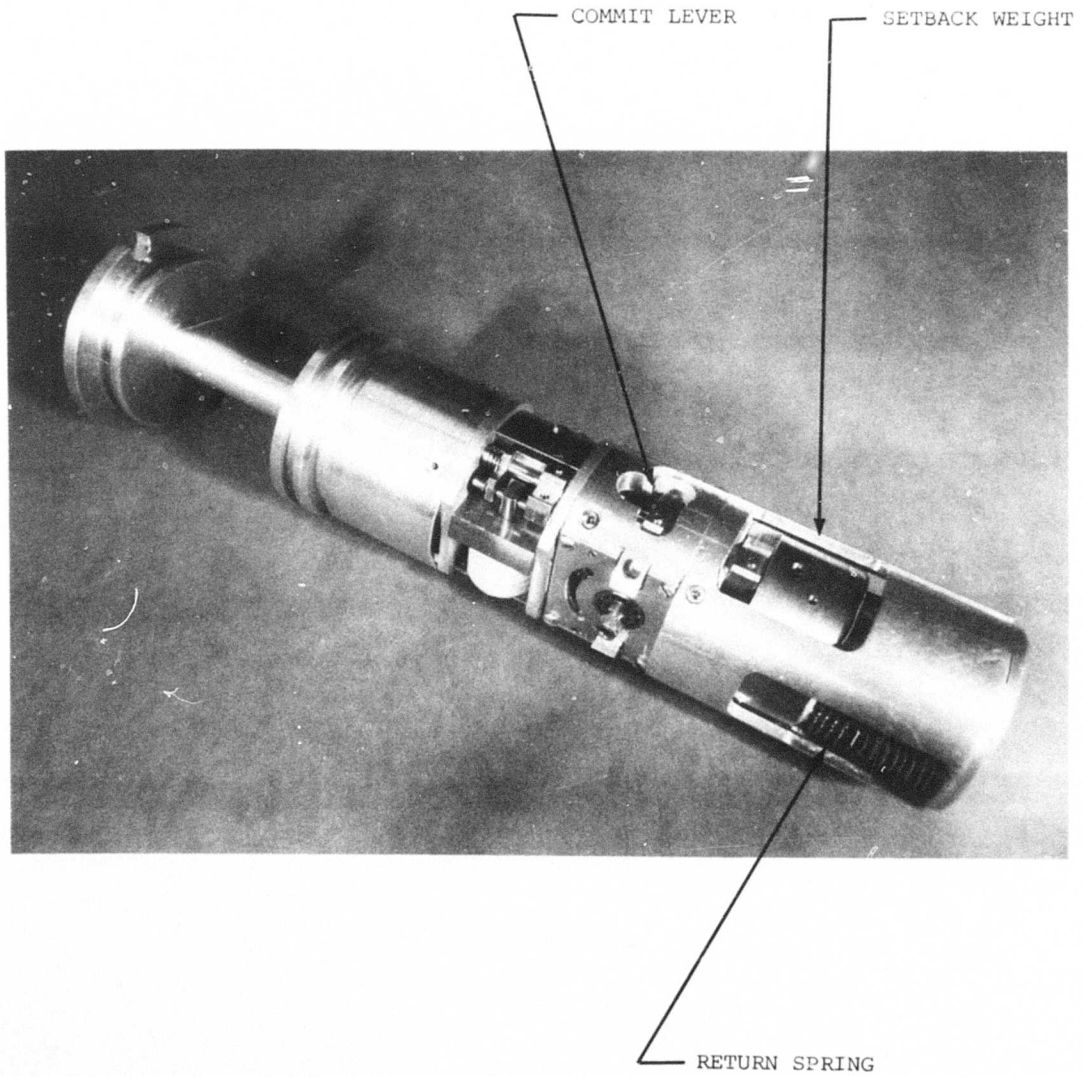


Figure 24. Top View of Safing and Arming Device

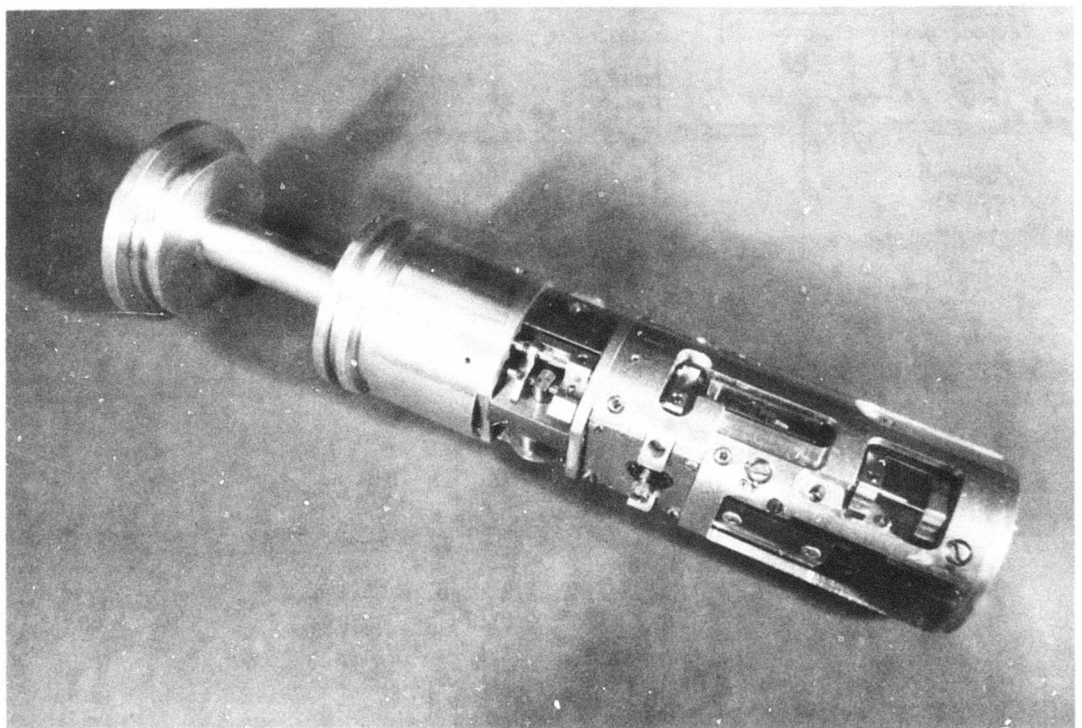
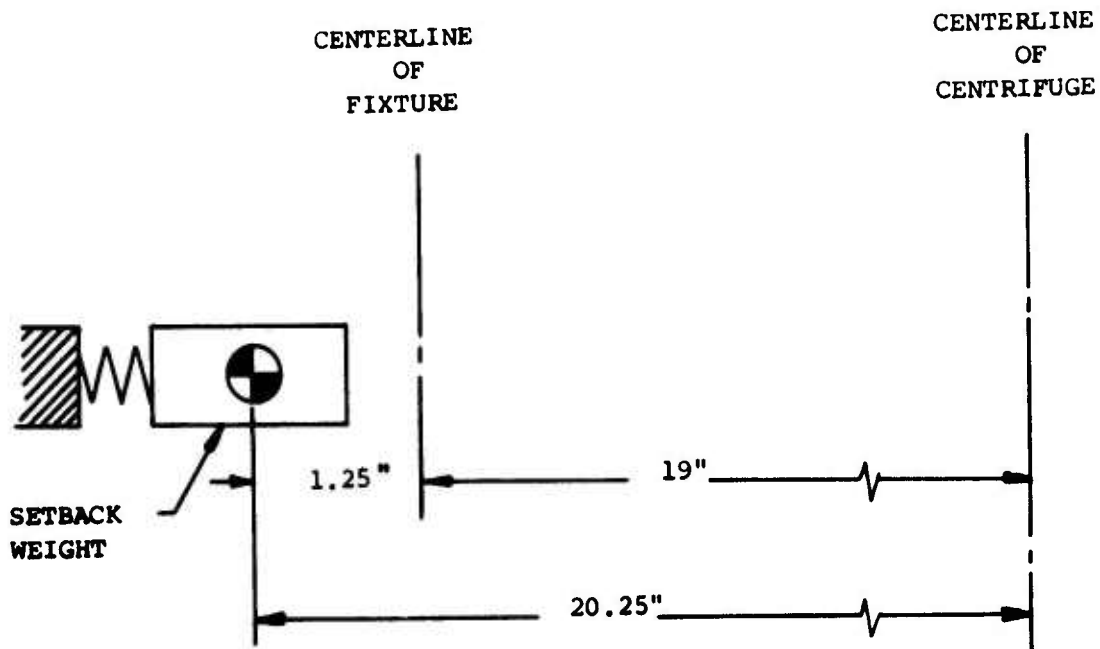


Figure 25. Bottom View of Safing and Arming Device.



$$G's = \frac{2.842 RN^2}{10^5}$$

Where R = 20.25

Then G = 0.0005755N²

N	G's
118	8.00
135	10.50
145	12.10
160	14.70
165	15.67
167	16.05
170	16.63
187	20.10
210	25.37
230	30.44
230 @ 45°	21.52

Figure 26. Acceleration Values Versus RPM for Centrifuge Tests

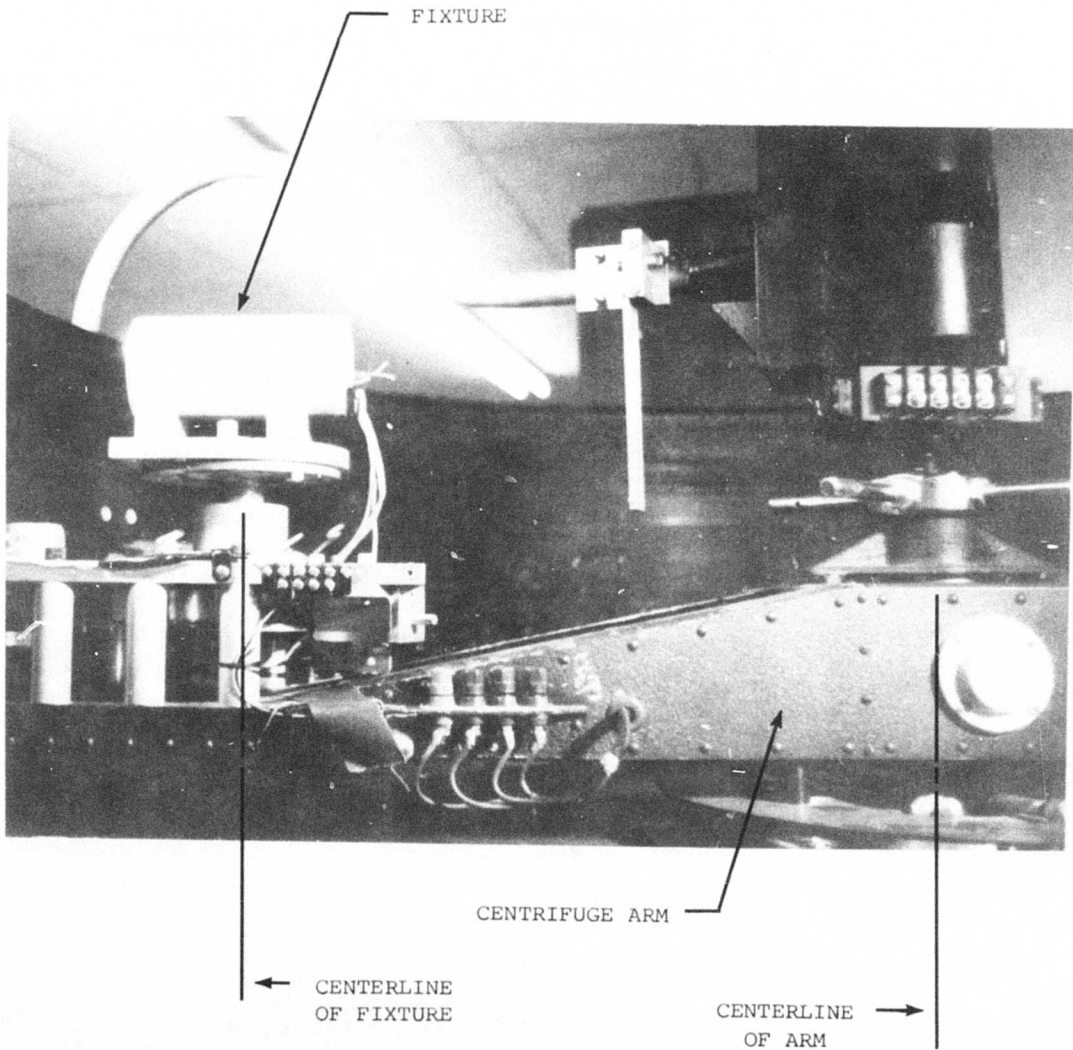


Figure 27. Fixture Orientation - Axial

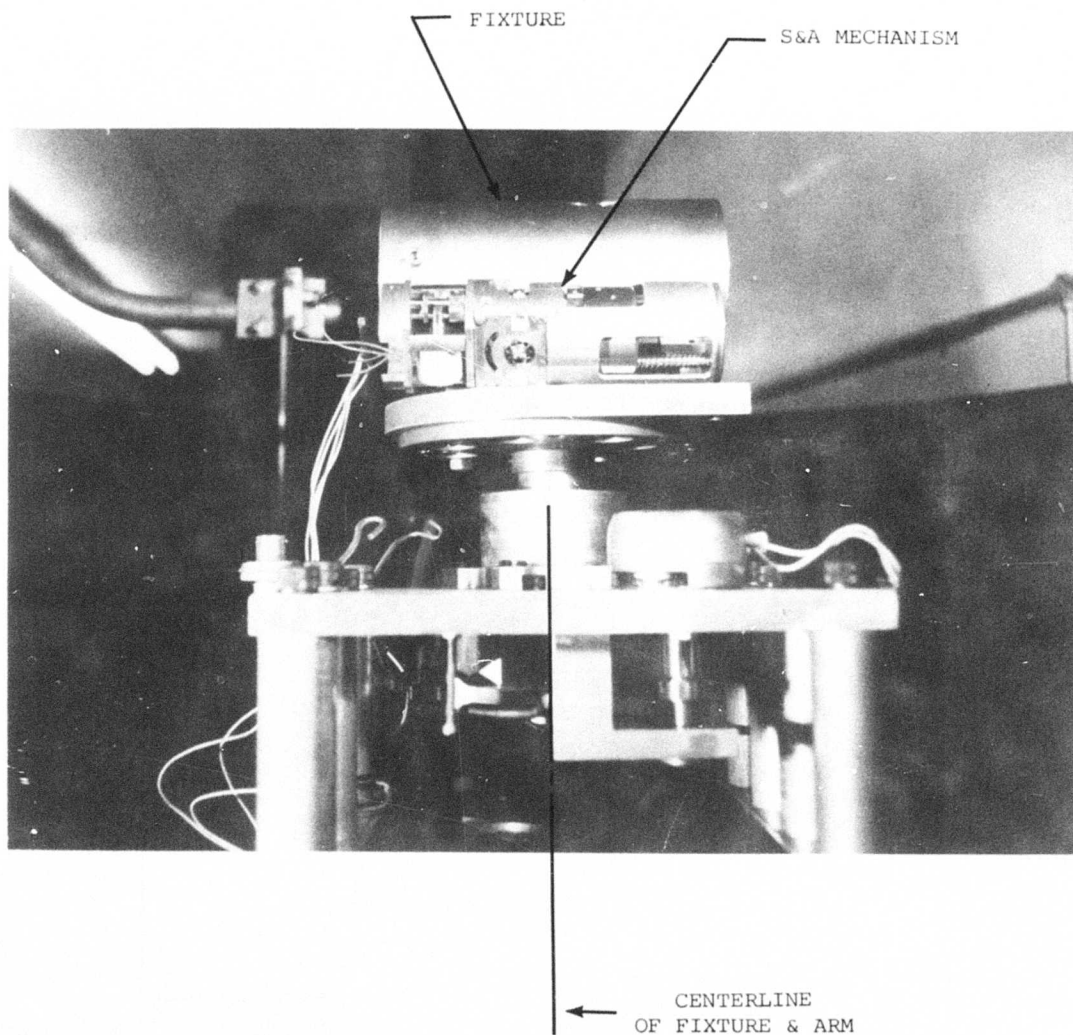


Figure 28. Fixture Oriented for Loading

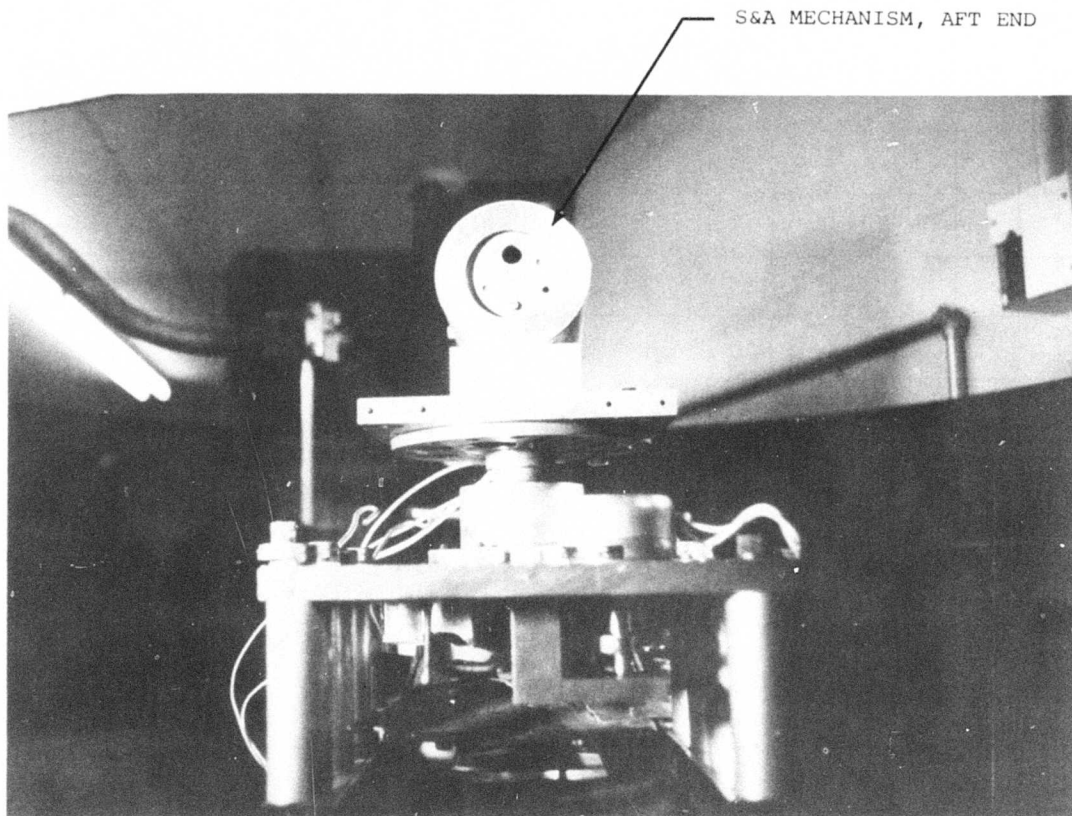


Figure 29. Centrifuge Fixture in Axial Position

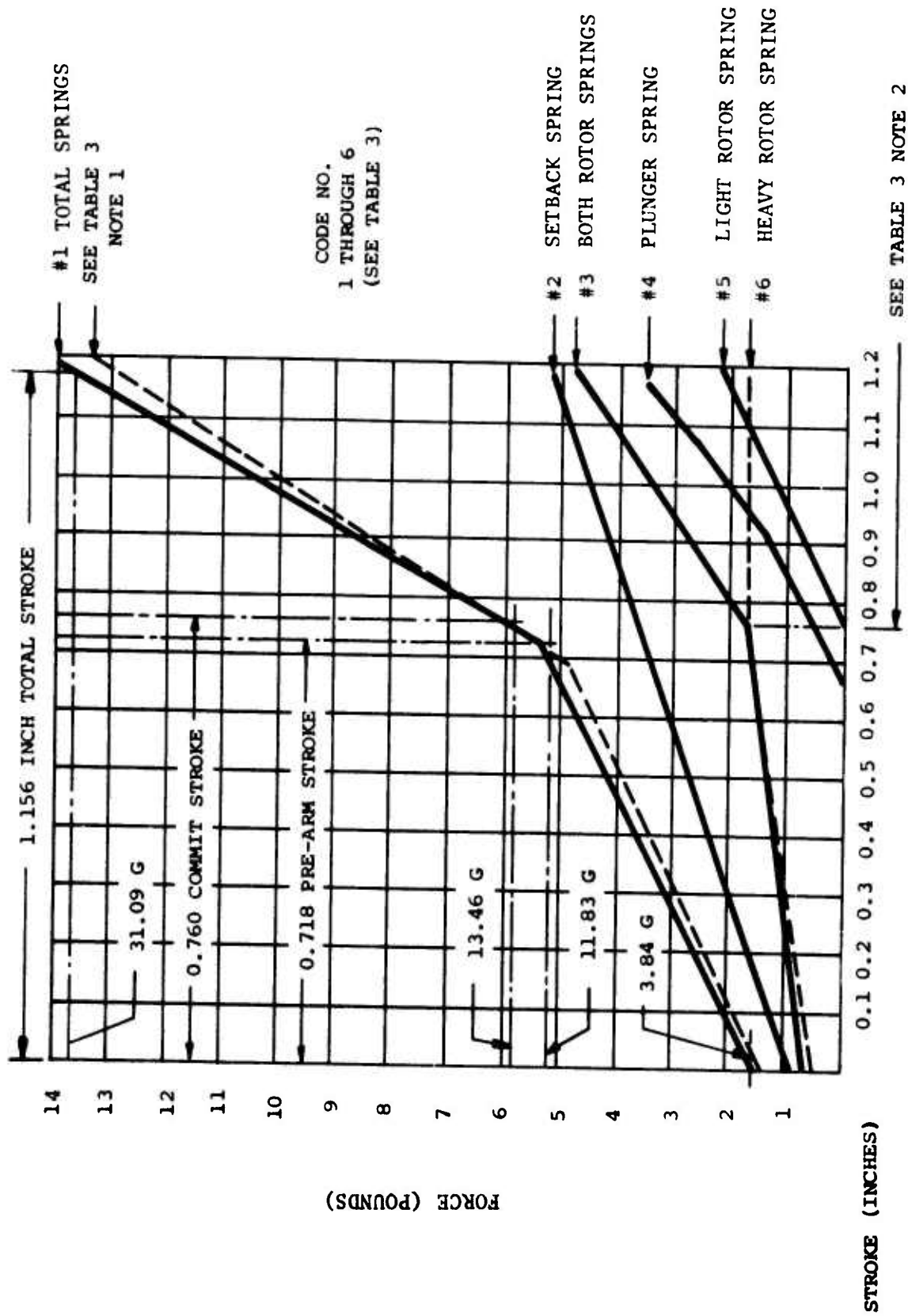


Figure 30. Spring System Characteristics

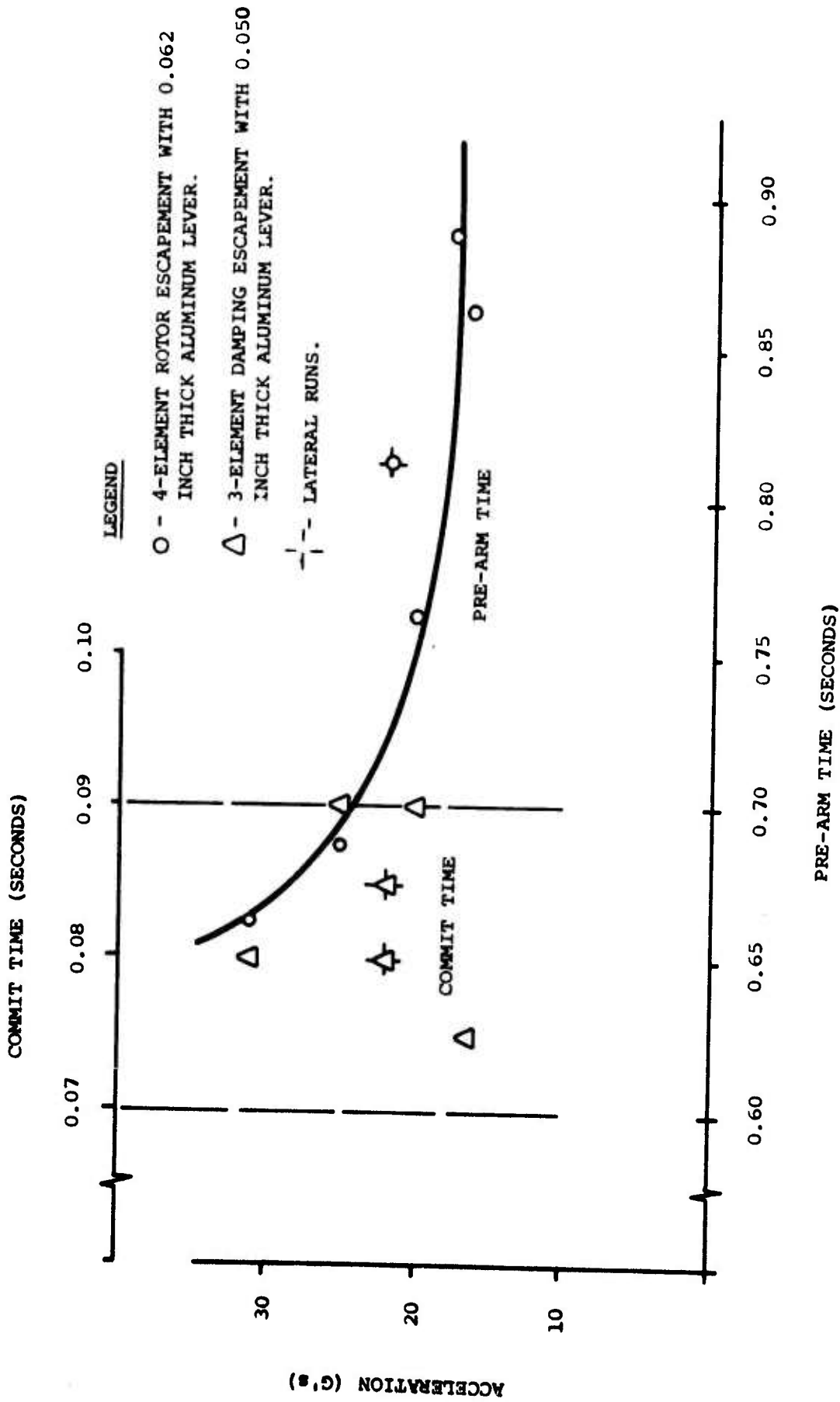


Figure 31. AWSAD Acceleration Test No. 1

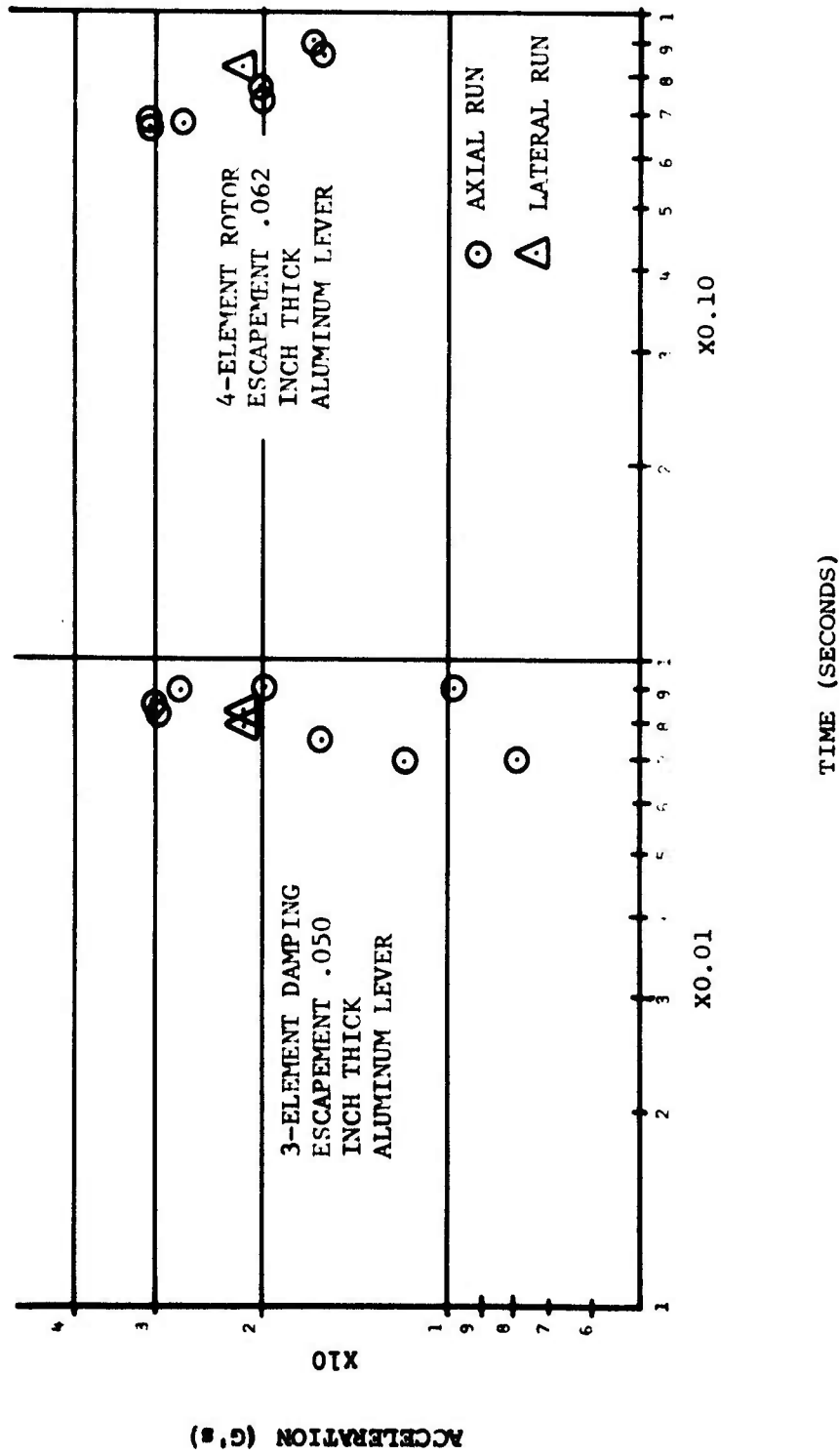


Figure 32. AWSAD, Centrifuge Test No. 1

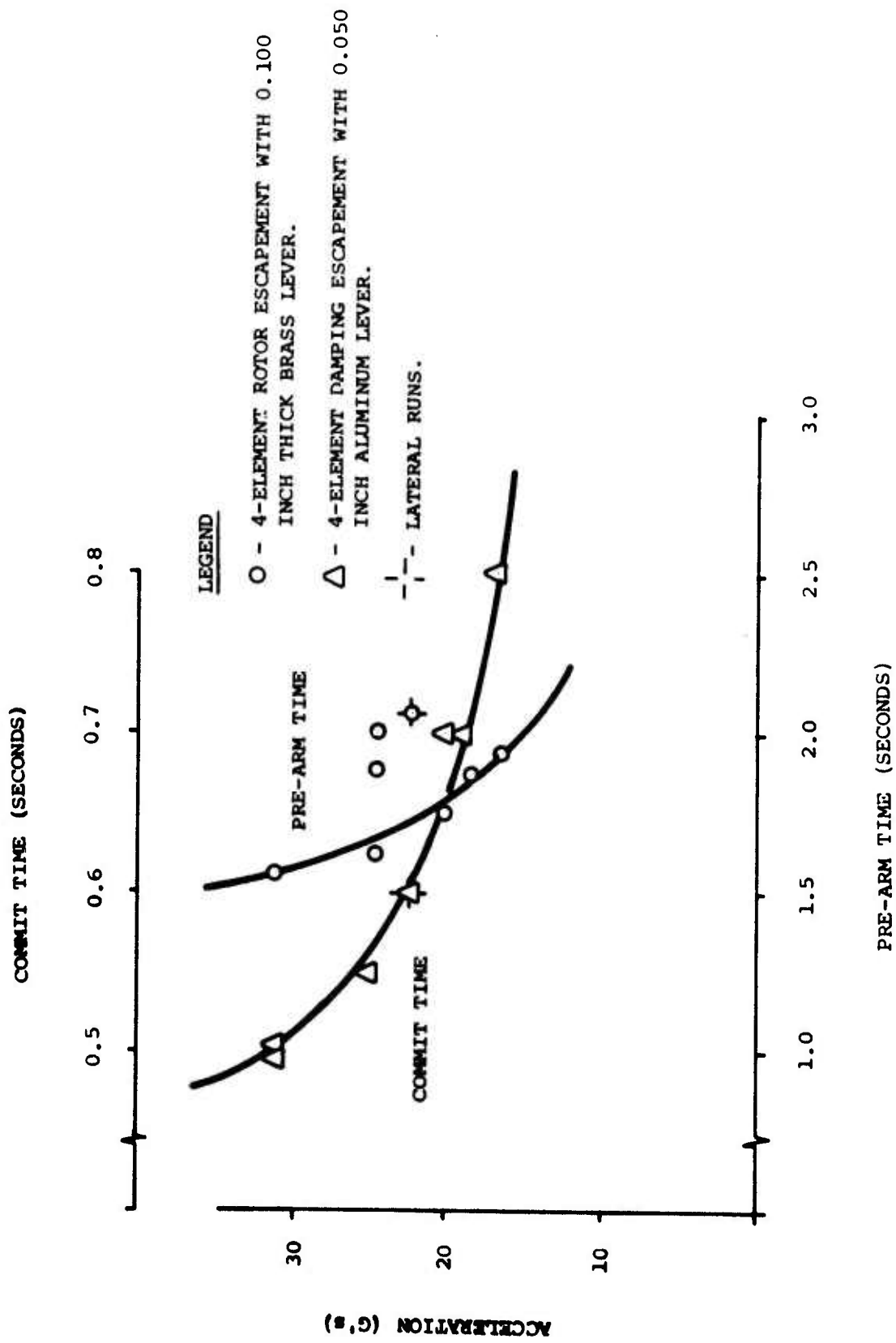


Figure 33. AWSAD Acceleration Test No. 2.

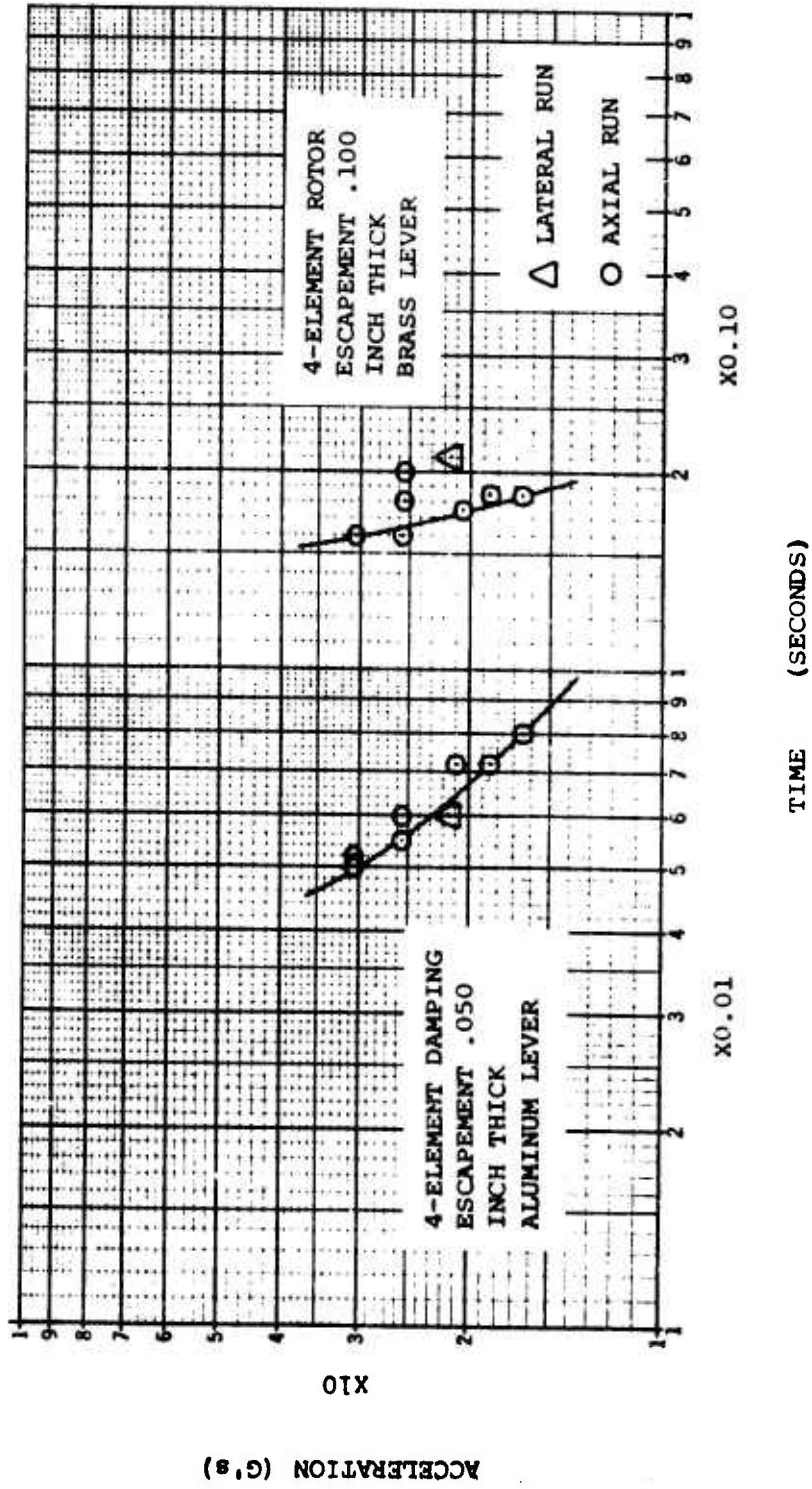
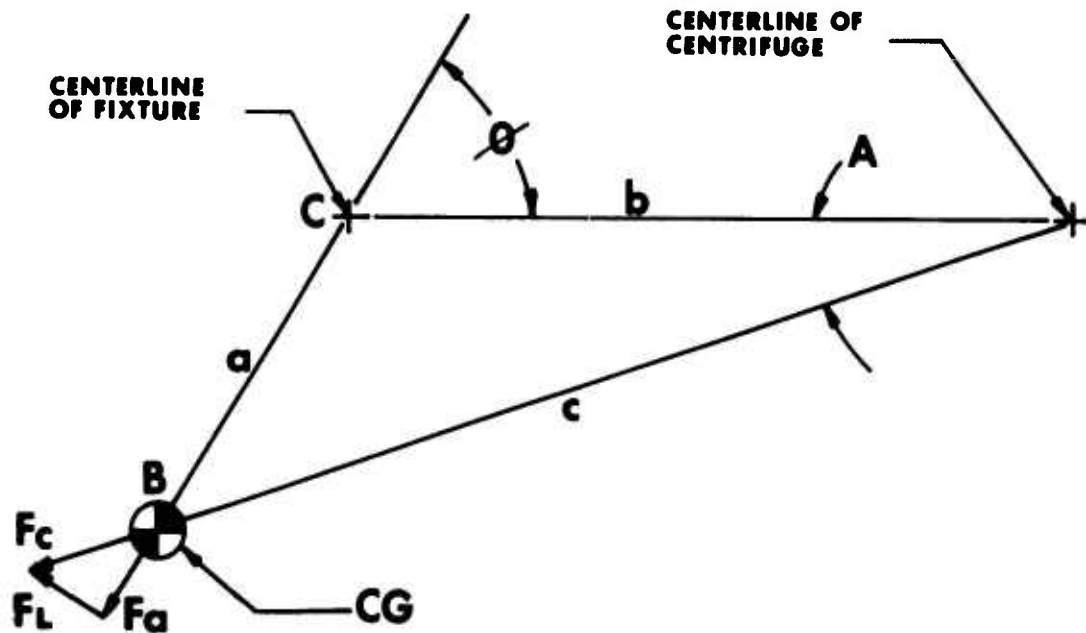


Figure 34. AWSAD Centrifuge Test No. 2



1.0 Given:

$\theta = 45^\circ$ Angle Setting of Fixture
 $b = 19$ Inch
 $a = 1.25$ Inch

$$\frac{b}{\sin B} = \frac{c}{\sin C}$$

$$\sin B = \frac{b}{c} \sin C$$

Determine: Radius C and Angle B $\sin B = \frac{19}{19.9} \times .70711$

$$C^2 = a^2 + b^2 - 2ab \cos C$$

$$= (1.25)^2 + (19)^2 - 2 \times 1.25 \times 19 \times (-.70711)$$

$$C = (396.16)^{1/2}$$

$$C = 19.9 \text{ Inches}$$

$$\sin B = .676$$

$$\text{Angle B} = 42.5^\circ$$

2.0 Determine Force Vectors

F_c , F_l and F_a

$$G = 2.842 \times 10^{-5} R N^2$$

$$R = c = 19.9 \text{ Inches}$$

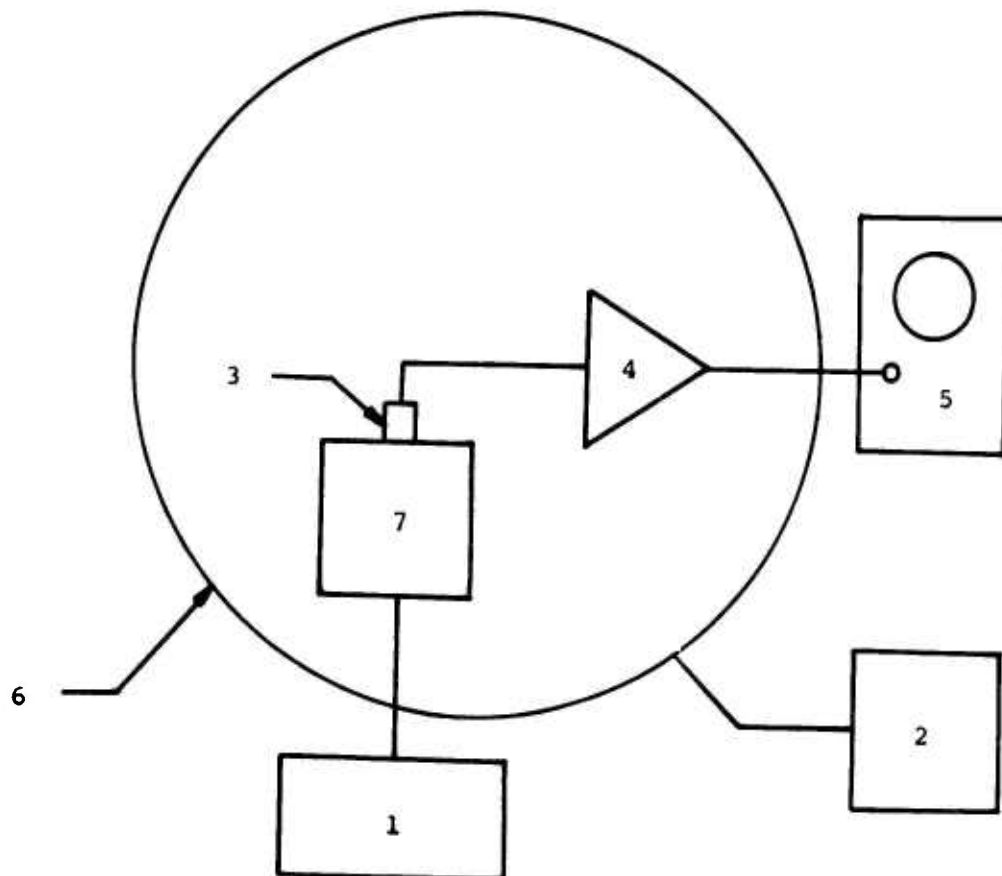
$$N = 230 \text{ RPM}$$

$$G = 2.842 \times 10^{-5} \times 19.9 (230)^2 = 29.9 \text{ G's} = F_c = \text{Centrifugal Force}$$

$$F_l = \sin 42.5^\circ \times 29.9 = 6.76 \times 29.9 = 20.2 \text{ G's} = \text{Lateral Force}$$

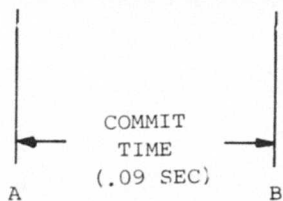
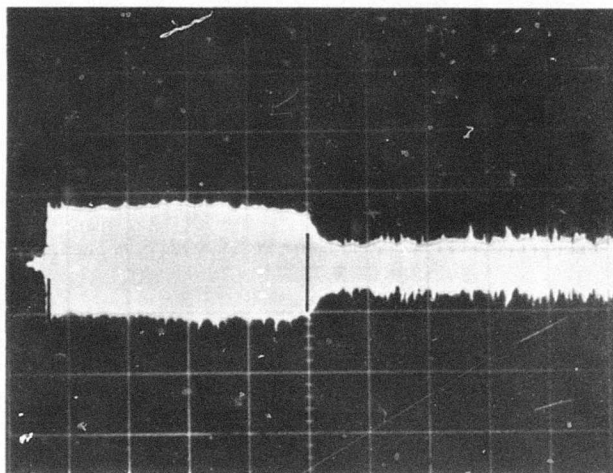
$$F_a = \cos 42.5^\circ \times 29.9 = .737 \times 29.9 = 22.0 \text{ G's} = \text{Axial Force}$$

Figure 35. Force Vectors at 45° Lateral Centrifuge Test



- 1 - Harrison Model 809A Power Supply.
- 2 - Hewlett-Packard Mod 523 DR Frequency Counter.
- 3 - Transducer, Piezoelectric for Sound Pickup.
- 4 - Hi-Gain/Hi-Input Impedance Pre-Amp.
- 5 - Tektronix 564B Storage Oscilloscope.
- 6 - Genisco Centrifuge.
- 7 - S&A Mechanism.

Figure 36. Acceleration Test Equipment Setup



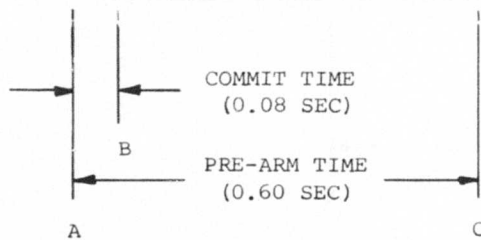
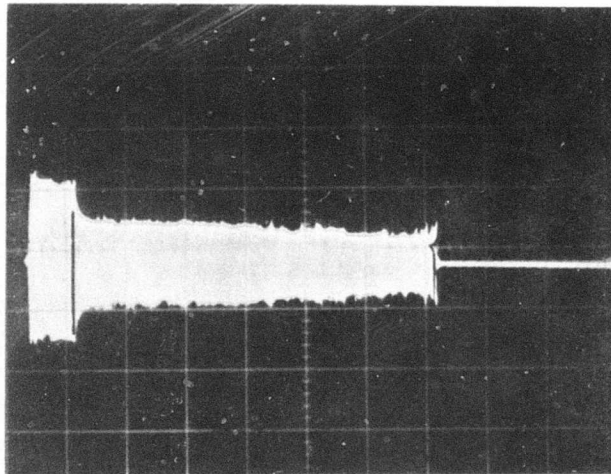
187 RPM CENTRIFUGE SPEED

20.1 G's ACCELERATION (AXIAL)

3 - ELEMENT DAMPING ESCAPEMENT WITH
.050 THICK ALUMINUM LEVER (COMMIT TIME)

4 - ELEMENT ROTOR ESCAPEMENT WITH
.062 THICK ALUMINUM LEVER (PRE-ARM TIME)

Figure 37. Typical Oscilloscope Trace (0.02 Second/CM Sweep Rate)



187 RPM CENTRIFUGE SPEED

20.1 G's ACCELERATION (AXIAL)

3 - ELEMENT DAMPING ESCAPEMENT WITH
.050 THICK ALUMINUM LEVER (COMMIT TIME)

4 - ELEMENT ROTOR ESCAPEMENT WITH
.062 THICK ALUMINUM LEVER (PRE-ARM TIME)

Figure 38. Typical Oscilloscope Trace (0.10 Second/CM Sweep Rate)

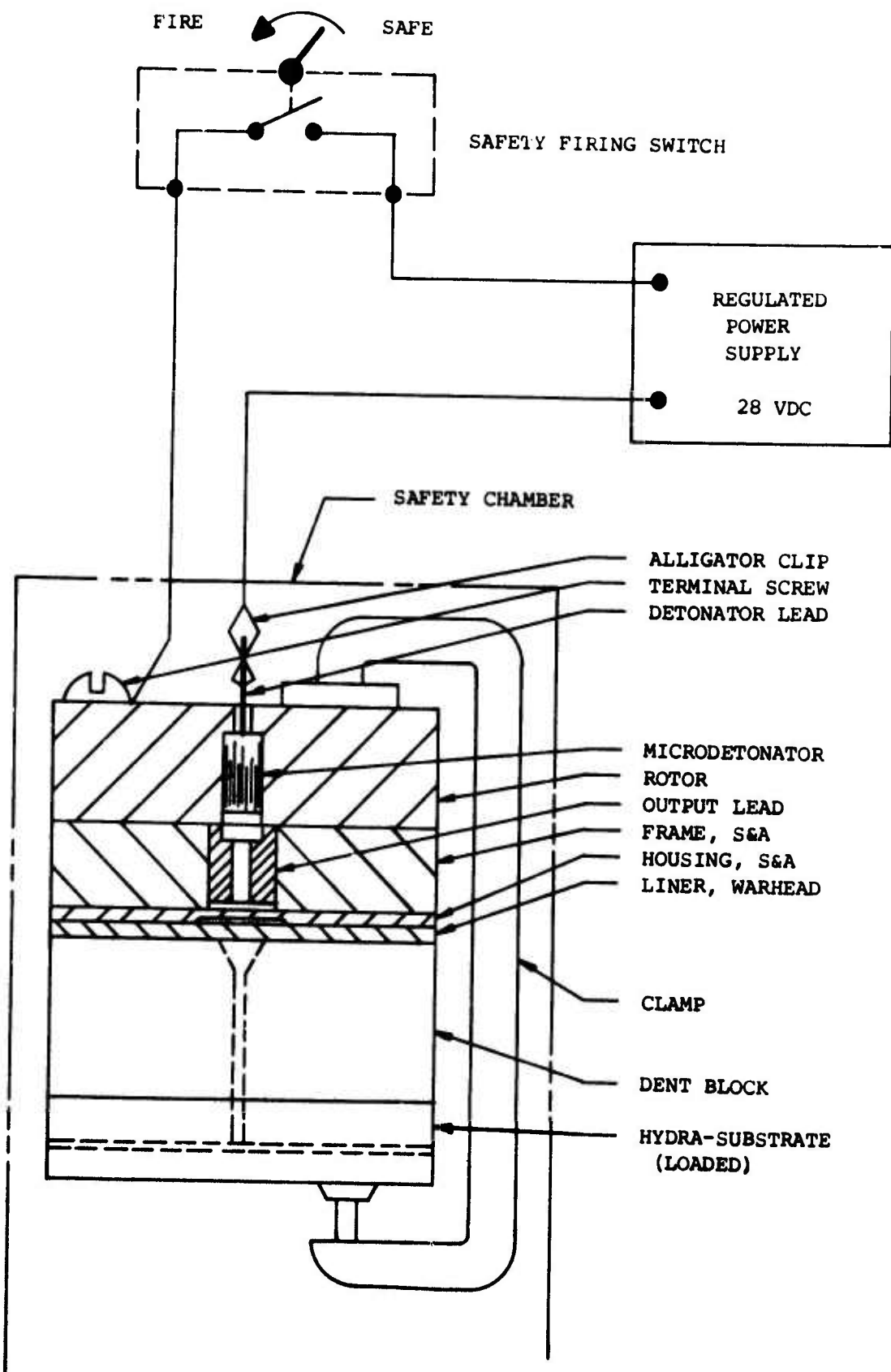


Figure 39. Explosive Train Test Setup

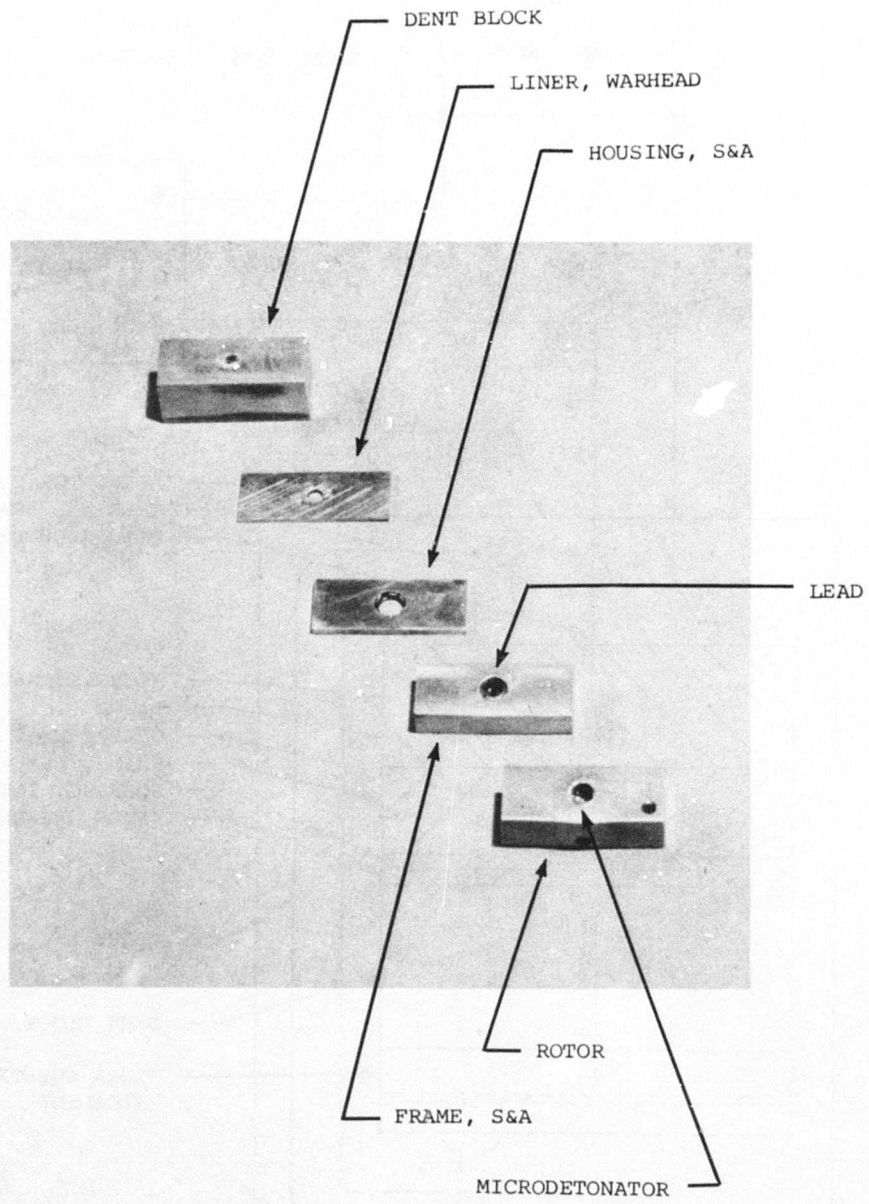


Figure 40. Aimable Explosive Train, Test No. 1

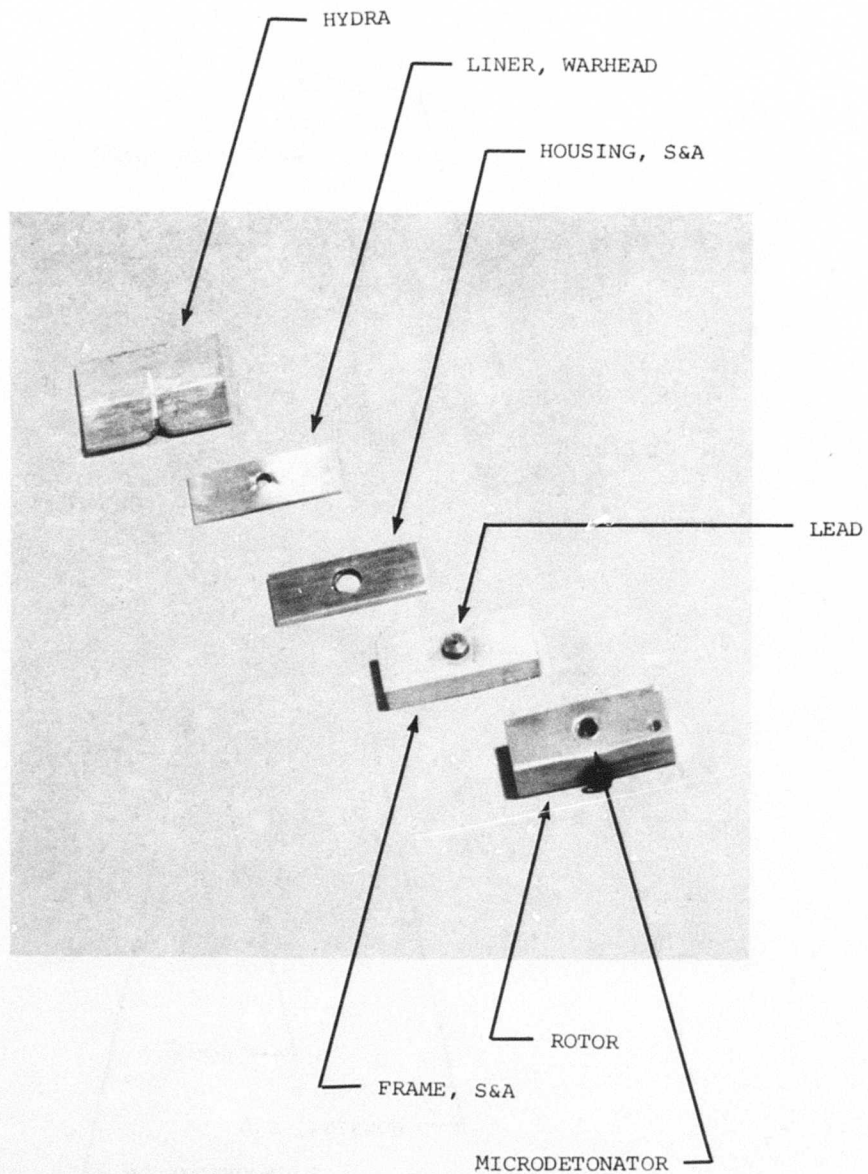


Figure 41. Aimable Explosive Train, Test No. 2

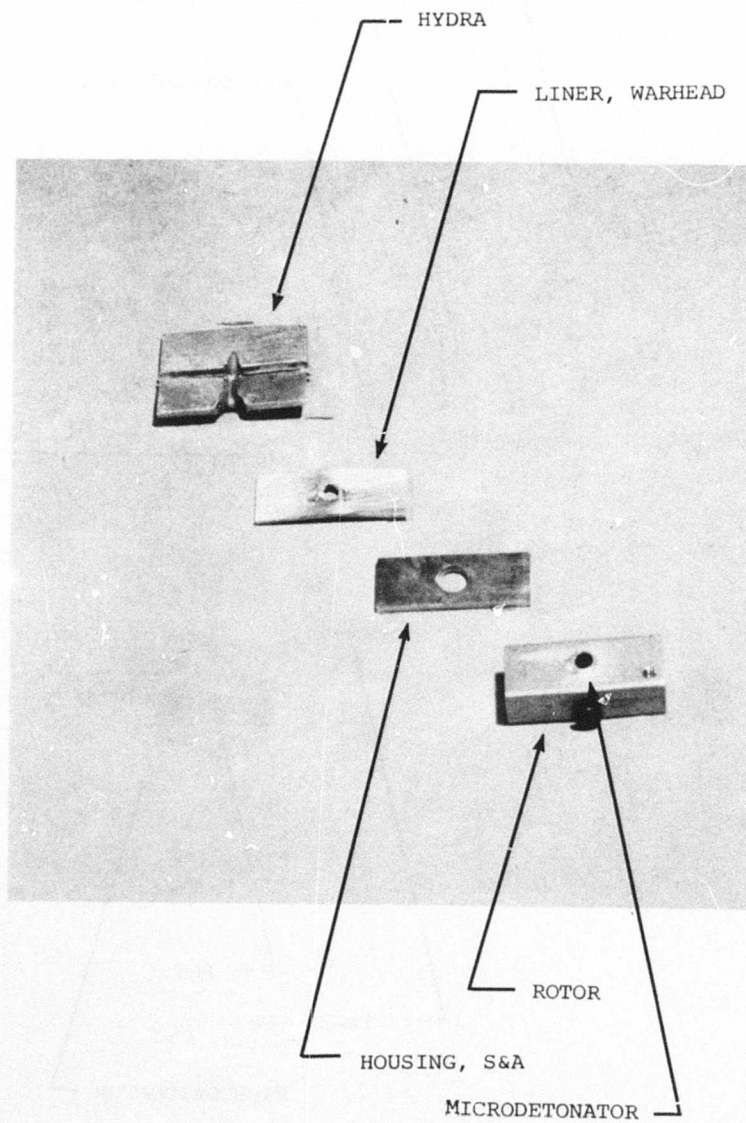


Figure 42. Aimable Explosive Train, Test No. 3

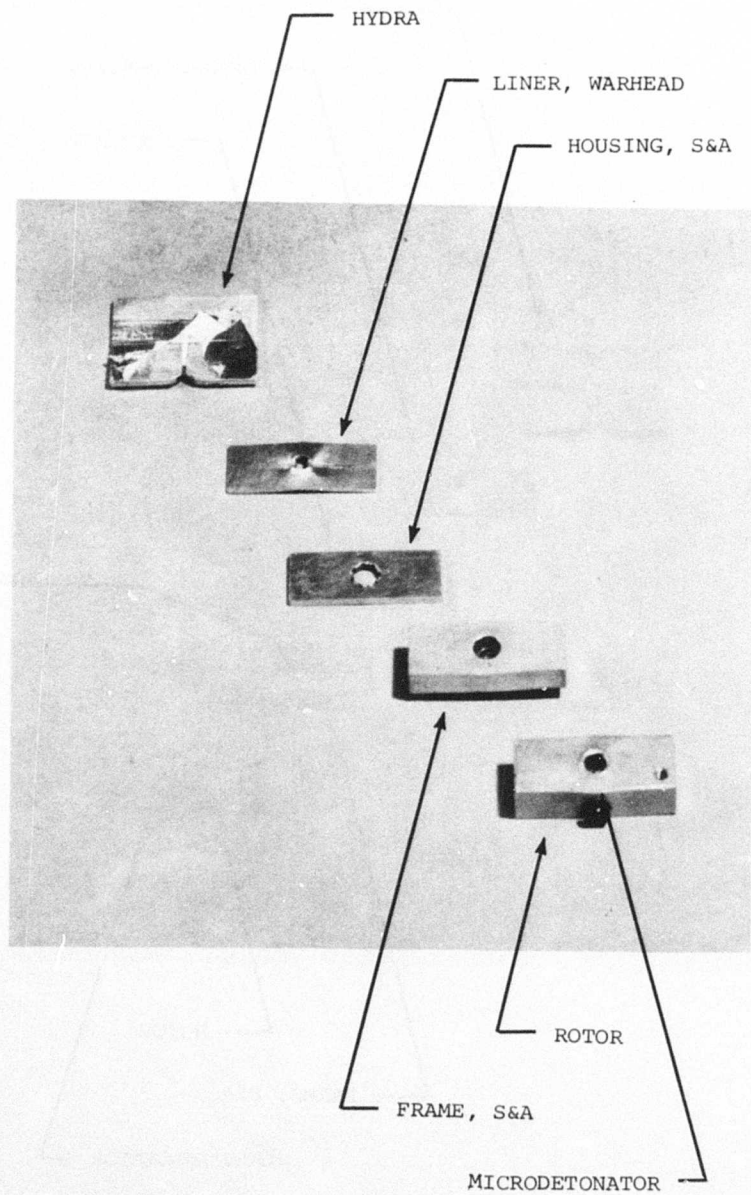


Figure 43. Aimable Explosive Train, Test No. 4

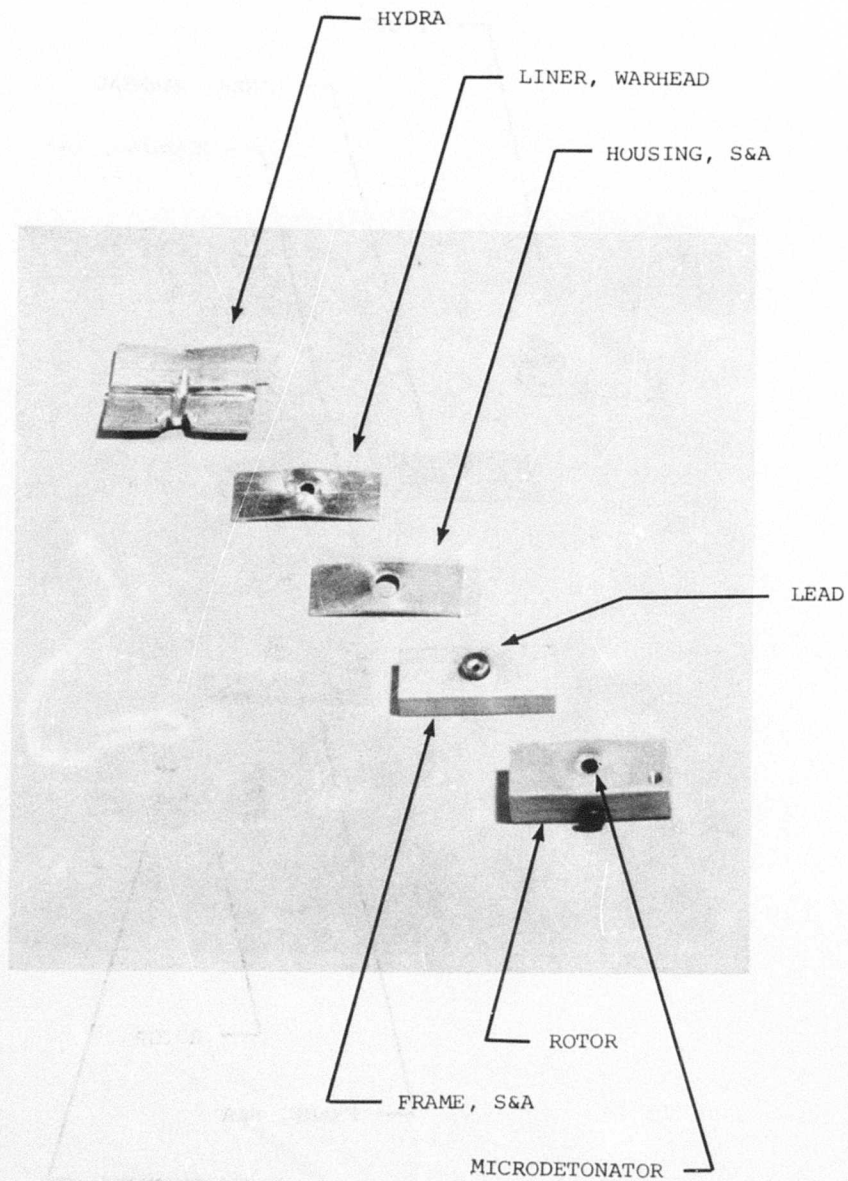


Figure 44. Aimable Explosive Train, Test No. 5

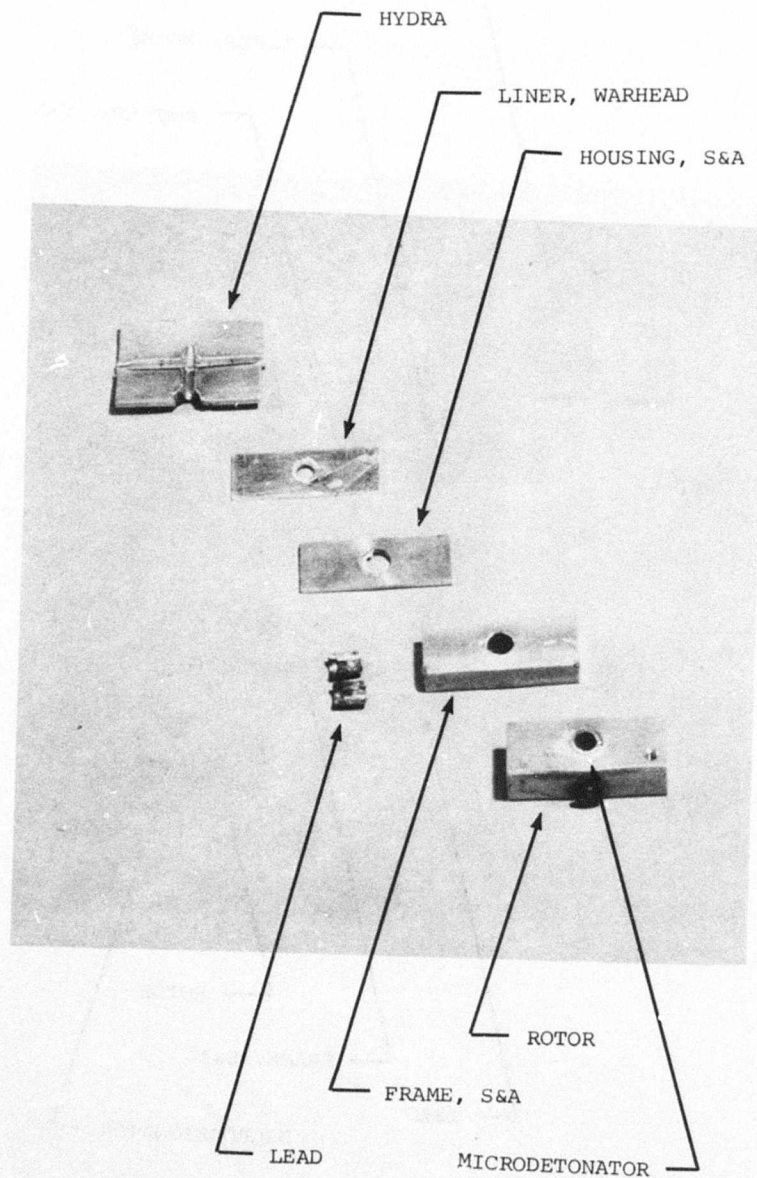


Figure 45. Aimable Explosive Train, Test No. 6

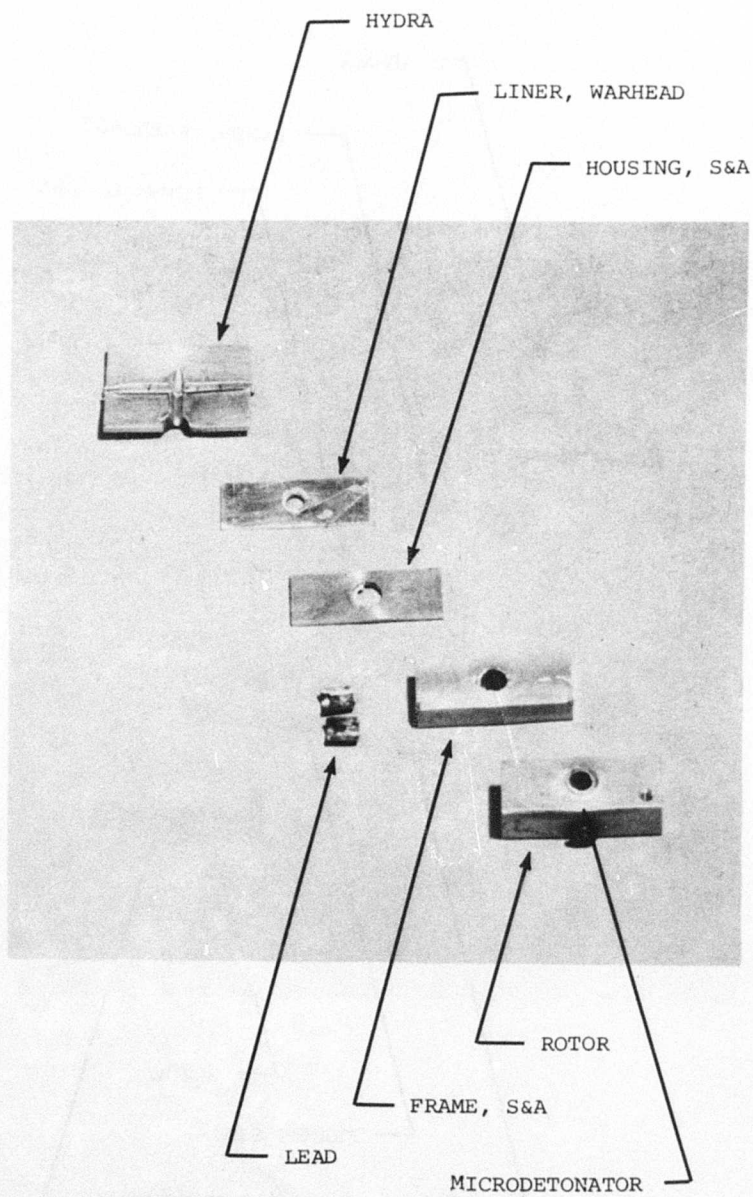


Figure 46. Aimable Explosive Train, Test No. 7

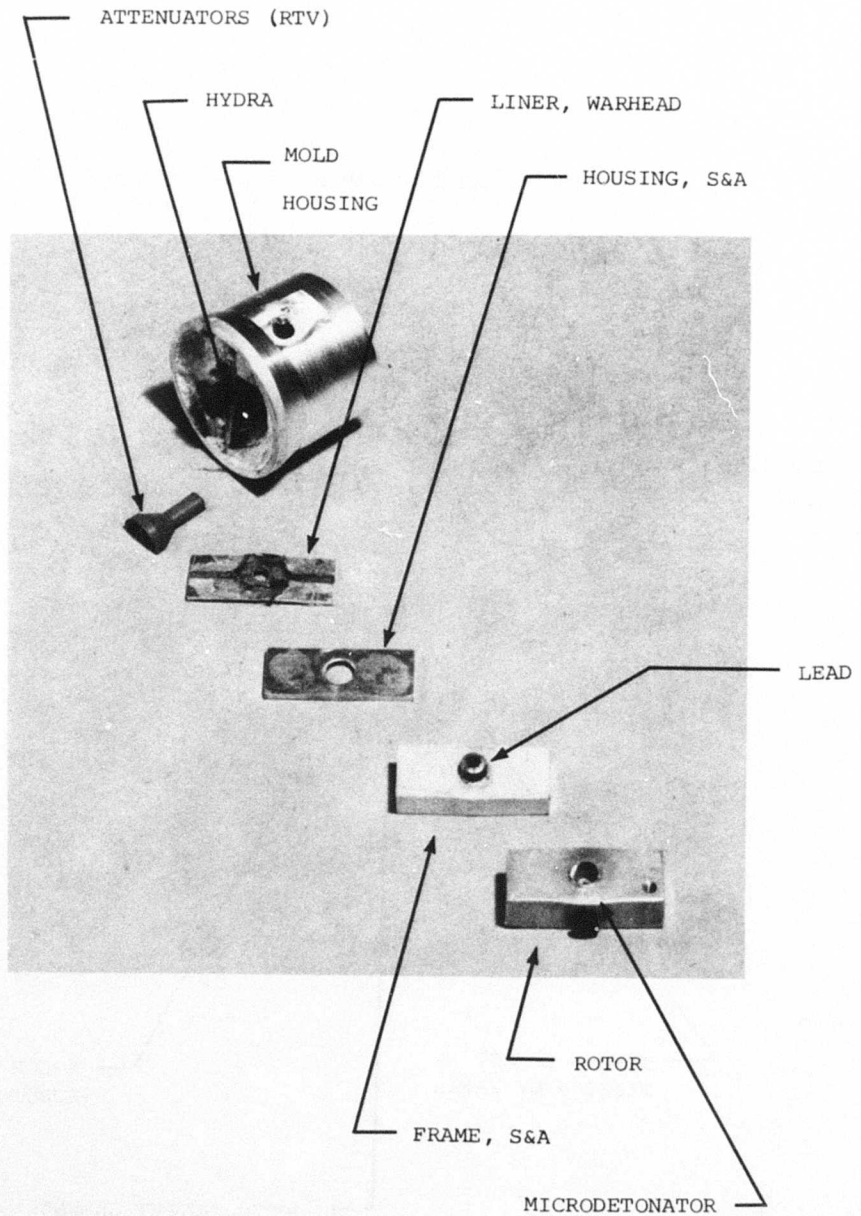


Figure 47. Aimable Explosive Train, Test No. 8

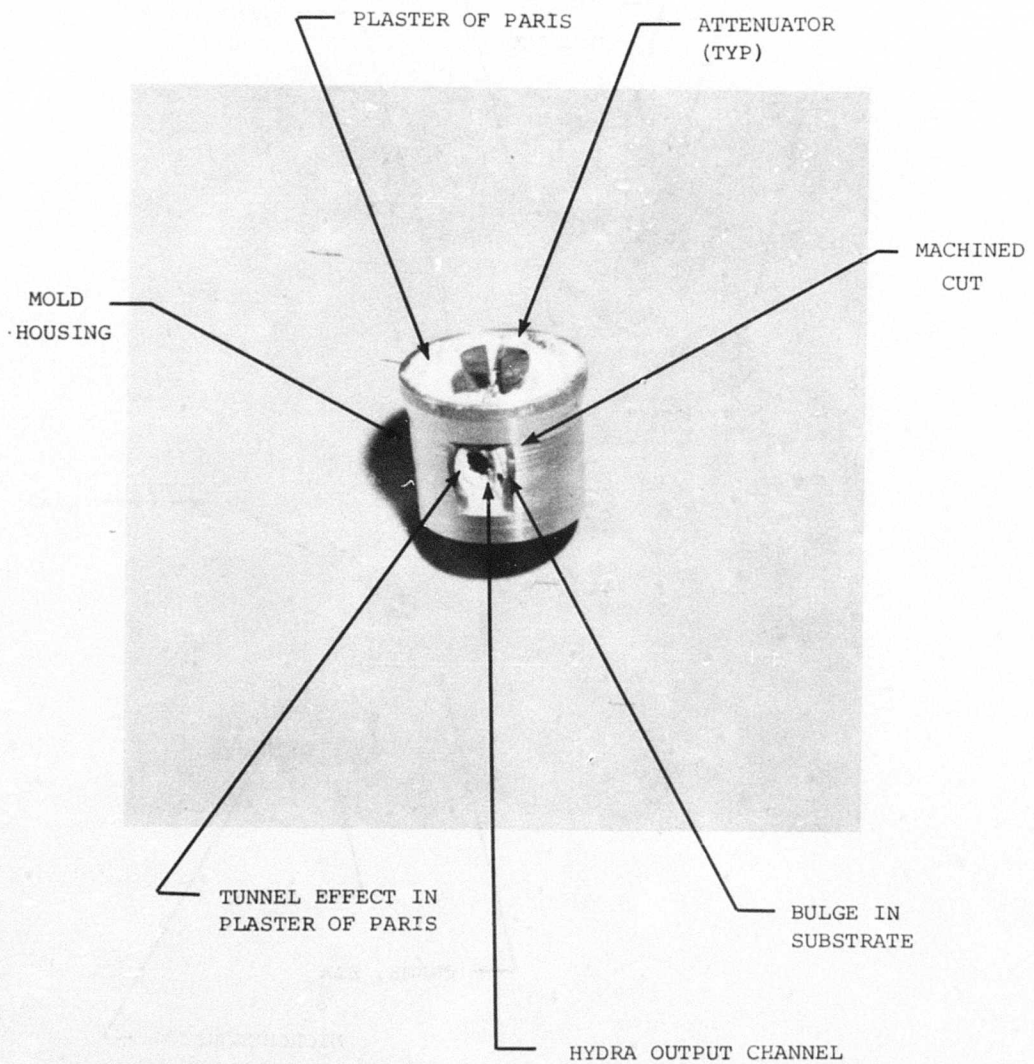


Figure 48. Detail of Hydra Substrate Test Sample

TABLE 1. AWSAD CENTRIFUGE TEST NO. 1 RESULTS

G-Level	RPM	Commit Time (Sec)	Pre-Arm Time (Sec)
8.0	118	0.070	No Pre-Arm
10.5	135	0.090	No Pre-Arm
12.1	145	0.070	No Pre-Arm
16.1	167	No Data Recorded	0.86
20.1	187	0.090	0.74
25.4	210	0.090	0.68
30.4	230	0.080	0.66
16.63	170	0.075	0.88
20.12	187	No Data Recorded	0.76
20.12	187	0.090	No Data Recorded
30.44	230	0.085	No Data Recorded
30.44	230	0.080	0.68
21.52 LAT	230 @ 45 ⁰	0.080	0.81
21.52 LAT	230 @ 45 ⁰	0.085	No Data Recorded

NOTE: The three-element damping escapement lever was 0.050-inch-thick aluminum and the four-element arming rotor escapement lever was 0.062-inch-thick aluminum.

TABLE 2. AWSAD CENTRIFUGE TEST NO. 2 RESULTS

G-level	RPM	Commit Time (Sec)	Pre-Arm Time (Sec)
16.63	170	0.80	= 1.84
18.65	180	0.72	= 1.82
20.12	187	0.72	= 1.76
25.37	210	0.60	= 1.60
30.44	230	0.50	= 1.60
25.37	210	0.55	= 1.80
21.52 LAT	230 @ 45 ^o	0.60	= 2.10
30.44	230	0.52	= 1.60
30.44	230	0.52	= 1.60
25.37	210	0.55	= 2.00

NOTE: The four-element damping escapement lever was 0.050-inch-thick aluminum and the four-element arming rotor escapement lever was 0.100-inch-thick brass.

TABLE 3. MEASURED LOADS OF SPRING FUNCTIONS

NOM. (DEFLEC) (INCHES) ALL SPRINGS (POUNDS) SETBACK SPRING (POUNDS) BOTH RTR SPRINGS (POUNDS) (DEFLEC) PLUNGER SPRING (DEFLEC) LIGHT RTR (DEFLEC) HEAVY RTR SPRING	0.10	0.20	0.30	0.40	0.50	0.60	0.70	0.77	0.87	0.97	1.07	1.17	CODE
	2.00	2.50	3.00	3.50	4.00	4.50	5.50	6.00	8.00	10.00	12.00	14.00	#1
	1.25	1.50	2.00	2.25	2.50	3.00	3.25	3.50	3.75	4.00	4.50	5.75	#2
	0.60	0.90	1.00	1.10	1.20	1.30	1.50	1.60	2.40	3.00	4.00	4.50	#3
					(INCHES)	0.68	0.76		0.87	0.97	1.07	1.17	#4
	0.04	0.14	0.24	0.34	0.44	0.54	0.64	(INCHES)	1.25	1.75	2.50	3.50	#5
	0.55	0.68	0.82	0.95	1.10	1.70	1.40	(POUNDS)					#6
					(INCHES)		0.76	0.86	0.96	1.06	1.50	2.00	
					(POUNDS)		0.00	0.50	1.00	1.50	2.00		

- CODE:
- #1 - CUMULATIVE SPRING CURVE (MEASURED)
 - #2 - SETBACK SPRING (MEASURED)
 - #3 - BOTH ROTOR SPRINGS (MEASURED)
 - #4 - PLUNGER SPRING (MEASURED INDEPENDENTLY)
 - #5 - LIGHT ROTOR SPRING (MEASURED INDEPENDENTLY)
 - #6 - HEAVY ROTOR SPRING (MEASURED INDEPENDENTLY)

INITIAL DISTRIBUTION

HQS USAF/RDORM	2	AFATL/DLJC	1
HQ USAF/SAMI	1	AFATL/DLJF	6
HQ USAF/XOXFM	1	AFATL/DLJK	1
AFIS/INTA	1	AFATL/DLJM	1
AFSC/DLCA	1	UNSWC (Code 335)	1
AFSC/IGFG	1	ASD/ENESS	1
AFSC/SDZA	1		
AFAL/DHO	1		
AFWAL	1		
ASD/ENFEA	1		
FTD/PDXA-2	1		
AFWL/NSC	1		
AFWL/NSE	1		
AFWL/SUL	1		
AFWC/SUR	4		
AUL (AU/LSE-70-239)	2		
DDC	2		
NRSLC/MMIRBD	1		
Ogden ALC/MMWM	2		
TAC/DRA	1		
57 FWW/DOS	1		
USAFTFWC/TA	1		
6510 ABG/SSD	1		
HQUSAFE/DOA	1		
HQUSAFE/DOQ	1		
HQPACAF/LGWSE	1		
HQPACAF/DOO	1		
SARRI-LW	1		
SARPA-TS-S#59	1		
USA Missile Cmd, Doc Sec	2		
Navair Sys Cmd, Code 530C	1		
Navair Sys Cmd, Tech Lib	1		
Naval Surf Wpn Cen	2		
Naval Ord Stn	1		
CT-176 TID/Tech Pubs	2		
USNWC (Code 533)	1		
Sandia Lab	1		
The Rand Corp	1		
TACTEC	1		
USAFTAWC/TEFA	1		
TAWC/TRADOCLO	1		
ADTC/SES	1		
ADTC/SD23	1		
AFATL/DL	1		
AFATL/DLOSL	2		
AFATL/DLY	1		
AFATL/DLJ	1		